Doctoral School in Health Sciences
Doctoral Programme in Drug Research
&
Institute of Biotechnology
Helsinki Institute of Life Science
&
Neuroscience Center
Helsinki Institute of Life Science
&
Division of Pharmacology and Pharmacotherapy
Faculty of Pharmacy

University of Helsinki
Finland

Development and optimisation of tools for preclinical studies on Parkinson's disease

Ilmari Parkkinen

ACADEMIC DISSERTATION

To be presented for public examination with the permission of the Faculty of Pharmacy, University of Helsinki, in auditorium 1041, Biocenter 2, Viikinkaari 5, on the 8th of April, 2022 at 12 o'clock

Helsinki 2022

Supervisors Professor Mikko Airavaara, PhD
Division of Pharmacology and Pharmacotherapy
Faculty of Pharmacy
University of Helsinki
Finland

Docent Andrii Domanskyi, PhD
Helsinki Institute of Life Science
Institute of Biotechnology
University of Helsinki
Finland

Reviewers Professor Timo T. Myöhänen, PhD
School of Pharmacy
Faculty of Health Sciences
University of Eastern Finland
Finland

Docent Šárka Lehtonen, PhD
A.I.Virtanen Institute for Molecular Sciences
University of Eastern Finland
Finland

Opponent Ari-Pekka Koivisto, PhD
Principal Scientist
Neurological Disorders Research
Orion Corporation, Orion Oyj
Finland

ISBN 978-951-51-8019-3 (paperback)
ISBN 978-951-51-8020-9 (PDF)
ISSN 2342-3161 (print)
ISSN 2342-317X (online)

The Faculty of Pharmacy uses the Ouriginal system (plagiarism recognition) to examine all doctoral dissertations

Dissertationes Scholae Doctoralis Ad Sanitatem Investigandam Universitatis Helsinkiensis

Unigrafia, Helsinki 2022

“Whenever a theory appears to you as the only possible one,
take this as a sign that you have neither understood the theory
nor the problem which it was intended to solve.”

— Karl Popper

“If it disagrees with experiment, it’s wrong.
In that simple statement is the key to science”

— Richard Feynman

Table of contents

Abstract

Successful drug development requires numerous tests to deem a drug safe and efficacious. Before clinical trials, preclinical testing is needed to ensure that the drug can be safely tried out in humans. In preclinical testing, efficacy is also assessed to minimise the risk of a drug failing in clinical trials. Parkinson's disease (PD) is a common age-associated neurodegenerative disease characterised by distinct debilitating motor symptoms caused by the dysfunction of the dopaminergic nigrostriatal pathway. For PD, a plethora of cellular and animal models have been developed to study the pathophysiology of the disease and to test potential new therapeutic interventions for treating the disease. New models are constantly created. However, methods to study outcomes also need to be developed and refined for reliable and reproducible results, which is pivotal to demonstrating the efficacy of drugs.

This dissertation work developed new tools and refined current methods to study PD in preclinical models and studied the characteristics of the cytomegalovirus (CMV) promoter and a primary culture of postnatal dopamine neurons used to model PD. First, we used infrared analysis of optical densities to assess the striatal innervation of tyrosine hydroxylase-positive (TH+) fibres in rat brain sections, a useful alternative to colourimetric optical density analyses. We also developed a novel method based on convolutional neural network algorithms to count dopaminergic neurons from rodent brain sections. The number of neurons counted had a high degree of correlation with results obtained using other counting methods, and counting was substantially faster with the algorithm.

Additionally, we developed reporter assays, both reporter plasmids, and cell lines, to measure the activity of a PD-associated drug target, Dicer. These assays, using either exogenous or endogenous fluorescent and bioluminescent indicators, were validated and produced comparable results to previously published similar assays in more physiologically relevant conditions. We also found out that a commonly used promoter in gene therapy, the CMV promoter, could be activated by neurotransmission. We showed *in vivo* that methamphetamine – a potent dopamine-releasing drug – activated the CMV promoter in the rat brain. Moreover, we observed differences in the distribution of the endoplasmic reticulum between different compartments of cultured mouse TH+ neurons.

In summary, the methods and refined tools obtained in these studies expand the toolbox of researchers engaged in studying PD preclinically and may be applicable to other disease areas and human clinical studies as well. Furthermore, our findings on the activation of the CMV promoter are important to consider when designing gene expression systems, reporter assays, or gene therapies for preclinical PD studies utilising amphetamines. And finally, we gained novel insight into the ultrastructural characteristics of cultured postnatal dopamine neurons and provided a valuable resource for the research community.

Tiivistelmä

Onnistunut lääkekehitys vaatii useita tutkimuksia, jolla lääkeaine voidaan osoittaa turvalliseksi ja tehokkaaksi. Ennen kliiniisiä kokeita, prekliinissisä kokeissa lääkeaineen turvallisuudesta tulee varmistua voidakseen sitä tutkia potilailla. Prekliinisissä kokeissa myös lääkeaineen tehoa tarkastellaan minimoidakseen riski epäonnistua kliinisissä tutkimuksissa. Parkinsonin tauti on yleinen hermostoa rappeuttava sairaus, joka aiheuttaa haitallisia ja tunnusomaisia liikehäiriöitä, jotka johtuvat keskiaivojen dopamiinijärjestelmän toimintahäiriöstä. Parkinsonin tautiin on kehitetty valtava määrä solu- ja eläinmalleja taudin patofysiologian tutkimiseksi ja uusien lääkkeiden tehon osoittamiseksi. Uusia malleja kehitetään jatkuvasti lisää, mutta myös lopputuloksia määrittäviä menetelmiä tulisi kehittää ja parantaa luotettavien ja toistettavien tulosten aikaansaamiseksi. Tämä on erityisen tärkeää, kun aikeena on osoittaa lääkeaine tehokkaaksi.

Tässä väitöskirjatyössä kehitettiin uusia työkaluja ja paranneltiin aiempia menetelmiä Parkinsonin taudin tutkimiseksi prekliinisissä malleissa, ja tutkittiin cytomegalovirus (CMV) promoottorin sekä Parkinsonin taudin mallintamiseen soveltuvan dopaamiinihermosoluviljelmän ominaisuuksia. Ensiksi hyödynsimme rotan striatumin tyrosiinihydroksylaasi positiivisten (TH+) hermosoluyhteyksien optisten tiheyksien mittaamisessa infrapuna-analyysiä, tavallisen väriaineanalyysin sijaan, tarjoten vaihtoehtoisen menetelmän optisten tiheyksien mittaamiseksi. Lisäksi kehitimme uuden hermoverkkoalgoritmeihin perustuvan menetelmän solujen laskemiseksi jyrsijöiden aivoleikkeistä. Solulaskelmat korreloivat voimakkaasti muilla laskentamenetelmillä saatujen tulosten kanssa ja algoritmilla saadut laskelmat olivat huomattavasti nopeampia.

Kehitimme myös, sekä plasmidi- että solupohjaisia, reportterikokeita Parkinsonin tautiin liitetyn entsyymin, Dicerin, aktivaation mittaamiseksi. Nämä reportterikokeet, jotka hyödynsivät ekso- ja endogeenisiä fluoresenssi- sekä luminesenssi-indikaattoreita, validoitiin ja tulokset olivat verrattavissa aiempiin julkaistuihin reporttereihin, paranneltujen fysiologisesti suotuisien olosuhteiden myötä. Näiden lisäksi huomasimme, että CMV promoottori, jota käytetään geeniterapioissa, voi aktivoitua neurotransmission myötä. Osoitimme *in vivo*, että metamfetamiinin – voimakas dopamiinia vapautta aine – annostelun myötä CMV promoottori aktivoitui rottien aivoissa. Viimeiseksi huomasimme eroja solulimakalvoston rakenteissa viljeltyjen hiiren TH+ hermosolujen eri osissa.

Yhteenvetona, tässä työssä kehitetyt ja parannellut työkalut laajentavat Parkinsonin taudin prekliinisten tutkijoiden työkalurepertuaaria, mutta ne ovat myös mahdollisesti sovellettavissa muiden tautien, sekä kliinisten tutkimusten, tutkimiseen. Lisäksi löydöksemme CMV-promoottorin aktivaatiosta, on tärkeä tieto ottaa huomioon suunnitellessa ekspressiovektoreita, reportterikokeita, ja geeniterapioita käytettäväksi prekliiniisissä Parkinsonin taudin kokeissa, joissa käytetään amfetamiineja. Ja lopuksi, saimme uusia havaintoja viljeltyjen dopamiinihermosolujen ultrarakenteellisista ominaisuuksista ja tuotimme hyödyllisen resurssin tutkijoiden käytettäväksi.

Abbreviations

6-OHDA	6-hydroxydopamine
ANOVA	analysis of variance
AAV	adeno-associated virus
BSA	bovine serum albumin
BDNF	brain-derived neurotrophic factor
CD	carbidopa
CLEM	correlative light and electron microscopy
CMV	cytomegalovirus
CNN	convolutional neural network
COMT	catechol-O-methyl transferase
DAB	3,3'-diaminobenzidine
DAT	dopamine transporter
DDC	dopa decarboxylase
DJ-1	protein deglycase DJ-1
DMEM	Dulbecco's modified Eagle's medium
DMSO	dimethyl sulfoxide
EGFP	enhanced green fluorescent protein
EM	electron microscopy
ENT	entacapone
ENX	enoxacin
ER	endoplasmic reticulum
FBS	fetal bovine serum
GBA	glucocerebrosidase
GDNF	glial-derived neurotrophic factor
GWAS	genome-wide association study
HEK	human embryonic kidney
HTS	high-throughput screening
IND	investigational new drug
i.p.	intraperitoneal
iPSC	induced pluripotent stem cell
LB	Lewy body
LD	levodopa (L-DOPA)
LRRK2	leucine-rich repeat kinase 2
Luc	luciferase
ML	machine learning
MAO	monoamine oxidase
mCherry	modified Cherry (red fluorescent protein)
Meth	methamphetamine
mRNA	messenger RNA

miRNA	microRNA
MPP+	1-methyl-4-phenylpyridinium
MPTP	1-methyl-4-phenyl-1,2,3,6-tetrahydropyridine
MoA	mechanism of action
NaCac	sodium cacodylate
NB-A	neurobasal-A medium
NCE	new chemical entity
PARK7	gene encoding DJ-1
PBS	phosphate buffered saline
PCR	polymerase chain reaction
PD	Parkinson's disease
PFA	paraformaldehyde
PFF	preformed fibril
PINK1	PTEN-induced putative kinase 1
PRKN	gene encoding parkin
PRS	polygenic risk score
RRF	retrorubral field
RT	room temperature
s.c.	subcutaneous
SD	standard deviation
SEM	standard error of mean
siRNA	small interfering RNA
SN	substantia nigra
SNpc	substantia nigra pars compacta
SNCA	gene encoding α-synuclein
SNR	signal-to-noise ratio
tdTomato	tandem repeat Tomato (red fluorescent protein)
TH	tyrosine hydroxylase
VMAT2	vesicular monoamine transporter 2
VTA	ventral tegmental area

List of original publications

This dissertation is based on the following publications and manuscript:

I Penttinen AM, **Parkkinen I**, Voutilainen MH, Koskela M, Bäck S, Their A, Richie CT, Domanskyi A, Harvey BK, Tuominen RK, Nevalaita L, Saarma M, Airavaara M: Pre-α-pro-GDNF and Pre-β-pro-GDNF Isoforms Are Neuroprotective in the 6-hydroxydopamine Rat Model of Parkinson's Disease. Front Neurol. 9: 457, 2018

II Penttinen AM*, **Parkkinen I***, Blom S, Kopra J, Andressoo JO, Pitkänen K, Voutilainen MH, Saarma M, Airavaara M: Implementation of Deep Neural Networks to Count Dopamine Neurons in Substantia Nigra. Eur J Neurosci. 48: 2354–2361, 2018

III Bäck S, Dossat A, **Parkkinen I**, Koivula P, Airavaara M, Richie CT, Chen YH, Wang Y, Harvey BK: Neuronal Activation Stimulates Cytomegalovirus Promoter-Driven Transgene Expression. Mol Ther Methods Clin Dev. 14: 180-188, 2019

IV **Parkkinen I**, Chmielarz P, Airavaara M, Domanskyi A: Novel reporter systems to study the activity of Dicer. *Manuscript*

V Sree S*, **Parkkinen I***, Their A, Airavaara M, Jokitalo E: Morphological Heterogeneity of the Endoplasmic Reticulum within Neurons and Its Implications in Neurodegeneration. Cells. 10: 970, 2021 (review article)

* Equal contribution

The publications and manuscript are referred to in the text by their corresponding Roman numerals (I-V). The manuscript of publication I is also included in the dissertation of Anna-Maija Penttinen (University of Helsinki). Additional unpublished data is included from studies III and V. Reprints were made with the permission of the copyright holders.

1 Introduction

Drug development is a highly intricate process, and a broad number of preclinical and clinical experiments must be conducted before a drug can be approved and used in hospitals or sold in pharmacies. It is usually divided into the discovery, preclinical, and clinical phases (Steinmetz and Spack 2009; Mohs and Greig 2017).

The preclinical phase, which lasts on average between 2-5 years, consists of multiple *in vitro* and *in vivo* experiments that aim to showcase that the drug has a beneficial physiological effect, i.e., that it is efficacious and safe. Preclinical experiments may include biochemical, cellular, and animal experiments. All of these are founded on a plethora of methods that have been developed solely to show safety or efficacy, i.e., pharmacology or based on methods created from basic research in the fields of physics, chemistry, and biology.

The importance of reliable methodology to produce ample proof of a drug's effects cannot be overstated. Particularly since compounds in drug development have high attrition rates. For example, the likelihood of preclinical projects advancing to clinical trials within academic drug discovery is only 31.8% (Takebe et al. 2018). Success in preclinical research depends highly on robust cellular and animal models of disease and methods used to assess efficacy in them. Many diseases, such as Mendelian diseases, can be quite precisely modelled due to their straightforward nature (Tadenev and Burgess 2019). However, common neurodegenerative diseases are perplexing and etiologically multifactorial consisting of a combination of polygenetic and environmental risk factors that make their pathogenesis and pathophysiology difficult to replicate.

Parkinson's disease (PD) is the second most common neurodegenerative disease which causes distinct motor symptoms caused by the loss of dopamine and the neurons producing it in the midbrain (Kalia and Lang 2015). The estimated costs of PD are over 50 billion dollars per year alone in the United States and it is thus a significant burden not only to patients and their caregivers but all of society (Yang et al. 2020). Particularly as the prevalence of PD increases with the ageing population.

As mentioned, drug development has low success rates and PD is no exception. The overall success rate of approved drugs for PD between the years 1999-2019 was only 14.9% illustrating the need for higher quality preclinical studies (Boucherie et al. 2021).

PD is preclinically modelled with multiple models replicating various aspects of the pathology from a cell biological perspective and more general animal models that replicate the symptoms from a clinical perspective (Duty and Jenner 2011; Airavaara et al. 2020). However, the models suffer from reproducibility issues, which arise, in part, due to a lack of robust methods to study outcomes aiming to modulate the pathobiology and to consequently develop potential disease-modifying therapies. As such, there is a need for better quantitative and unbiased measures, and the development and optimisation of methods and reporter assays aiming to show drug efficacy within these models are of high importance in the quest to cure PD.

2 Review of the literature

2.1 Parkinson's disease

PD is the most common movement disorder and after Alzheimer's disease the second most prevalent neurodegenerative disease by current clinical diagnostic standards (Kalia and Lang 2015; Poewe et al. 2017). It mainly affects the older population as incidence increases after the age of 50. Currently, more than 6 million individuals in the world suffer from PD (Armstrong and Okun 2020). It is a debilitative progressive neurodegenerative disease that causes distinct worsening motor symptoms due to the loss of the neurotransmitter dopamine and the dopaminergic neurons in the midbrain and is associated with the occurrence of Lewy bodies (LBs) (Kalia and Lang 2015).

The first recordings of a disease with Parkinsonian-like symptoms, later known as Kampavata, dates back to 300 BC from ancient Indian literature (Ovallath and Deepa 2013). Later on, scientifically, Parkinsonism came to be known as any disorder causing symptoms described by James Parkinson in his seminal monograph "An essay on the shaking palsy" in 1817 (reprinted as (Parkinson 2002)). Primary parkinsonism, which consists of 80% of cases, is most commonly known today as PD (Fahn 2003). About 90% of PD cases are idiopathic and sporadic i.e. the aetiology is unclear and who will develop it is unpredictable, however, it is highly associated with ageing (Kalia and Lang 2015). The rest are hereditary and have a known genetic aetiology and thus the development of the disease depends mainly on certain genetic defects rather than other factors. Even though primary parkinsonism cases are diagnosed as PD, like many other diseases, PD is highly heterogeneous and thus stratification of patients, based not only on the clinical manifestation of the disease but also pathological markers, would be instrumental for reliable and earlier diagnoses and better choice of treatments (Lang et al. 2019).

Nowadays it is known that the motor symptoms are mainly caused by the aforementioned loss of striatal dopamine, and the nigral cell bodies producing it (Gonzalez-Hernandez et al. 2010; Kalia and Lang 2015). There are differences in estimates on how much dopamine and dopaminergic marker loss in the striatum, and dopamine neuron loss in the substantia nigra (SN) occurs before the appearance of motor symptoms. The most consistent findings suggest that motor symptoms manifest when approximately 30% of the dopamine neurons are lost in the

SN assessed by quantitative neuromorphometry and regression analyses (Fearnley and Lees 1991; Ma et al. 1997; Greffard et al. 2006). Estimates for loss of dopamine in the striatum range between 50-70%, however, biochemical measurements are more affected by the quality and delay of *postmortem* tissue assessments, and concerns about the validity of results are higher than that of SN cell counts. Nevertheless, available data suggest that the loss of striatal dopaminergic markers exceeds the loss of SN dopamine neurons (Cheng et al. 2010). The extent of neurodegeneration at the time of diagnosis has implications for the development of disease-modifying therapies. Other areas of the brain are also affected to varying degrees such as neuron loss in the locus coeruleus and ventral tegmental area (VTA) (Uhl et al. 1985; Sulzer 2007; Giguere et al. 2018).

The specific pathological underpinnings behind the substantial loss of dopamine and degeneration of the dopamine neurons are still enigmatic, even though multiple hypotheses have been presented and extensively studied (Sulzer 2007; Gonzalez-Hernandez et al. 2010; Giguere et al. 2018). There are currently no treatments that would halt or reverse the progression of the disease and no reliable clinical biomarkers to diagnose the disease in its early stages or other diagnostic tools and clinical strategies to stratify between the different subtypes of PD (Wu et al. 2011; Armstrong and Okun 2020; McFarthing et al. 2020; Mitchell et al. 2021). Unravelling the detailed mechanisms of pathogenesis is the foremost goal for developing better diagnostic tools, stratifying patients, and developing disease-modifying therapeutics.

2.1.1 Midbrain dopamine neurons

The first descriptions of the SN were made by Vicq d'Azyr and Soemmering in the late 1700s. They observed a black pigment in the nigral cells which is why it was termed “locus niger crurum cerebri” (Parent and Parent 2010). Later, in the late 1800s, Blocq, Marinesco, and Brissaud observed Parkinsonism in a patient who had a tuberculoma that had selectively degenerated the patients’ right SN. Combined with the clinical observations of James Parkinson in the early 1800s and later studies of Lewy (1912), Trétiakoff (1919), and Hassler (1938, 1955), the hypothesis that cell loss in the SN was the basis for PD in its postencephalitic, idiopathic and hereditary forms was confirmed. Later, anatomical, morphological, and ultrastructural studies revealed the specific projections of midbrain dopamine neurons, showing the afferent

projections between the SN and striatum that forms the nigrostriatal pathway, which is focal in PD. Further, using electron microscopy (EM), characterisation of the SN ultrastructure and degeneration of dopamine neurons have shown more precisely various changes, e.g., how drug treatments disrupt the organelles, in cellular morphology and ultrastructure in different animals (Bak et al. 1969; Gulley and Wood 1971; Domesick et al. 1983).

In the late 1950s, a landmark study by Carlsson and collaborators showed that dopamine is an independent neurotransmitter instead of a precursor for the other catecholamine neurotransmitters, noradrenaline, and adrenaline (Carlsson et al. 1957; Carlsson 1959). Dopamine pathways and the neurons within them have been extensively studied after this groundbreaking discovery. Dopamine is synthesised from L-tyrosine and L-phenylalanine in enzymatic steps, the most crucial ones being the oxidation of L-tyrosine into L-DOPA, also known as levodopa, by tyrosine hydroxylase (TH), and the decarboxylation of levodopa into dopamine (Meiser et al. 2013). Dopamine can then be further converted into noradrenaline which is converted into adrenaline. As dopamine neurons mainly use dopamine for synaptic signalling, it is one way to categorise types of neurons. Dopamine neurons are involved in various physiological functions such as the regulation of motivated behaviour and its reinforcement through reward signalling and associative learning (Wise 2004). Furthermore, dopamine neurons have a significant role in regulating emotions, mood, decision-making, attention, working memory, and movement through fine-tuning of motor functions and programming of motor behaviours.

Dopamine neurons are located in the mesencephalon (midbrain), diencephalon, and olfactory bulb and constitute less than 1% of overall neurons. The total amount of ventral midbrain dopamine neurons is approximately 20000-30000 in mice, 40000-50000 in rats, and 400000-600000 in humans (Bjorklund and Dunnett 2007; Bolam and Pissadaki 2012). Most of the dopamine neurons in the human central nervous system are found in the midbrain, and about 70% are located in the SN (German et al. 1983; Pakkenberg et al. 1991; German and Manaye 1993; Bjorklund and Dunnett 2007). Different populations of dopamine neurons can be found in nine distinct neuronal groups (A8-16). The main dopaminergic circuits are located in the A8, A9, and A10 groups (Figure 1A). A8 and A10 clusters are found primarily in the retrorubral field (RRF) and the VTA, respectively, while the A9 cluster forms the neurons found mainly in the SN pars compacta (SNpc), which project to the dorsal striatum forming the

nigrostriatal pathway. This pathway is crucial for the function of the basal ganglia, which are comprised of the striatum, globus pallidus, subthalamic nucleus, intralaminar nuclei of thalamus, and SN (Lanciego et al. 2012). The basal ganglia are responsible for the execution of controlled movement patterns together with the cortex. In PD, the function of the basal ganglia is disrupted due to the loss of dopamine neurons in the nigrostriatal pathway, which causes the manifestation of the typical motor symptoms diagnosed in PD (Surmeier et al. 2014).

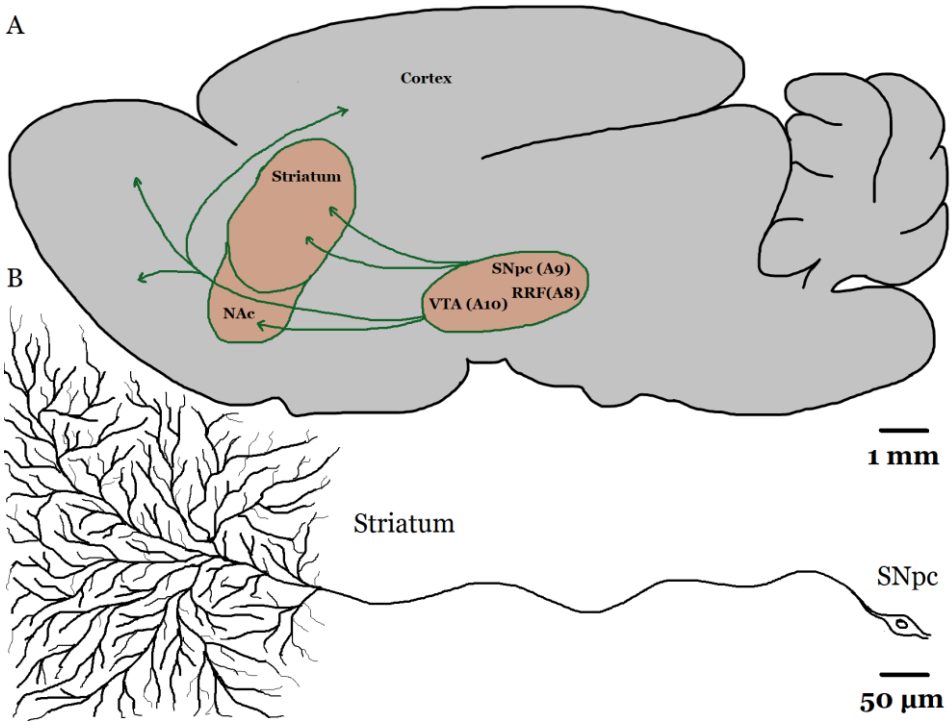

Figure 1. Dopamine projections from the ventral midbrain. Simplified schematic of a rodent brain where the dopamine pathways from the substantia nigra pars compacta (SNpc, A9), ventral tegmental area (VTA, A10), and the retrorubral field (RRF, A8) to the forebrain are displayed (**A**). Dopamine neurons within these groups project axons to the dorsal striatum, nucleus accumbens (NAc), and cortex forming the nigrostriatal, mesolimbic, and mesocortical pathways. An illustration of the extensive axonal arborization of a single dopamine neuron projecting from the SNpc to the striatum (**B**). Note that in reality the arborization is substantially vaster and the dopamine cell body thus smaller compared to the total volume covered by the axon. Scale bars are approximations. Figure drawn by the author, inspiration from Björklund and Dunnett, 2007, Trends Neurosci.

Dopamine neurons in the SN have highly complex morphologies, with expansive arborization of the axons (Figure 1B). They project from the SN to the striatum and each axon forms up to 100000-400000 synapses, and non-synaptic boutons, in a rodent brain and 10 times more in the human brain (Matsuda et al. 2009; Bolam and Pissadaki 2012). This arborization enables a single neuron to cover 6% of the total volume of rat striatum innervating up to 75000 striatal neurons. They also have extensive dendrites expanding in the whole SN and thus the cell body represents only about 1% of the total volume of a singular dopamine neuron (Matsuda et al. 2009). The reason for this perplexing arborization and redundancy of extensive synapses is not known but has been speculated to be required for the refinement of complex motor programs and/or be a compensatory mechanism due to their inherent vulnerability (Surmeier et al. 2017). It may be that the reliability for firing for rapid motor responses is favoured instead of cellular homeostasis, e.g. energy production, done at the cost of excess oxidative stress, and hence the compensation by cell amount and volume.

Since these neurons primarily die in the course of PD, a myriad of studies has been conducted to find the reasons for their selective vulnerability (Gonzalez-Hernandez et al. 2010; Giguere et al. 2018; Aguila et al. 2021; Zaccaria et al. 2021). The neurons have been under scrutinous characterisation in healthy subjects and PD patients, and multiple studies have aimed to shed light on their developing-stage and mature molecular architectures. Numerous RNA sequencing studies determining which genes they express, proteomic studies for which and what kind of proteins are produced, and metabolomic studies for which lipids and metabolites they make have been done. Yet, due to technological and methodological limitations, the full repertoire of what constitutes a dopamine neuron has not been resolved, although their complexity as such is appreciated and understood. Notwithstanding, we now know that they express certain distinct genes or molecular patterns which can be used to discern subtypes of dopamine neurons (Tiklova et al. 2019; Aguila et al. 2021). Generally, dopamine neurons can be labelled by using distinguishable dopamine markers, mainly the aforementioned TH, dopamine transporter (DAT), and vesicular monoaminergic transporter 2 (VMAT2) (Bjorklund and Dunnett 2007). When a neuron expresses all of these and/or other dopaminergic markers, it can be considered a *bona fide* 'dopamine neuron', however, if a neuron is known to express TH but the presence of other markers are not assessed, it could still be a noradrenergic neuron, as

they also express TH, and is thus only considered 'dopaminergic'. The subsets of SN dopamine neurons and VTA dopamine neurons of the midbrain can be discerned by G-protein-regulated inward-rectifier potassium channel 2 and Calbindin, respectively, as a clear majority of dopamine neurons within these areas express them (Thompson et al. 2005; Reyes et al. 2012). Thus, comparative studies looking at differences in these subtypes have been thought to be able to decipher the reason why SN dopamine neurons die more readily.

2.1.2 Risk factors and pathogenesis of Parkinson's disease

The median lifetime risk for developing PD is 2% for men and 1.3% for women at age 40 in the United States (Ascherio and Schwarzschild 2016). Environmental and genetic risk factors both contribute to the development of the disease with varied importance (Sulzer and Schmitz 2007; Kalia and Lang 2015). Some of the most widely studied risk factors are shown in Figure 2.

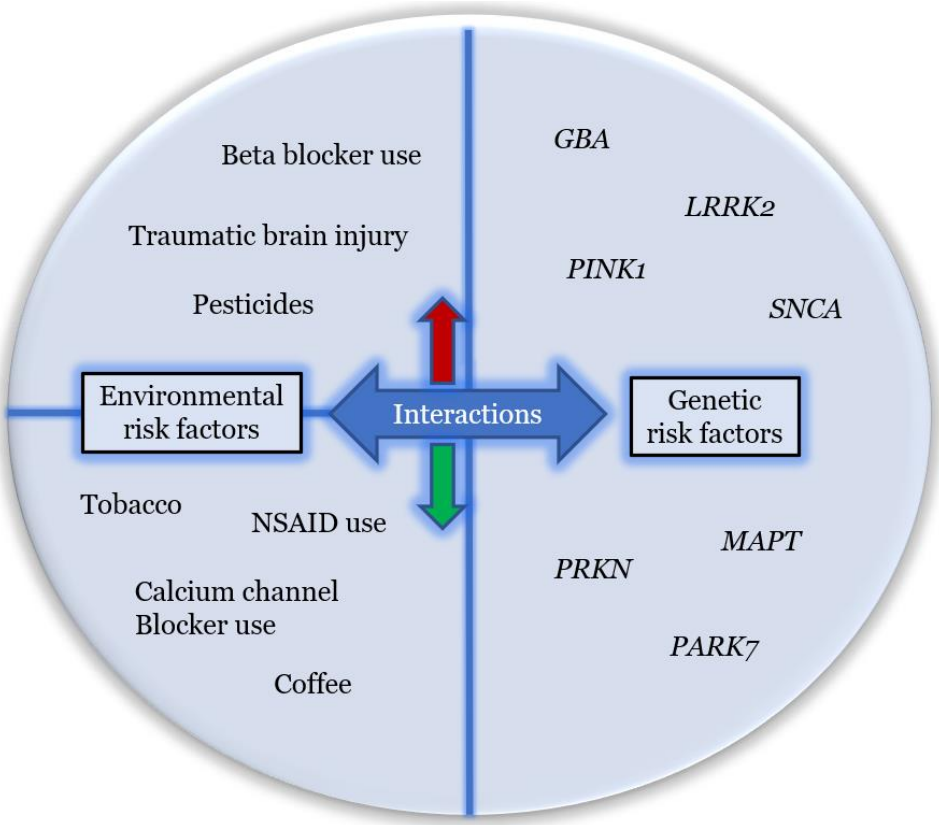

Figure 2. Examples of well-known environmental and genetic risk factors of PD. Several risk factors may reduce (green arrow) or increase (red arrow) the risk of developing PD. The genetic risk factors (right) comprise polymorphisms within these genes that influence the risk of developing PD. *GBA*: glucocerebrosidase, *LRRK2*: leucine-rich repeat kinase 2, *MAPT*: microtubule-associated protein tau, NSAID: non-steroidal anti-inflammatory drugs, *PARK7*: gene encoding DJ-1, *PINK1*: PTEN-induced putative kinase 1, *PRKN*: gene encoding parkin, *SNCA*: gene encoding α-synuclein. Figure drawn by the author, inspiration from Kalia and Lang, 2015, Lancet.

Of the environmental risk factors that significantly increase the risk of developing PD, exposure to certain toxins, drug abuse, heavy metals and pesticides, traumatic brain injury, and chronic use of beta-blockers have been detected to be significant in meta-analyses (Noyce et al. 2012). Protective environmental factors include the use of tobacco, consumption of coffee, and physical activity. Environmentally caused PD, when the aetiology is known, is classified as secondary parkinsonism. A criterion for

primary parkinsonism, or PD, is that drugs increasing dopamine signalling should alleviate the symptoms, which is not the case for secondary parkinsonism (Fahn 2003).

Most, approximately 90%, of PD cases are idiopathic, and approximately 10% are inherited (Kalia and Lang 2015). There are over 20 gene variants causing inheritable or familial PD and almost 100 variants that increase the risk of developing PD (Li et al. 2021). Five of the genes are very well known and have been widely studied. Two of them, *SNCA* and *LRRK2*, cause autosomal dominant forms of the disease, and three genes, *PRKN*, *PINK1*, and *PARK7* cause autosomal recessive PD. These develop quite early in the patient's life, usually before the age of 45. One additional gene, *GBA*, encoding a lysosomal enzyme, β-glucocerebrosidase (GBA) is also a major early-onset PD risk factor and it causes a more aggressive phenotype of PD, associated with more severe non-motor symptoms and decreased survivability (Sidransky et al. 2009; Sidransky and Lopez 2012). Modern genome-wide association studies (GWAS) have identified numerous additional genes associated with PD and their role and contribution are only starting to be uncovered (Grenn et al. 2020). These are essential when clinically assessing polygenic risk scores (PRS) in preventive or prophylactic medicine and for studies aiming to elucidate PD pathogenesis, particularly from a systems-wide perspective.

The precise causative mechanisms behind the environmental and genetic factors implicated in PD are not yet known. A multitude of cellular events has been attributed to the pathophysiology of PD based on human genetic studies and neuropathological modelling of PD in animal models (Figure 3) (Michel et al. 2016). As previously mentioned, comparative studies have been instrumental in understanding the mechanistic pathogenesis of SN dopamine neuron demise (Giguere et al. 2018; Monzon-Sandoval et al. 2020; Aguila et al. 2021; Zaccaria et al. 2021). For example, in comparative studies, it was noted that LBs are found in both SN and VTA dopamine neurons, and other areas of the brain e.g. locus coeruleus and the dorsal raphe nucleus, even though the neurons in VTA die to a lesser extent than the SN dopamine neurons and not at all in the raphe nucleus, which argues against the occurrence of LBs being the main culprit of why the neurons die (Parkkinen et al. 2011; Giguere et al. 2018). Nevertheless, SN dopamine neurons have certain distinctive characteristics which have been postulated to be responsible for their susceptibility towards neurodegeneration (Pacelli et al. 2015; Aguila et al. 2021). One of them is the noteworthy morphology – their vast arborization – which places the neurons under enormous stress just to maintain the homeostasis

throughout the axodendritic compartment of the neurons (Matsuda et al. 2009). They also have low intrinsic calcium buffering capacity compared to VTA dopamine neurons due to high cytosolic calcium oscillations produced by their autonomous pacemaking activity (Grace and Bunney 1983; Overton and Clark 1997; Guzman et al. 2009). The Cav1.3 (L-type) calcium channels that they express, which are critical for pacemaking, stimulate dopamine synthesis. Additionally, studies have shown that calbindin expressing SN dopamine neurons are relatively spared compared to those that do not express calbindin (Yamada et al. 1990). Furthermore, calbindin is more prominently expressed in the less susceptible VTA dopamine neurons (Thompson et al. 2005). The pacemaking activity and low calcium sequestering capacity combined with the distinct morphology, have been shown to produce significant oxidative-phosphorylation-related oxidative stress due to arduous bioenergetic requirements of the neurons (Pacelli et al. 2015). This high metabolic demand relies on optimal mitochondrial function and, because mitochondria are responsible for cellular bioenergetics, may contribute to PD pathogenesis.

Mitochondria are implicated both in sporadic and familial forms of PD. Toxins that are also used in modelling PD, such as 6-hydroxydopamine (6-OHDA), 1-methyl-4-phenyl-1,2,3,6-tetrahydropyridine (MPTP), rotenone, and paraquat disrupt mitochondrial function, and deficiencies in mitochondrial complex I have also been observed in *postmortem* PD patients (Schapira et al. 1989). Moreover, induced pluripotent stem cells (iPSC) extracted from patients and derived into neurons have alterations in mitochondrial function (Malpartida et al. 2021). The genes *PRKN*, *PINK1*, and *PARK7*, in which mutations cause autosomal recessive forms of PD, have roles in mitochondrial function (Vila et al. 2008; Malpartida et al. 2021). *PRKN* encodes for parkin which is a ubiquitin ligase that specifically recognises proteins on the mitochondrial membrane and is involved in mitochondrial autophagy, or mitophagy. PINK1 is a mitochondrial kinase that activates parkin to bind mitochondria destined for mitophagy. *PARK7* encodes for DJ-1 which is a multifunctional protein, acting as a sensor, antioxidant, chaperone, protease, and glyoxalase all aiming to protect mitochondria against oxidative stress. DJ-1 is primarily cytosolic but translocates to mitochondria under cellular stress to maintain their homeostasis. It does this in multiple ways: by assisting parkin and PINK1, maintaining the activity of mitochondrial complex I, and regulating the function of endoplasmic reticulum (ER)-mitochondria contact sites.

Besides the calcium hypothesis, oxidative stress, and mitochondria, there are other organelles, cellular pathways, and proteins attributed to idiopathic PD pathogenesis (Figure 3). The most widely studied topics are posttranscriptional RNA regulation, nuclear and growth factor signalling, the immune system, neuroinflammation, autophagy, the ubiquitin-proteasome system, lysosomal biology, protein accumulation, and the ER (Valente et al. 2012; Michel et al. 2016; Poewe et al. 2017; Elkouzi et al. 2019). There are multiple excellent reviews covering these topics and thus this dissertation will give examples only on a select few. Although the occurrence of LBs in PD has been known for over 100 years, and various intraneuronal proteinaceous inclusions have been studied since Friedrich Lewy found LBs in 1912, protein misfolding and aggregation became a popular topic among PD researchers after the discovery of α-synuclein in LBs, which are a prime hallmark of the disease (Spillantini et al. 1997; Spillantini et al. 1998; Elkouzi et al. 2019). LBs consist of degraded organelles, lipids, and various proteins, of which the major one is α-synuclein (Shahmoradian et al. 2019). Interestingly, α-synuclein binds to lipid membranes and seems to either tether the organelles in the LBs leading to their disruption or compromise the membrane integrity leading to fragmented organelles and sequestering them into LBs. Either way, the process by which LBs form may be a major factor driving neurodegeneration in PD (Mahul-Mellier et al. 2020).

There are multiple indications why dysfunctions of autophagy, proteasomes, and lysosomes are a cardinal feature of PD (Klein and Mazzulli 2018; Lehtonen et al. 2019). Lysosomes have been implicated through GBA-PD and mutations in ATP13A2 which is a part of the lysosomal acidification machinery. Loss-of-function mutations in GBA1, encoding a lysosomal β-glucocerebrosidase responsible for degrading glucosylceramide, in a single allele, pose a significant risk factor for developing PD (Sidransky et al. 2009). However, lysosomal storage disorders do not display PD-like symptoms which could argue against lysosomes being a major culprit in idiopathic PD pathogenesis. Dysfunctions in autophagy and the ubiquitin-proteasome system have been widely observed in PD (Lehtonen et al. 2019; Hou et al. 2020). Intriguingly, many studies show that *postmortem* brain samples and patient iPSC-derived neurons and/or astrocytes display abnormalities in autophagy.

The ER is the largest organelle of the cell and expands throughout the cell even in polarised cells such as neurons (Terasaki et al. 1994; Berridge 1998; Luarte et al. 2018). The neuronal ER is responsible for many functions

including the synthesis, folding and posttranslational modifications, secretion, and membrane insertion of proteins, accounting for approximately a third of the whole proteome (Luarte et al. 2018; Öztürk et al. 2020). It is also involved in phospholipid, sterol, and carbohydrate synthesis in conjunction with mitochondria and is the largest intracellular reservoir of calcium, thus partaking in calcium homeostasis and signalling. The ER has been associated with all of the most common neurodegenerative diseases, PD included (Mercado et al. 2013; Jung et al. 2017). In PD, the role of the ER has been studied, especially with regard to misfolded proteins and ER stress, and there are multiple good reviews addressing the involvement of the ER in PD (Tsujii et al. 2015; Hetz and Saxena 2017; Colla 2019; Fowler et al. 2019; Öztürk et al. 2020). Contact sites between the ER and other organelles, in particular mitochondria, may also contribute to the pathobiology as mitochondria-ER contact (MERC) sites have been linked to PD (Gomez-Suaga et al. 2018). Notable MERC proteins that are attributed to PD are mortalin, also known as glucose-regulated protein 75, and vesicle-associated membrane protein-associated protein B. Mortalin levels are reduced in PD patients while vesicle-associated membrane protein-associated protein B has significant interactions with α-synuclein (Jin et al. 2006; Burbulla et al. 2010; Skibinski and Finkbeiner 2011; Paillusson et al. 2017). α-synuclein is also enriched in the MERC sites (Colla et al. 2012; Guardia-Laguarta et al. 2014). Yet, the role of ER morphology in the disease has received less attention and there is considerable precedent to study this as mutations in proteins that regulate ER morphology have been shown to cause axonal degeneration, and the distinct morphology of the dopamine neurons seem to have a role in their selective vulnerability (Pacelli et al. 2015; Öztürk et al. 2020). Especially since the ER is found in all compartments of the neuron – and has significant roles in axonal and dendritic homeostasis regulating central functions with other organelles – it would be crucial to thoroughly characterise the ultrastructure of the ER and its contact sites with other organelles in all compartments of dopamine neurons in PD patients.

Additionally, due to the disproportionate loss of dopamine markers in the striatum and loss of SN dopamine neurons, it has been suggested that the neurons degenerate in a process starting from the terminals, and then along the axon towards the cell somas (Fearnley and Lees 1991; Hornykiewicz 1998; Cheng et al. 2010). This is supported by large-scale *postmortem* studies showing differences in striatal and SN dopaminergic markers, as five years after diagnosis there is near complete loss of TH, while dopamine neurons in SN are detected even decades after diagnosis

(Kordower et al. 2013). Therefore, studying the cell death mechanisms – apoptosis, autophagic cell death, and necrosis – of dopamine neurons in different pathological contexts could yield clues on the specific demise of dopamine neurons and reveal novel converging therapeutic targets which could ameliorate multiple pathological aspects of the disease (Burke 1998; Venderova and Park 2012; Onate et al. 2020). Indeed, it has been shown that apoptosis is involved in PD in somal death through caspase-dependant, UPR-initiated, and mitochondrial intrinsic pathways (Venderova and Park 2012). However, the mechanism for axonal degeneration was shown in *postmortem* brain tissue from PD patients and *in vitro* and *in vivo* models of PD to be mediated by the necroptosis machinery, providing a novel druggable pathway to treat the axonopathy observed in PD, which could prove to be the key to therapies capable of slowing down or arresting the development of the disease (Onate et al. 2020).

Other notable biological pathways implicated in idiopathic PD have less human pathology-based evidence to support their involvement in the development of the disease, albeit they may have a significant role in some patients. One example is the role of Dicer in PD (Simunovic et al. 2010; Chmielarz et al. 2017; Leggio et al. 2017). Dicer is an integral enzyme in microRNA (miRNA) biogenesis, responsible for cleaving precursor microRNAs (pre-miRNA) into mature miRNAs, which posttranslationally regulate gene expression. Dicer's postulated role in PD was realised when it was noticed that PD patients have reduced expression of Dicer in *postmortem* analysis of their dopamine neurons (Simunovic et al. 2010; Chmielarz et al. 2017). Aged mice also have reduced expression of Dicer in dopamine neurons. Conditional Dicer knockout mice also show progressive loss of nigrostriatal dopamine neurons, and enhancing the activity of Dicer, with a small-molecule drug enoxacin, is protective in stressed embryonic dopamine neuron cultures (Pang et al. 2014; Chmielarz et al. 2017). Thus, it would be helpful not only to focus on mutated genes but to find all defects related to gene expression, i.e., the RNA species regulating these genes, in PD and elucidate their role comprehensively. As such, besides human genetic studies, reporter assays and models based on these findings could unravel the perplexing nature and complete pathogenesis of PD.

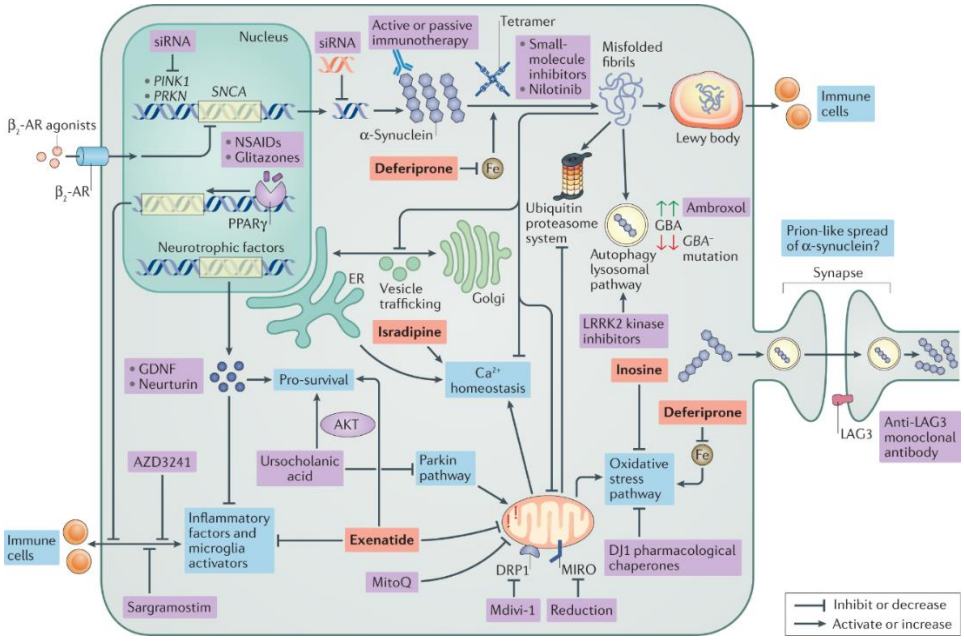

Figure 3. Factors involved in PD pathogenesis and select drugs that are currently under investigation for the treatment of PD. The figure shows the main organelles, cellular pathways, and mediators (blue) implicated in the pathogenesis of PD: Nuclear transcription and RNA regulation, growth factor and G-protein coupled receptor signalling, endoplasmic reticulum (ER), chaperones, mitochondria, autophagy, lysosomes, protein aggregation, calcium homeostasis, oxidative stress, inflammation, and immune cells. In addition, certain therapies (purple and orange), e.g. the glucagon-like peptide-1 agonist exenatide, that are presently studied for potential therapeutic effects in PD and how they affect the pathogenetic features are displayed. Bolded (orange) drugs are at advanced stages of testing. Bars indicate inhibition or decrease, and arrows indicate activation or increase. Arrows also showcase a sequence of events in a pathway. AKT: protein kinase B, β2-AR: Beta 2-adrenergic receptor, DRP1: dynamin-related protein 1, GBA: glucocerebrosidase, GDNF: glial cell line-derived neurotrophic factor, LAG3: lymphocyte activation gene 3, LRRK2: leucine-rich repeat kinase 2, MIRO: mitochondrial Rho GTPase 1, NSAID: non-steroidal anti-inflammatory drug, PPAR-γ: peroxisome proliferator-activated receptor gamma, siRNA: small interfering RNA, *SNCA*: gene encoding α-synuclein, *PINK1*: PTEN-induced putative kinase 1, *PRKN*: gene encoding parkin. Reprinted, with permission, from Elkouzi et al. 2019, Nat Rev Neurol, © Springer Nature Limited

2.1.3 Clinical aspects of Parkinson's disease

PD manifests with a multitude of clinical symptoms; classical motor dysfunctions and non-motor symptoms (Cheng et al. 2010; Kalia and Lang 2015; Armstrong and Okun 2020). The characteristic motor symptoms consist mainly of postural instability, rigidity, slowness of movement or bradykinesia, festinating gait, and resting tremor. Other motor abnormalities are related to speech, swallowing, reflexes, and eye movements. They are usually accompanied by some, not as prevalent, largely heterogenous non-motor symptoms, including cognitive impairment (dementia), anxiety, depression, sleep disturbances (REM sleep disorder), olfactory deficits (hyposmia, loss of smell), urinary and sexual dysfunction, constipation, and various types of pain (Schapira et al. 2017). Many of these are prodromal and precede the onset of motor symptoms, even by a decade, and often negatively affect the patients' quality of life even more so than the motor symptoms (Postuma et al. 2012). Some clinical manifestations of the prodromal phase of PD, such as the REM sleep disorder and olfactory deficits, may herald PD but are insufficient to support its diagnosis.

Clinically, PD is diagnosed when bradykinesia is present in addition to at least one other motor symptom; postural instability, resting tremor or rigidity (Postuma et al. 2018; Armstrong and Okun 2020). Currently, there is not a single definitive test or clinical parameter that would ascertain the diagnosis of PD. Certainty of the diagnosis is fully possible only after *postmortem* evaluation showing the presence of neuropathological markers, such as LBs, however, a certain degree of confirmation is achieved by excluding alternative diseases and disorders (secondary Parkinsonism) and with additional supportive criteria, e.g. progression of the symptoms and responsiveness to levodopa treatment.

Reliable early-stage biomarkers and methods for diagnoses have long been sought in PD patients (Wu et al. 2011). Neuroimaging is used to diagnose progression and disease state in preclinical, prodromal, early, and moderate to late-stage PD patients (Mitchell et al. 2021). The most used imaging methods are magnetic resonance imaging and positron emission tomography, or single-photon emission computed tomography, of dopamine, serotonin, or acetylcholine. To detect prodromal progression, dopaminergic imaging of the striatum, metabolic imaging, free-water imaging, and T1-weighted structural magnetic resonance imaging are applied. In early-stage PD, besides the aforementioned excluding T1-weighted imaging, neuromelanin-sensitive imaging in the posterior SN is

also utilised, and moderate to late-stage patients can be monitored using free-water imaging of the anterior SN and metabolic imaging. The methods detect progression over 12-18 months or longer. One of the most studied disease progression biomarkers for PD is α-synuclein. Multiple studies have measured α-synuclein and its various forms – conformations and posttranslational modifications – from bodily fluids, mainly blood, cerebrospinal fluid, and saliva (Schmid et al. 2013; Ganguly et al. 2021). Although some forms, such as serine 129 phosphorylated α-synuclein, which is the most commonly found pathological posttranslational modification of α-synuclein, have been extensively studied and significant differences between patients and healthy controls have been found, no reliable markers have been found for measuring the severity and stages of PD.

Machine learning (ML) -based methods have been implemented in diagnostics and have shown promise in the diagnosis of PD (Mei et al. 2021). Mainly, they have been applied to be used with neuroimaging such as magnetic resonance imaging or positron emission tomography scans or based on movement data such as computer keystrokes with relatively high accuracy rates (Liu et al. 2016; Pham 2018; Wu et al. 2019). PD diagnosis has been studied in plenty of other ways such as the use of omics data, e.g., metabolomics which has been used to reveal reductions in catecholamines of biological fluids from PD patients (Trifonova et al. 2020). One of the most promising recent developments in diagnostics has been the development of a skin test that can possibly predict PD early and late-stage phenotypes by measuring sebaceous lipids (Manne et al. 2020; Sinclair et al. 2021). Moreover, speech or voice recordings can detect PD with high accuracy (Dastjerd et al. 2019). Other diagnostic methods that have been studied are, for example, retinal alterations, a decrease in the size of handwriting, or analysis of blood-based gene expression profiles (Shamir et al. 2017; Pereira et al. 2018; Nunes et al. 2019). However, despite the enthusiasm toward ML in PD diagnostics, all of these need to be validated before they can potentially be used in the clinic.

2.1.4 The treatment landscape of Parkinson's disease

Despite decades of research, a therapeutic strategy for PD that would either halt or reverse the progression of the disease remains elusive. All approved therapies for PD so far treat only the symptoms and help patients manage the disease. Both motor and non-motor symptoms are treated, with most

of the treatment being pharmacological but there are also other options available, such as deep brain stimulation (Elkouzi et al. 2019; Armstrong and Okun 2020). The developmental scope of drugs for PD is quite broad and many different therapeutic modalities are being investigated for both curative and symptom alleviation purposes (Elkouzi et al. 2019; Armstrong and Okun 2020; McFarthing et al. 2020; Ntetsika et al. 2021; Prasad and Hung 2021).

Current pharmaceutical treatments include those that aim to manage the motor symptoms such as levodopa (precursor for dopamine), dopamine agonists e.g., pramipexole, ropinirole, apomorphine, and various enzyme inhibitors, mainly monoamine oxidase B (MAO-B) inhibitors, catechol-O-methyltransferase (COMT) inhibitors, and dopa decarboxylase (DDC) inhibitors. A gold standard is to give levodopa concomitantly with enzyme inhibitors, mainly DDC, e.g. carbidopa, and COMT, e.g. entacapone, to decrease the peripheral metabolism of levodopa to dopamine (Prasad and Hung 2021). Levodopa has been the standard for over 50 years since its approval in 1970 and PD-related successful drug development since then has been underwhelming (Figure 4) (Przedborski 2017; Charvin et al. 2018). Unfortunately, the main problem with the use of levodopa is that it leads to a fluctuated motor response, also called the “on” and “off” effect, and levodopa-induced dyskinesias, which remain unresolved. It also may take months before showing prominent efficacy. Thus, multiple drugs have been developed to treat levodopa-induced dyskinesias as add-on therapies in drug regimens. Other drugs used to treat motor symptoms include anti-dyskinetic medication such as amantadine and anticholinergics (Armstrong and Okun 2020). Non-pharmaceutical interventions are deep brain stimulation of basal ganglia and psycho- and physiotherapy. Therapeutics that are used for treating non-motor symptoms include antidepressants, anticholinesterase inhibitors for dementia associated with PD, antipsychotics, melatonin to treat insomnia, drugs to treat constipation e.g., laxatives, and dietary supplements.

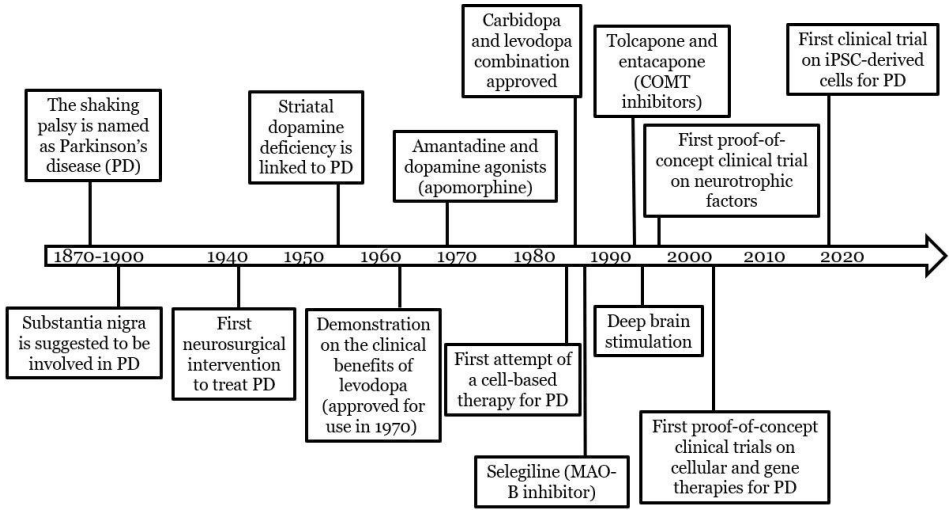

Figure 4. Timeline on important events in PD research with a focus on developing disease-modifying therapies. COMT: catechol-O-methyltransferase, MAO-B: monoamine oxidase B. Figure drawn by author inspired from Charvin et al. 2018, Nat Rev Drug Discov, and Przedborski 2017, Nat Rev Neurosci, Springer Nature Limited.

Based on meta-analyses the most effective and tolerable drugs, assessed by different Unified Parkinson's Disease Rating Scales, currently prescribed for patients are levodopa, ropinirole, rasagiline, rotigotine, entacapone, apomorphine, pramipexole, sumanirole, bromocriptine, and piribedil (Zhuo et al. 2017; Li et al. 2018).

Regarding prospective therapies, the most notable drug groups in clinical trials currently are α-synuclein targeting compounds, kinase inhibitors, neurotrophic factors, immunotherapies and microglial activators, antioxidants, Beta-2-adrenergic receptor agonists, peroxisome proliferator-activated receptor gamma agonists, compounds or probiotics affecting the microbiome, calcium stabilisers, agents enhancing mitochondrial activity, and glucagon-like peptide-1 agonists (Figure 3) (Elkouzi et al. 2019; McFarthing et al. 2020; Ntetsika et al. 2021). Examples of α-synuclein targeting antibodies are prasinezumab (PRX002) and cinpanemab (BIIB054) which have been tested in phase 2 trials. These aim to reduce pathological levels of α-synuclein. Notable kinase inhibitors inhibit LRRK2 and the c-abl kinase. C-abl kinase has been found to be active in *postmortem* PD patient brains and tyrosine-phosphorylates parkin (Ko et al. 2010). Neurotrophic factors that have been explored for

treating PD include brain-derived neurotrophic factor (BDNF), glial-derived neurotrophic factor (GDNF), neurturin, and cerebral dopamine neurotrophic factor (Chmielarz and Saarma 2020). Neurotrophic factors are important for neural growth and development and promote the survival of neurons. The glucagon-like peptide-1 agonists studied are semaglutide, liraglutide, lixisenatide and exenatide. The favourable effects seen in preclinical models of PD of these compounds is attributed to enhancing mitochondrial biogenesis and autophagy, suppressing microglial activation and inflammation, and clearance of aggregated proteins (Athauda and Foltynie 2016). Other noteworthy drugs include ambroxol, a GBA chaperone, isradipine, a calcium channel blocker and deferiprone, an iron chelator (Elkouzi et al. 2019). Of these, the latter two and exenatide are or have been, studied in late-stage clinical trials.

Cellular transplantation has also been investigated as a therapeutic approach to treat PD, with the first human trial initiated already in the late 1980s using human fetal ventral mesencephalic cells (Jang et al. 2020). Human embryonic stem cells have also been prospectively investigated for use in cellular transplantation with less ethical controversy than using fetal ventral mesencephalic cells. However, after the famous discovery and development of human iPSC:s in 2007, transplanting cells derived from iPSC:s has also been tested in rats and non-human primates, with even fewer ethical issues concerning the origin of the transplanted cells (Kikuchi et al. 2011; Barker et al. 2017). So far, results have been mixed, but interest is still considerable after the discovery of moderate amelioration using fetal ventral mesencephalic tissue in humans, successes in animal models using the iPSC-derived dopamine neurons, and a report of a possible benefit for a patient implanted with iPSC-derived autologous dopaminergic progenitor cells over a period of 24 months (Jang et al. 2020; Schweitzer et al. 2020). Furthermore, because cell transplantation has the potential to replace whole tissues it could, in theory, be curative for late-stage patients who have lost most of their SN dopamine neurons. Thus, it is very tempting to speculate that further human trials might have a considerable impact if successful. Particularly because reliable early diagnoses cannot be made and considering that the degree of neurodegeneration is highly advanced when the first motor symptoms appear.

2.2 Drug development and discovery

Drug development is a long and tedious process involving years of research and experimentation aimed at assessing the safety and efficacy of a drug candidate. The pharmaceutical industry is notorious for its high attrition rates (Drews 2000; Hutchinson and Kirk 2011). Most drug development programs fail, and the stellar results attributed to best-selling blockbuster drugs are rare. Drug development is divided into the discovery, preclinical, clinical, and marketing stages (Figure 5). The early stages of drug development, which encompasses the discovery phase and preclinical phases, consists of basic chemical, biological, and pharmaceutical research to ensure that a drug candidate is ready for clinical trials (Brodniewicz and Grynkiewicz 2010; Mohs and Greig 2017; Merchant et al. 2019). In the discovery phase, the pathobiology of diseases is illuminated, new drug targets are identified and validated, and new chemical entities (NCE), to be chosen as drug candidates, are created or discovered. Traditionally the sources have been of natural origin but with modern chemistry, semisynthetic and fully synthetic molecules have become very common. Also, the introduction of biologics since the era of biotechnology from the cloning of the first protein in the 1980s has enabled efficient production, instead of extraction, of multiple new non-small-molecule candidates including peptides, proteins, RNA, DNA, virus vectors, and cell-based therapeutics. After the NCE has been discovered and deemed drug-like from a chemical perspective, i.e. has favourable properties such as adhering to the Lipinski rule of 5, it will be tested in a variety of tests that measure the biological activity, efficacy and safety of the NCE (Lipinski 2000).

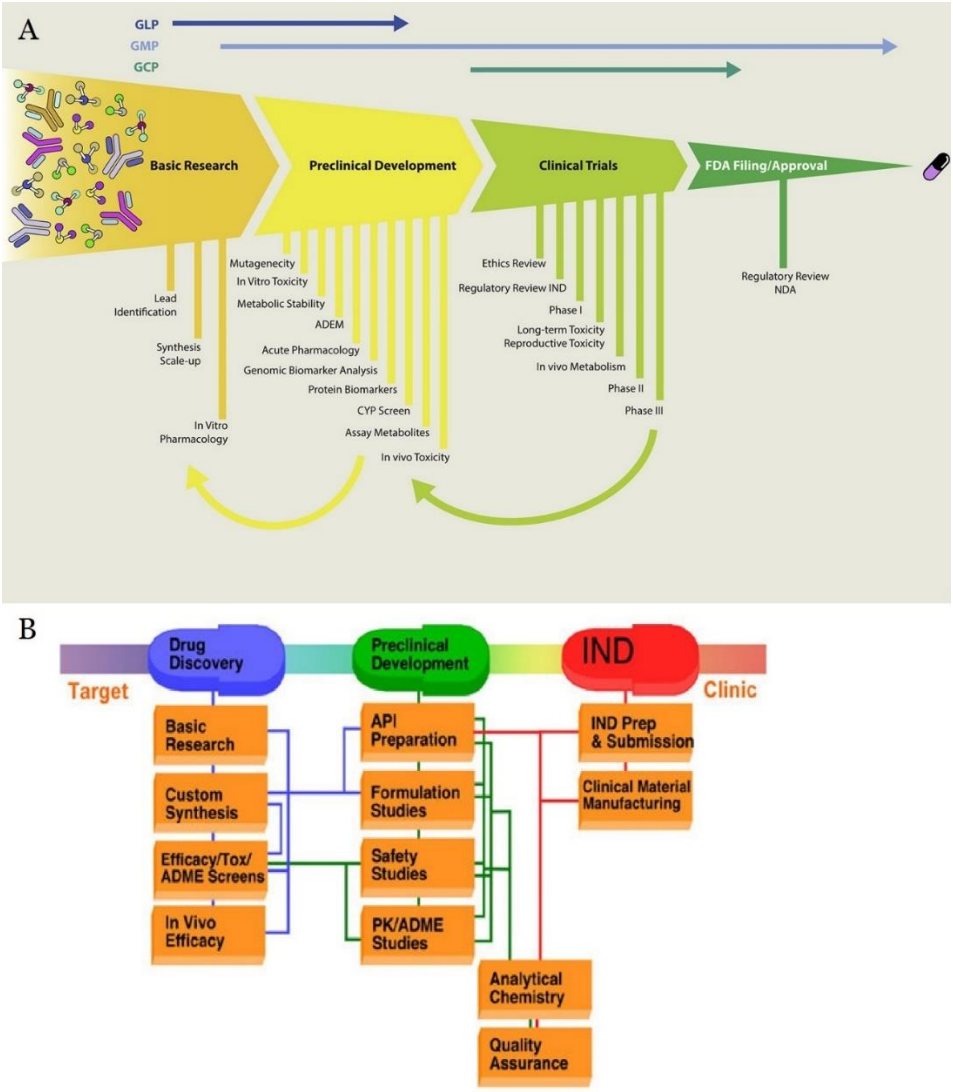

Figure 5. Stages of drug development with a focus on discovery and preclinical studies. The full developmental cycle of a drug from discovery to marketing (**A**) and studies to be conducted before the drug candidate can achieve an investigational new drug (IND) status and enter clinical trials (**B**). ADME/ADEM: absorption, distribution, metabolism and excretion, API: active pharmaceutical ingredient, CYP: cytochrome C oxidase, FDA: Food and Drug Administration, GCP: good clinical practice, GLP: good laboratory practice, GMP: good manufacturing practice, IND: investigational new drug, PK: pharmacokinetics, NDA: new drug application. Reprinted (adapted), with permission, from Mohs and Greig, 2017 (A), and Steinmetz and Spack, 2009 (B).

In the discovery stage, the potential drug target (gene/nucleic acid/protein/metabolite) is identified from mechanistic biological studies, e.g. on gene-protein associations, expression profiles, phenotypic analysis or functional screening (Hughes et al. 2011). The goal is to reveal its function and role in the disease or indication that the drug is developed for and to determine whether it is druggable, meaning that it can be targeted with the developed modality; the small-molecule or biological drug candidate. Then the target is validated which aims to demonstrate that the target is involved in the disease and that modulating it has a therapeutic effect. This is done with pharmacological and genetic methods by demonstrating the structure-activity relationship of analogous drug candidates, generating resistant mutants of the target, and the knockdown/knockout, or overexpression of the target and/or its partners in the targets' up/downstream signalling pathway(s). After this, hit compounds are generated and the best ones are selected for lead development from which they move into the preclinical development stages. An integral part of drug discovery is the use of biochemical and biological reporter systems which are widely implemented in target validation, and NCE/drug candidate screening and validation.

Drug discovery relies on phenotypical screening, rational design of compounds, or anything in between (Swinney and Anthony 2011; Swinney 2013). Historically many drugs have been found through luck and serendipitous efforts, such as the famous discovery of penicillin. In the 20th century, new technological advancements, such as crystallography and EM have enabled scientists to illuminate biomolecular structures, especially proteins which are the targets of most drugs. This, combined with modern organic chemistry and particularly computational chemistry, have enabled rational drug design. Nowadays a general protocol in rational drug design is to find a drug target, figure out its structure, and design compounds *de novo*, or virtually screen the copious chemical space for ligands, that bind the target in a desired manner, i.e. inhibiting or enhancing (activating) its function. Meanwhile, modern phenotypical screening has had considerable advancements in terms of the throughput of experiments and the models used for screening new therapeutics. Both are still utilised today, and new drugs entering the market have been found using one or the other method, although rational drug design is most likely to become dominant at some point through major technological advancements in structural biology and computational chemistry. To mention a few, improvements in cryo-EM have enabled precise estimation of protein structures with increasing speed and it is overshadowing the use of crystallography. Studies using cryo-EM and additions of structures to the

protein data bank have increased substantially during the past 10 years (Renaud et al. 2018; Robertson et al. 2021). On the computational side, better programming has enabled efficient software to study molecular modelling and docking, and this combined especially with increased computational power and ML-based algorithms have enabled the study of the structures, ligands, and their interactions, with higher speed and precision. Particularly, ML is emergent in the field and the latest demonstration of this is AlphaFold, a deep learning neural network algorithm that can accurately predict structures of proteins (Jumper et al. 2021). On the other hand, miniaturisation, robotics, and microfluidic technologies have also augmented the throughput of screening experiments and this combined with more pertinent and accurate cellular and animal models, and analysis methods have made phenotypical screening very time- and cost-effective and more reliable (Swinney and Lee 2020). A modern phenotypical screen can combine robotics, microfluidics to reduce variables, a good well-characterised disease model, and fast computer-assisted imaging to analyse millions of images of thousands of compounds screened in multiple models in a matter of days which can yield hits faster than rational drug design. It is important to note that these two are not mutually exclusive and research groups and biopharmaceutical companies can even combine both for desired results.

Phenotypical screening looks at phenotypical effects of compounds in cellular and animal models (Swinney 2013; Swinney and Lee 2020). Screening is done using libraries of chemical compounds or biomolecules. The libraries can be either small-molecule compounds of natural origin, synthetic compounds, drug-like compounds already found or even marketed drugs that could be repurposed. For biologics, a battery of potential proteins such as various antibodies and their derivatives e.g., fragmented antibodies or nanobodies, other peptides or proteins with good binding properties or RNA/DNA libraries of various forms (miRNAs or other non-coding RNAs such as small interfering RNAs, siRNAs) or even cells can be screened to look for effects in the models. Most commonly cell lines or cellular models of disease are used in high-throughput screening (HTS), but also canonical animal models can be implemented into HTS settings, mainly with simple model organisms such as *Caenorhabditis elegans* (nematode), *Drosophila melanogaster* (fruit fly), and *Danio rerio* (zebrafish) (Giacomotto and Segalat 2010). Nonetheless, even higher-order organisms like mammals, for example, the common laboratory animal *Mus musculus* (mouse), can be used for screening, albeit using them comes with reduced throughput and/or higher costs (Maggi and Ciana 2005). The advantage of using higher-order animals is that they are

more likely to yield good hit compounds as their biology is more similar to humans. Ergo there is a trade-off between translatability and throughput.

Rational drug design, or target-based drug discovery, as the name implies, is the design of therapeutics affecting a pre-specified target that holds the potential to have a beneficial effect to treat a disease (Croston 2017). Rational drug design relies on insights mainly from human biology and animal models of disease. Since the beginning of the 21st century, after the sequencing of the human genome, the era of genetics and genomics has revealed a multitude of drug targets from finding gene candidates implicated in disease and GWAS of large cohorts of humans. Especially genes associated with loss-of-function or gain-of-function variants and mutations have been under scrutinous investigation to find out whether they could be targeted with drugs. Examples of successful rational drug design have been the blockbuster drug imatinib, which was designed to inhibit a specific mutation in a kinase causing chronic lymphocytic leukaemia, and the development of proprotein convertase subtilisin/kexin type 9 antibodies for lipid disorders, of which the loss-of-function mutation has a protective effect in humans revealed by sequencing studies (Capdeville et al. 2002; Jaworski et al. 2017). Nevertheless, a highly important part of both phenotypical screening and rational drug design are reporter assays which are used to screen for desired effects or to make sure that the rationally designed drug functions as hypothesised.

2.2.1 Preclinical drug development

After the discovery phase, drug candidates enter the preclinical phase in which the preclinical profile of the candidates are studied using cellular and animal models that aim to showcase that the drug candidates are safe enough to enter human clinical trials (Hughes et al. 2011). Additionally, multiple pharmaceutical studies – chemistry, formulation pharmacology, pharmacokinetic, toxicology tests – are conducted to find out the optimal dose, method and frequency of administration and formulation of the candidates for scaled production (Figure 5). Further *in vitro* and *in vivo* experiments are conducted and all of these are iterated until a candidate is found to be suitable for entering clinical trials.

For a drug to get an investigational new drug (IND) status, the preclinical evidence required must be substantial enough for drug regulatory agencies to approve the IND application (Figure 5). This means that the tests and

methods used to showcase the safety and efficacy must be well-established and reliable based either on scientific consensus or, in the case of new methods, careful scientific assessment (Hughes et al. 2011; Swinney and Anthony 2011). Standards set too low increase attrition rates as unreliable methods will not promote positive clinical results (Hutchinson and Kirk 2011). In many cases, the focus is too much on the models, and the development of methods assessing outcomes of drugs investigated in the models is overlooked, and outdated, possibly not critically reviewed, methods are used (Airavaara et al. 2020). An example of a test in need of evaluation is the drug-induced rotation test. The test was developed in the 1970s but only recently its usefulness in assessing neurorestorative or neuroprotective effects was critically examined, and various pitfalls realised that may lead to misinterpretations of data and misleading or false conclusions (Bjorklund and Dunnett 2019).

Although efficacy studies are not as prevalent in the preclinical stages and focus is mostly on safety, they are highly important for helping identify candidates for further development and optimisation, and as such are many times conducted before, or concurrently with, pharmacokinetic and toxicological studies (Steinmetz and Spack 2009). *In vivo* proof of mechanism studies are also critical for clinical trials aiming to demonstrate proof of principle and proof of concept for a drug (Merchant et al. 2019).

2.2.2 Reporter assays for novel therapeutic targets

A reporter is an indicator of a biological phenomenon or process and as such reporter assays are systems that give readouts or indications of these. Reporter assays are an integral part of biological research and drug development (Giacomotto and Segalat 2010; Hughes et al. 2011). Screening to find hit compounds is the next step in the discovery stage of drug development after target identification. Reporter assays can also be used in phenotypical screening, without prior knowledge of the target. Reporter systems, or the assays, can be endogenous or exogenous, chemical, or genetic and can be based on *in vitro* or *in vivo* models. Reporter assays rely on a variety of measurable factors or proxies utilising quantifiable detection in the form of fluorescent, bioluminescent or colourimetric markers. An ideal reporter assay is easy to implement, sensitive, stable, and well-controlled, i.e., is not affected by too many variables.

Endogenous reporters are used to measure changes in a cell related to DNA, RNA, proteins, or metabolites as these are the main building blocks for a cell (Schenborn and Groskreutz 1999). Alterations in DNA can be measured with chromatin assays, RNA can be measured *in situ*, and numerous proteins can be assayed using immunological-based methods and mass spectrometry, which is also used with nuclear magnetic resonance spectroscopy to study ions, lipids, carbohydrates, and metabolites. Exogenous reporters, however, use these building blocks and their functionality to elicit changes in the reporter itself. This is useful in multiple ways. For instance, one can get the reporter systems to report in a very precise spatiotemporal manner, i.e., from specific cells at a specific time point. They can also be used to visualise biological events in real-time and have a high signal-to-noise ratio (SNR). The systems can also be easily developed into a simple and standardised workflow for higher throughput of experimentation.

The proxies used to detect and quantify effects are mainly based on colourimetric, fluorescent, or bioluminescent probes (England et al. 2016; Lopreside et al. 2019). Colourimetric, or chromogenic, compounds, such as 3,3'-diaminobenzidine (DAB), which produces a brown precipitate, have been widely used in biology to stain samples (Litwin 1979). However, many biological organisms have evolved to produce fluorescent and luminescent small-molecule compounds and proteins which have useful properties compared to colourimetric options, such as reduced toxicity, use in heritable genetic systems, and signal specificity (Rodriguez et al. 2017). The green fluorescent protein (GFP) was discovered in 1962 by Shimomura and colleagues who isolated and purified it with aequorin, a luminescent protein, from the *Aequorea victoria* jellyfish (Shimomura et al. 1962). It was then cloned by Douglas Prasher who published the findings in 1992 (Prasher et al. 1992). Since then, it has been the most widely used fluorescent marker. Nowadays multiple different fluorescent proteins have been engineered to be better for use in biological settings. One of the most common GFP variants is the enhanced GFP (EGFP) which is brighter than the original GFP and matures faster at 37°C (Zhang et al. 1996). When choosing fluorescent proteins, brightness, autofluorescence, photostability, toxicity, and maturation time should be considered respective to the application. For example, red fluorescent proteins have generally less autofluorescence and phototoxicity than green ones but may take more time to mature or may not be as sensitive (Graewe et al. 2009; Lopreside et al. 2019). Most used fluorescent proteins are between 17-28 kDa in size.

The most commonly used luminescent proteins originate from *Gaussia princeps* (Gaussia luciferase, GLuc), *Photinus pyralis* (Firefly luciferase, FLuc), *Renilla reniformis* (Sea Pansy, RLuc), *Pyrophorus plagiophthalamus* (Click beetle luciferase, CBLuc), *Cypridina noctiluca* (Cypridina luciferase, CLuc) or *Oplophorus gracilirostris* (OLuc and NanoLuc) (Fan and Wood 2007; Nakajima and Ohmiya 2010; England et al. 2016). They all use either D-luciferin, coelenterazine or furimazine as the substrates to produce the bioluminescent reactions. Their sizes range from 64 kDa (CBLuc) to 19 kDa (NanoLuc) and have different emission wavelengths ranging from 460 to 600 nm. RLuc and GLuc reactions are shorter (<60 min) and thus follow flash kinetics, while FLuc, CBLuc and NanoLuc reactions stay for longer periods and thus follow glow kinetics. While flash kinetic proteins have higher sensitivity and are suitable for proximal *in vitro* measurements with a plate reader, glow kinetic proteins are better for *in vivo* use.

Choosing which promoters to use is one of the most important considerations when developing reporter assays (Alam and Cook 1990; Qin et al. 2010). Promoters initiate gene expression and have various properties which are important to consider for optimal spatiotemporal expression of wanted genes. They can be constitutive, activity-dependent, and have different degrees of expression. Some promoters are cell-type specific and others ubiquitous, depending on the size of the promoter sequence and transcription factor binding. Most promoters used in reporter assays are either endogenous with regards to the system they are used in, to match normal physiological expression levels, or from viruses, as viral promoters are efficient and can elicit supraphysiological expression levels which may be optimal for the assay in some cases.

The cytomegalovirus (CMV) promoter was first used in mammalian expression systems in the late 1980s and the full genome of the human CMV was sequenced in 1990 (Foecking and Hofstetter 1986; Chee et al. 1990). Since then, it has been widely used in expression vectors due to its ability to drive high expression of transgenes and compatibility with multiple cell types. Due to its stability and the ability to maintain long-term transgene expression, it has been exploited in gene therapy trials.

Besides choosing the indicator compounds and promoters, other factors to be considered when designing genetically-encoded reporter assays are genetic elements that affect transcription and/or translation and vectors or methods to transform, transfect or transduce them (Alam and Cook 1990; Jayawickreme and Kost 1997; Kobayashi et al. 1997). Numerous ways to control expression have been developed, such as activatable

promoters and/or indicators, for example, the tet-On system so that promoter activity and expression levels can be controlled using tetracycline and its derivatives, such as doxycycline. Also, elements that enhance expression are commonly utilised, such as the Woodchuck Hepatitis virus posttranscriptional regulatory element, which stabilises the transcript for amplified expression (Zufferey et al. 1999).

Transfection can be achieved by reagents that enhance uptake of genetic material to cells, such as polyethylenimine, or physical methods such as electrophoresis, or cell squeezing which disrupts the cell membrane for passage of genetic material into the cell (Yamano et al. 2010; Fajrial et al. 2020). When using viral vectors, i.e. viruses that cannot replicate, the viral proteins enable transduction of genetic material into cells utilising receptor-mediated entry and other viral elements, such as reverse transcription for insertion of the material into the genome (Bouard et al. 2009). The advantage of using viral vectors, such as different adeno-associated virus (AAV) -variants or lentiviral vectors is increased efficiency, and tissue or cell-type specificity to ensure that only wanted cells are transduced.

When the purpose of a reporter assay is to specifically use it to find novel therapeutic drugs, HTS compatibility is a desired feature as it enables large compound libraries to be screened efficiently (Inglese et al. 2007; Plate et al. 2016). This increases the chances of finding hit compounds and reduces the time it takes to do so. However, a reporter assay with HTS compatibility may not be easy to develop depending on the target that it aims to measure. HTS requires that the reporter has a significant enough effect size combined with minimal variation and that the effects of multiple compounds can be studied in a relatively short amount of time. Usually, this means that the assay should be scalable to a high multiwell plate format, such as 384 or 1586 wells.

2.3 Preclinical modelling of Parkinson's disease

PD can be modelled *in vitro* in cells and *in vivo* in animals, by using toxins, genetically modified animals or various proteins delivered into the brains of naïve animals (Figure 6) (Airavaara et al. 2020). Cellular and animal models are used to assess both the efficacy and safety of therapeutic interventions. A myriad of methods has been developed and implemented specifically for this purpose or repurposed from general biological methods to assess readings or outcomes of the interventions.

Validity is crucial in the evaluation of animal models. An animal model should exhibit considerable construct validity, i.e. similar pathogenesis to the modelled disease, face validity in that it recapitulates pathological aspects of the disease and predictive validity, the ability to assess therapeutics with the model, which is the key feature for drug discovery (Duty and Jenner 2011). Considering this from a PD point of view, for a model to have good construct, face, and predictive validities, it should display most, if not all pathological phenomena presented in section 2.1.2, show dysfunctions in the nigrostriatal dopaminergic pathway and both motor and non-motor behavioural deficits, and the model should be responsive to treatments enhancing dopamine-signalling. In addition to validity, reproducibility is pivotal for the reliability and successful assessment of therapies with the model. The models used in preclinical PD studies and methods to measure outcomes are discussed in the following section.

2.3.1 Cellular and animal models of Parkinson's disease

The first case of modelling PD-like symptoms with animals was developed over 50 years ago by Ungerstedt after the discovery by Anden et al. of the nigrostriatal tract in the rat (Anden et al. 1964; Anden et al. 1966; Ungerstedt 1968). A unilateral lesion to this tract caused vigorous ipsilateral turning behaviour after inducing dopamine release with reserpine and an MAO-B inhibitor. Ungerstedt et al. went on to use the newly discovered neurotoxin 6-OHDA to induce a selective lesion and developed a quantifiable test based on this drug-induced turning behaviour (Ungerstedt and Arbuthnott 1970).

The most commonly used toxins that have been used to model PD are 6-OHDA, MPTP and its metabolite 1-methyl-4-phenylpyridinium (MPP+),

lactacystin, and the pesticides, rotenone and paraquat (Duty and Jenner 2011; Airavaara et al. 2020) (Figure 6). All of them cause quite selective lesions to the dopaminergic pathways through damage to mitochondria or proteosomes. The advantages of these models are that they are easy to implement, they replicate the degeneration of the nigrostriatal dopaminergic circuitry, and the behavioural effects can be readily measured in unilateral lesion models. The behavioural and functional effects are quantifiable and useful for studying new restorative or protective drugs with these models. 6-OHDA and MPTP models are generally quite reproducible, with the unilateral 6-OHDA being very well-tolerated by the animals (Kirik et al. 1998). However, the major drawback of these two models is that, besides the specific mitochondrial dysfunction, they do not exhibit other pathological features of idiopathic PD such as the deposition of α-synuclein. The presence of this pathological marker is seen with lactacystin, rotenone, and paraquat which is why some researchers prefer to use them to model PD (Airavaara et al. 2020). However, these models suffer from a lack of robust effects in causing prominent lesions, behavioural symptoms, and reproducibility between studies.

A plethora of transgenic mice and rat models have been created to model PD, both GWAS-based and etiological (Figure 6). Most models have aimed to modify the familial early-onset PD genes, *SNCA* and *LRRK2* (autosomal dominant inheritance) and genes that encode DJ-1, PINK1, and parkin (autosomal recessive inheritance). Etiological models have been created which disrupt dopaminergic transcription factors and mitochondrial proteins (Airavaara et al. 2020). For example, heterozygous deletions of the transcription factors, Nurr1, Foxa2, and Engrailed1, and factors causing disruptions in the mitochondrial respiratory chain proteins, such as mitochondrial complex I, show motor abnormalities and progressive loss of dopamine neurons in aged animals. One of the most successful etiological models is the MitoPark mouse, which recapitulates many facets of the disease besides locomotor deficits and loss of dopamine neurons, such as certain aggregates, gastrointestinal dysfunction, and alterations in the microbiota observed in the early stages of PD (Ekstrand and Galter 2009). In addition, they respond to levodopa treatment and thus are very useful in preclinical testing of treatments for PD. One interesting, less studied model in the context of PD are conditional Dicer knockout mice which develop robust nigrostriatal degeneration (Pang et al. 2014; Chmielarz et al. 2017). The GWAS-based models have suffered from the fact that the variants are not penetrant enough to cause significant pathology. The best option would be to find the highest risk variants by determination of PRS and modify multiple variants in a mouse or

preferably create humanised mice that would express the human variants so the pathology would most closely resemble that of the human.

In addition to the genetic models, overexpression models, using viral vectors and injected proteins, have also been implemented (Albert et al. 2017) (Figure 6). Mostly these have focused on α-synuclein although certain other proteins could be of use but have not been as widely studied in modelling PD, e.g. mutant Parkin overexpression which has shown progressive degeneration of dopamine neurons in the rat SN (Van Rompuy et al. 2014). Some of the most used models are the AAV-based overexpression of α-synuclein or injection of α-synuclein preformed fibrils (PFFs) into the brains of animals (Decressac et al. 2012; Albert et al. 2017). PFFs are produced for monomeric α-synuclein and can seed endogenous α-synuclein to aggregate and spread (Luk et al. 2012). These models show loss of TH in the SN and may cause some behavioural changes but many of the other measures are not consistently observed, such as reduction in dopamine release or TH in the striatum or correlation between the levels of α-synuclein, TH, and motor behaviour (Albert et al. 2017). Combining AAV-mediated overexpression of α-synuclein and injection of PFFs in the SNpc elicits a rapid development of PD-like pathology with decreased dopamine levels, progressive loss of dopamine neurons, and impaired motor behaviour, which seems to be the most replicable approach when using exogenous α-synuclein to model PD (Thakur et al. 2017).

Surprisingly, the GWAS-based mouse models have not been successful in recapitulating human PD pathology, while the etiological models seem to replicate these features more prominently supporting their use in preclinical studies assessing the efficacy of new therapies (Airavaara et al. 2020). However, an important consideration in using any model is the stage of the disease to be modelled. With toxins, the size of the lesion can be controlled to study the late or end-stage of the disease but with genetic models, the early-stage phenomena attributed to the disease can be modelled and thus they can serve as good models to study preventative therapies.

Cellular models are also highly used in modelling PD (Figure 6). The advantages of using *in vitro* cellular models are that large quantities of data can be produced in a short amount of time, with relative ease and reduced costs compared to animal modelling (Eglen et al. 2008; Kepp et al. 2011; Linsley et al. 2019). Cell cultures can be well-controlled and easily manipulated and they also decrease the use of animals, particularly when using immortalised cell lines or stem cells. Combining microfluidics, automated cell culturing and microscopy with ML-based image analysis, a

vast amount of multimodal data can be acquired both for studying pathogenesis and for drug discovery (Bassil et al. 2021). Cellular models utilise the same ways to induce PD pathology as previously mentioned: toxins, genetic methods, and overexpression or induction of pathology-associated proteins.

Immortalised cell lines, such as SH-SY5Y, PC12, and MN9D cells have been used to model PD (Skibinski and Finkbeiner 2011; Airavaara et al. 2020). These cells are of neuronal origin and can be relatively easily differentiated into dopaminergic cells, such as treating the neuroblastoma cells with retinoic acid and BDNF, or they have dopaminergic features. However, they do not fully recapitulate dopamine neuron features such as the spontaneous pacemaking activity. Moreover, immortalisation causes the cells to have enhanced and altered proliferative or growth properties not seen with postmitotic dopamine neurons within organisms in their native context and, as such, contribute to issues on translatability. The advantage of using these cell lines is their scalability, genetic malleability, and availability. The cells can be expanded almost limitlessly and nearly all assays can be used with them as there is never a shortage of samples.

Primary cells derived from rodent brains are commonly used to model PD *in vitro* (Rayport et al. 1992; Eglen et al. 2008). Cultures are most commonly done from embryonic or early postnatal stages. Adult animal-derived primary 2D cultures are not as widely used due to lower viability, and 3D tissue or slice cultures are alternatively implemented. Postnatal and adult neurons have the advantage of maturity and increased physiological relevance toward PD as it mainly affects aged neurons (Rayport et al. 1992; Skibinski and Finkbeiner 2011). They are highly susceptible to insults and when cultured for longer periods they exhibit electrophysiological activity which, taken into account the dopaminergic pacemaking activity, is important to account for all metabolic alterations that the neurons may encounter (Rayport et al. 1992; Lautenschlager et al. 2018). However, they have reduced survivability and are demanding to culture for long periods. Furthermore, efficient gene transfer cannot be achieved as readily as in immortalised cells, and isolation of material only from these cells would require sorting as the cultures are always heterogenous containing other neurons, glia, and other cells, depending on from which developmental stage they are cultured. As material may be limited due to the use of animals for studies, and high dopaminergic neuron yielding cultures are difficult to produce, these cultures are pertinent for single-cell analyses using e.g., immunofluorescence and automated imaging methods (Chmielarz et al. 2017; Chmielarz et al. 2020)

Although primary hippocampal cultures have been implemented successfully to model the progression of LBs, for instance, by treating the neurons with α-synuclein PFFs for 3 weeks, the use of dopamine neurons would have better relevance (Mahul-Mellier et al. 2020). The use of embryonic dopaminergic cultures has been established for modelling PD but postnatal or adult dopaminergic cell culturing protocols, are not routinely used in combination with α-synuclein PFFs to model PD (Chmielarz et al. 2017; Albert et al. 2021). The advantage of postnatal and adult cultures are in the maturity and the possibility to do cultures from different areas of the midbrain (Lautenschlager et al. 2018). In optimal models for comparative studies, subsets of dopamine neurons should be cultured, e.g., VTA and SN dopamine neurons, and the underlying pathology of interest modulated within these neurons.

The most recent advances, however, have been in utilising iPSC-derived dopamine neurons and midbrain organoids (Skibinski and Finkbeiner 2011; Smits et al. 2019; Boussaad et al. 2021). With good differentiation protocols, specific neuronal subtypes can be grown, and midbrain organoids show structural architecture resembling the human midbrain which can be used to model network effects. Translatability is already increased due to the human origin and iPSC-derived dopamine neurons have shown to be vulnerable to insults not observed in rodent-derived dopamine neurons. However, using PFFs and other α-synuclein strains in these models, significant differences in aggregation have been observed which may suggest that these cultures need optimisation for successful modelling of PD based on α-synuclein (Tanudjojo et al. 2021). Furthermore, they are expensive and require cumbersome protocols to obtain and can have high variability between differentiations requiring isogenic controls, all of which reduce the widespread and reliable implementation of using these cultures to model PD.

Regardless, the best practice so far, as suggested with animal modelling, would be to find and stratify the idiopathic PD patients with the highest PRS, collect samples from these patients, and produce iPSC-derived organoids or cells affected in the disease (mainly dopamine neurons, but preferably other cells too such as astrocytes and microglia) (Lang et al. 2019). Then use the iPSC-derived cells or organoids to screen for potential new compounds and confirm biological activity and efficacy in animal models that most closely model the pathway-associated degeneration, i.e. mice genetically edited to express the high-risk variants.

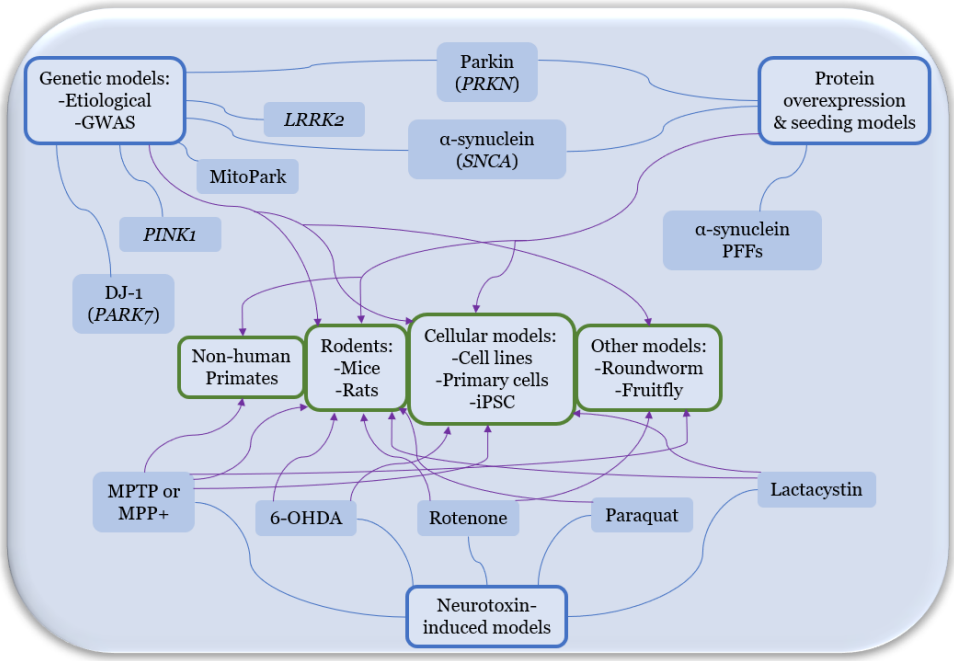

Figure 6. Parkinson's disease *in vitro* and *in vivo* models. Arrows indicate the most widely used models in different cellular and animal models. 6-OHDA: 6-hydroxydopamine, DJ-1: protein deglycase DJ-1, GWAS: genome-wide association study, iPSC: induced pluripotent stem cell, *LRRK2*: leucine-rich repeat kinase 2, MPP+: 1-methyl-4-phenylpyridinium, MPTP: 1-methyl-4-phenyl-1,2,3,6-tetrahydropyridine, *PARK7*: gene encoding DJ-1, PFF: preformed fibrils, *PINK1*: PTEN-induced putative kinase 1, *PRKN*: gene encoding parkin, *SNCA*: gene encoding α-synuclein.

2.3.2 Assessing the efficacy of therapeutics in preclinical models of Parkinson's disease

The endpoints used to measure whether a therapeutic intervention is regarded as efficacious are highly important to classify and define thoroughly before engaging in an experiment (Merchant et al. 2019). A very common battery of tests is to first use cell models and reporter assays to study the efficacy of the interventions (Hughes et al. 2011). After this, in animal models, efficacy is further demonstrated by various behavioural and cellular or biochemical methods which show improvements in the animal's behaviour from the insult and biochemical markers or readings

from alterations in the brain chemistry. This is done by measuring either the change in neurotransmitters or the cells producing them.

To assess neuroprotective and/or neurorestorative effects, a combination of methods needs to be used to show effects on the cellular level and improvements in functionality through behavioural analysis (Bjorklund et al. 2000). Since PD has very clear behavioural effects with regard to motor functions which can be attributed to the nigrostriatal system, animal models and behavioural analysis have been relatively easy to implement to study the progression and reversal of neurodegeneration. Using various insults to cause lesions in the nigrostriatal system, there is a clear change in the behaviour of the animals which can be assessed by different tests (Asakawa et al. 2016). The most used tests are drug-induced rotations, the cylinder test, the rotarod, and the staircase test. Other, not as commonly used tests include the open field, elevated body swing test, tail suspension swing test, stride length test, pole test, stepping test and balance beam. The alterations in behaviour measured in the rotation test, cylinder test and rotarod correlate with the loss of dopamine to the striatum and/or loss of dopamine cell bodies in the SN (Iancu et al. 2005). However, as previously mentioned, this may not always be the case and critical evaluation of the usefulness of the tests should be revisited and refined accordingly, or novel and better tests developed (Bjorklund and Dunnett 2019).

Since the nigrostriatal system controls motor behaviour, neurodegeneration can be approximated with animal behavioural deficits, therefore efficacy in PD is measured by the reduction or alleviation of motor symptoms in animals and functionally with biochemical or histological methods, such as increases in dopamine or dopamine neuronal markers (Kirik et al. 1998). Currently, the only way to measure neuroprotection and/or neurorestoration is using a model that causes distinct PD-like symptoms and pathology, and treatment protocols that aim to either prevent (administer before the onset of pathology/symptoms) or restore (after the pathology/symptoms appear) them, and then analysing it with behavioural and functional assays (Bjorklund et al. 2000; Asakawa et al. 2016). However, as most neurorestorative experiments model late stages of PD, for example, when causing a full lesion of the nigrostriatal tract, most optimal experiments would be something in between neuroprotection and neurorestoration, where the modelling of the disease would be in its mid-stages. As early-stage diagnosis for PD is currently not possible and the late or end-stage patients are more difficult to treat, these mid-stage 'neuromodulatory' experiments would be best for studying potential disease-modifying

interventions. To fully conclude neurorestorative effects, behavioural recovery must correlate with dopaminergic striatal innervation or dopamine concentrations in the striatum. These changes are usually assessed by measurements of dopamine concentrations in the striatum using e.g., high-performance liquid chromatography and immunolabelling of dopaminergic markers of the nigrostriatal areas (Figure 7). Most noteworthy markers are the previously mentioned TH, DAT, and VMAT2, and if there is a marked decrease in neurite densities or cell numbers positive for any or all of these markers, that usually points to a loss of dopaminergic phenotype or cell death (Bjorklund and Dunnett 2007; Tenenbaum and Humbert-Claude 2017). Histological assessments should take into account that the spatiotemporal expression levels of individual markers can vary as their regulation depends on a multitude of factors and thus a combination of markers should be used for definitive conclusions (Kumer and Vrana 1996). Studies have shown that loss of neurites or cell bodies can occur without any behavioural deficits, which either means that this loss was not properly quantified using appropriate measures or markers, or that the loss is not significant enough, as substantial depletion of dopamine or loss of neurons in the nigrostriatal tract is needed to cause severe motor behaviour impairments (Decressac et al. 2012). Alternatively, if a study were to show behavioural improvements but no effects on cellular or biochemical outcomes, then it cannot be concluded that the improvements were due to direct effects on the nigrostriatal tract, but more likely some other reason.

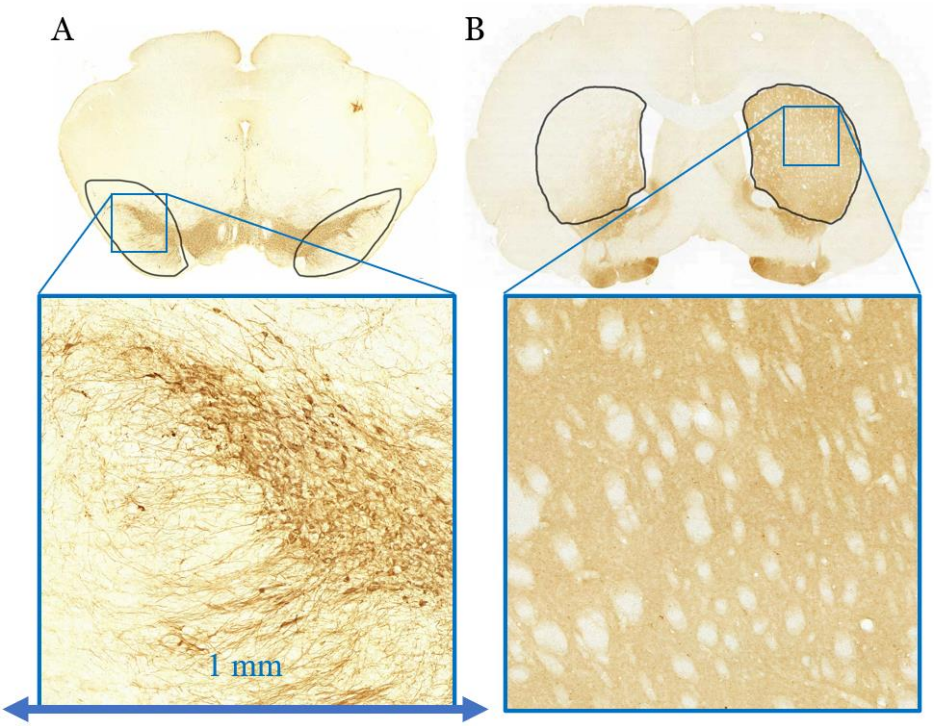

Figure 7. Rodent brain sections stained to visualise dopaminergic neurons using antibodies against tyrosine hydroxylase and an avidin-biotin-peroxidase complex followed by a 3,3'-diaminobenzidine reaction**.** The region marked with black demarcates the substantia nigra (**A**) and the striatum (**B**) with zoomed-in views of specified areas showcasing the dopamine neurons and the dopaminergic fibres in the respective brain areas. Note the lesioned (left) and non-lesioned (right) sides of the striatum with differences in staining intensities. Scale bar (1 mm) is an approximation.

In cellular models, as inducing the pathology is similar to *in vivo* models, efficacy measurements are also the same, that is measuring dopamine concentrations or counting the number of dopamine neurons and assessing their viability by looking at their morphological characteristics, e.g. neurite length and pathological markers within them, e.g. α-synuclein inclusions or various stress markers (Albert et al. 2021; Dagra et al. 2021). In neuronal cultures with spontaneous electrical activity, recording of the electrical activity can also be measured to assess functionality and restoration of the electrophysiological capabilities of the neurons.

Considering which methods to use to assess outcomes is highly important, especially from a drug development perspective. It is very important to consider the mechanism of action (MoA) of the studied drug candidate and its known effects in choosing the best model and outcome measures. For example, if the MoA is targeting a specific aspect of PD pathophysiology, such as α-synuclein it is important to assess the drug's effects on this measure (Merchant et al. 2019). In human trials, proof of principle and proof of concept studies can be well-defined due to better outcome measures, at least with regards to scores in behaviour or clinical improvement, however, in preclinical α-synuclein-based animal models, it can be difficult. Large heterogeneity in animal behavioural and functional deficits with a minor correlation between behaviour, amount of α-synuclein, and loss of dopaminergic markers has been reported and, as such, using typical measures, used with the toxin models are not appropriate (Airavaara et al. 2020; Oliveira et al. 2021). Thus other, possibly new, methods and behavioural assays should be used. In addition, models implementing α-synuclein PFFs, have demonstrated contradictory results, with some studies showing dopamine neuron death and others not (Luk et al. 2012; Albert et al. 2021). However, if the MoA is not of focus, as it does not need to be known for a drug to be deemed efficacious, any model which recapitulates the behavioural deficits and loss of dopamine neurons should suffice in assessing efficacy regardless of alterations in other pathological features.

An example of a drug approved for the treatment of PD, the MAO-B inhibitor safinamide, has the following preclinical efficacy profile. In *in vitro* studies, it was shown that in rat liver homogenates the IC50 value (which means the concentration required to inhibit 50% of MAO-B enzyme activity) was 0.250 μM after 2 min of pre-incubation and 0.14 μM after 60 min, but MAO-A was not affected even in high micromolar concentrations (Benedetti and Dostert 1994). The IC50 and MAO-B selectivity were also assessed in human platelet-rich plasma, in addition to the brain and liver mitochondria of human and rat tissue. The selective, reversible and dose-dependent inhibition of MAO-B by safinamide was also demonstrated in mice and cynomolgus monkeys (Caccia et al. 2006). Oral administration in mice inhibited MAO-B in a dose-dependent manner, but not MAO-A substantially. The reversibility was shown in mice treated with 20 mg/kg (i.p.) safinamide and sacrificed at different times between 0-24 h. Maximum inhibition of MAO-B was observed 1 h after administering and it reduced significantly after 4 h. In monkeys, two different doses (10 and 20 mg/kg) were attributed to 27 and 48% respective increases in dopamine levels after 24 h of administration with

reduced levels of MAO-B in the striatum. A study examining chronic administration over 39 weeks at doses of 0, 3.2, 8 and 20 mg/kg of safinamide in monkeys also showed a dose-dependent increase in dopamine and no evidence of tolerance to the treatment.

Besides these, the efficacy of safinamide was further studied in two different models of PD, the MPTP and 6-OHDA model (Caccia et al. 2006). In mice treated with MPTP safinamide increased brain dopamine levels by 60% when co-administered with levodopa and benserazide. It also inhibited microglia and pre-treatment provided non-dopaminergic neuroprotection showing that it prevented neuronal death, by counting neurons in the SN, but did not affect dopamine levels in the striatum. In MPTP lesioned macaque monkeys, pre-treatment also inhibited levodopa-induced dyskinesia (Gregoire et al. 2013). In 6-OHDA-lesioned rats, 25 mg/kg levodopa treatment for 28 days decreased rotational behaviour, and safinamide administered on day 29 concomitantly with levodopa, reversed the effect on rotations of levodopa (Caccia et al. 2006). Reduced microglial activation and protection of SN dopamine neurons was also demonstrated in 6-OHDA-lesioned rats by treating the animals for 7 days with safinamide (Sadeghian et al. 2016). Based on these studies the potential of safinamide for treating PD was realised and warranted testing of safinamide in clinical trials.

Due to the low translatability of preclinical studies to clinical studies, there are numerous examples of drugs that have shown potential in preclinical studies demonstrating efficacy but ultimately failed to show similar therapeutic effects in humans (Elkouzi et al. 2019; Prasad and Hung 2021). One such example is exenatide, a glucagon-like peptide-1 agonist, which in preclinical studies demonstrated disease-modifying potential by delaying or even reversing nigral lesions but did not conclusively demonstrate more than symptomatic relief in a human trial (Harkavyi et al. 2008; Athauda et al. 2017). Hence, preclinical efficacy assessment should be improved by better disease models and methods to assess efficacy outcome measures.

2.3.3 Cell counting and neuromorphometrics

Cell counting has been an essential part of biological research since the discovery of the microscope. Counting can be done by multiple different methods, from manual counting using microscopes, to counting from images or flow cytometry from homogenates or various other biochemical

assays, however, microscopy and imaging are very widely used and thus further covered from hereon. The first instances of accurate methods to estimate cell numbers were described in the late 1800s, and in 1946 refined by Abercrombie (Abercrombie 1946). Then in 1961 the term stereology was coined and became a very prominent method in neuromorphometrical studies with methods being continuously developed, and in 1991 West demonstrated an unbiased stereological method for efficient quantification of neurons (Sterio 1984; West et al. 1991). Multiple studies have been conducted to quantify cell loss in PD using observational, computer-assisted, and stereological methods (Giguere et al. 2018). The most consistent results supporting the finding that motor symptoms of PD appear when approximately 30% of total SN neurons are lost compared to age-matched controls have been acquired using stereological approaches.

For unbiased quantification of cells in a 3D environment, unless counting all cells by exhaustive methods, systematic random sampling, and equal probability assuming counting rules need to be implemented (Sterio 1984; Gundersen 1986; West et al. 1991; Boyce et al. 2010). In large tissues with numerous cells, such as the brain or its areas, it is not feasible to count all cells and thus other methods must be used. This can be achieved by design-based stereology. Stereology is defined as statistical inference of geometric parameters from sampled data, which in practice utilises the aforementioned sampling and counting methodology. Sampling is commonly done using the optical fractionator, which patterns unbiased virtual counting spaces, with uniform distance, covering the entire region, enabling all parts of the region to be counted with equal probabilities. Counting is commonly conducted using an unbiased 3D probe, with a defined volume, called an optical disector allowing cell estimates regardless of spatial and morphological characteristics. Hence, stereology is a way to obtain unbiased quantitative data on estimations of cell numbers without having to count the whole volume of the tissue. However, like any method, stereology suffers from drawbacks, the pivotal one being that it is very time-consuming. Thus, stereology has been developed and refined throughout the years and automated platforms and programs for sampling and counting have been implemented (Schmitz and Hof 2005). Commercial stereology set-ups have reduced worktime but require specialised microscopes and software, such as the StereoInvestigator. However, counting accuracy is similar to stereology done using standard light microscopes and free access software (Ip et al. 2017). Stereological methods are continuously improved and newer methods have been developed and optimised, such as the automatic optical disector and proportionator (Keller et al. 2013; Mouton et al. 2017). These have

improved the workflow and reduced the counting time. Nevertheless, there is always room for improvement and finding ways to streamline the work, reduce bias between users, and make it even faster is a worthy endeavour.

Besides counting, morphometric measurements, i.e. the shape or size of a tissue, a cell, organelle or biological structure, are utilised (Khudoerkov et al. 2014). For morphometric assessments, measuring pixel lengths and intensities is used when quantifying biological imaging data (Boutros et al. 2015; Caicedo et al. 2017). Using immunolabelling and different staining methods, the stained molecules emit light in different wavelengths with, or without, excitation using lamps or lasers. The more of the stained compound there is in the sample the higher the amount of light will be emitted and recorded by the camera used within microscopes. This serves as a good proxy on the volume covered by the stained material or amount, if the labelling is done specifically, i.e. with antibodies, and thus, morphometrics are used to estimate changes in levels of the antibody-targeted biological molecule of interest. Pixel intensities are usually measured using various programs, such as FIJI/ImageJ.

Densitometric measurements have been used in biological research for over 40 years since computer-assisted image analysis was introduced to biological research (Cassell et al. 1982). Optical density measurements were applied to PD research in 1990 when Burke et al. demonstrated that two measures – per cent area of staining and average optical density – measurements of TH+ fibres in the striatum of 6-OHDA treated rats could reliably provide a relative indication on the extent of fibre innervation (Burke et al. 1990). The optical density is based on the numeric pixel intensity values from images. Using the rotation assay they showed that apomorphine induced rotations in animals when the area measured was 2% or less than the control side or density was 15% or less. They compared these results to biochemical assays of TH which had similar results showing rotations when activity was reduced to 10% or less. Based on these findings they concluded that the average optical density measurements were sensitive and could be used to approximate striatal TH+ innervation. Since then, it has been widely used in preclinical PD studies in combination with counting TH+ cell numbers from the SN to biochemically assess nigrostriatal degeneration, neuroprotection and/or neurorestoration (Kirik et al. 1998; Bjorklund et al. 2000; Lindholm et al. 2007; Penttinen et al. 2016; Runeberg-Roos et al. 2016). However, depending on other measures of interest, striatal dopamine measurements are also used, in case biochemical stainings are not needed for another reason or the focus is on alterations in the dopamine neurochemistry.

2.3.4 Quantitative analyses using machine learning

Artificial intelligence encompasses all research studying intelligence that aims to mimic human intelligence or is used as a term to classify machines aiming to do this. A subset of artificial intelligence research is the study of mathematical models, more specifically computing algorithms, which have the capacity to learn. When used with computer systems, this field of study is called machine learning (ML). ML is mainly based on various regression algorithms that comprise of four main components: inputs, weights, a bias or threshold, and an output. One subset of ML algorithms that have been heavily studied is neural networks, which have been inspired by studying the function of biological nervous systems, i.e. trying to mimic the human brain (McCulloch and Pitts 1990). The difference between neural networks and regression is that in regression changing weights can be done without affecting the other inputs in a function, whereas in neural networks, the outputs of a layer are passed on to the next layer of neurons in the network so any change may have cascading effects (LeCun et al. 2015; Jahn et al. 2020; Laine et al. 2021). Deep learning algorithms are neural network algorithms that have multiple hidden layers and convolutional neural networks (CNN) are specialised deep neural networks that perform mathematical convolution operations in their hidden layers. ML can be supervised or unsupervised. Supervised learning has labelled datasets, the input and output data, while unsupervised does not. Supervised learning is used in the classification or categorisation of data, and regression, which aims to understand a relationship between variables. Unsupervised learning is used in clustering, association, and dimensionality reductions. Clustering is used for grouping unlabelled data based on differences or similarities, useful, for example, in image segmentation. Association is trying to find relationships between variables that do not necessarily regress or cannot make predictions as with regression. Dimensionality reduction is used in reducing the features of a dataset when it is too high. The aim is to reduce inputs while preserving integrity to processable data, such as removing noise from images to improve quality.

ML has recently been implemented in the quantification of cells and other biological objects of interest (Patel and Goyal 2007; Mamoshina et al. 2016). The main advantages of using ML-based methods are automation and increased speed and accuracy. However, accuracy is highly dependent, not only on the learning parameters but more so on the ground truth, that is the bulk material (images or other data) that the ML algorithms are trained upon. If the data is incorrect or has artefacts, the algorithm can

learn the wrong things to find, so it is of utmost importance that the training set is right on all accounts. In this case, with a large enough training set and using unsupervised learning the ML algorithm can even find information that the human observer cannot. However, the caveat with using deep neural networks and unsupervised learning is in dissecting the parameters of what was learned and why, as the layers used in deep learning can get very complex. This is called the black box problem, knowing the input and output but not the process in between (Mamoshina et al. 2016; Laine et al. 2021). From a practical point of view, it may not matter how the algorithm has learned if it does what it was meant to do reliably, but from a scientific view, it would be important to know as then the learning could be further optimised and controlled to make it even better. Drug development serves as a good analogy. There are multiple efficacious drugs on the market for which the MoA is not fully known, such as the widely used analgesic paracetamol. However, knowing the precise MoA of a drug aids in developing better, safer, and more efficacious derivatives of the drug.

Automated microscopy and ML are ideal when studying cellular models of PD (Bakkar et al. 2017; Kraus et al. 2017). A considerable amount of data can be acquired using HTS utilising multiwell plates and automatic scanners in combination with ML-augmented imaging and analyses. There are multiple programs that implement ML for image analyses. Most publicly available image analyses software such as ImageJ have platforms and plugins to analyse images with ML. CellProfiler and CellProfiler Analyst are commonly used programs for high-throughput image analyses. The program can be used to identify objects, i.e., cells and cell structures, by segmenting them based on pixel size and intensity (Carpenter et al. 2006; Jones et al. 2008). They have been successfully used in PD studies for quantifying midbrain neuronal cultures. For example, counting TH immunoreactive dopamine neurons with α-synuclein positive inclusions (Chmielarz et al. 2020; Er et al. 2020; Albert et al. 2021).

2.3.5 Resources and databases

Plenty of useful resources such as databases, web portals, and interactive maps of PD-related information and research tools have been published and set up, however, the information on where to find them, i.e. their outreach, is lacking. As the number of PD models and omics data acquired from patients increases it will be more important to have good repositories

and databases for storing, sharing, and upkeeping the new information. This is done with many large-scale mapping studies but should also be done with any study that has large datasets, as a lot of important information may not be as easily available or accessible only through publications. Especially information-rich data such as gene expression patterns, protein interactions, and imaging data on morphological characteristics of neurons are invaluable for preclinical PD researchers, especially for those aiming to develop new drugs (Table 1).

Table 1. Useful resources and databases for preclinical PD researchers.

Resource/database	Link*	Publication
Allen Brain Atlas	https://mouse.brain-map.org/	(Lein et al. 2007)
Brain RNA-Seq	https://www.brainrnaseq.org/	Multiple
Fine Structure of the Aging Brain	https://www.bu.edu/agingbrain/introduction/	(Peters and Kemper 2012)
FOUNDIN-PD	https://www.foundinpd.org/	Multiple
Gene4PD: A Comprehensive Genetic Database of Parkinson's Disease	http://genemed.tech/gene4pd/	(Li et al. 2021)
Genetic variants associated with PD	https://www.omim.org/phenotypicSeries/PS168600	Multiple
Parkinson's Disease Genome-Wide Association Study Locus Browser	https://pdgenetics.shinyapps.io/GWASBrowser/	(Grenn et al. 2020)
Parkinson's disease map	https://pdmap.uni.lu/minerva/	(Fujita et al. 2014)
Parkinson's disease mouse model resource	https://www.jax.org/research-and-faculty/resources/parkinsons-resource#	Multiple
Proteome-scale measurements of human protein localisation and interactions	https://opencell.czbiohub.org/	(Cho et al. 2021)
Protein Atlas	https://www.proteinatlas.org/humanproteome/brain	(Uhlen et al. 2005; Uhlen et al. 2015; Sjostedt et al. 2020)
Ratlas: An MRI template of the Lister hooded rat brain with stereotaxic coordinates for neurosurgical implantations	https://www.nitrc.org/projects/ratlas-lham	(Prior et al. 2021)
Reactome pathway database	https://reactome.org/	(Gillespie et al. 2022)

*Accessed in January 2022

3 Aims of the study

The overall aim of this work was to develop, refine, and characterise new tools and tools already in use for preclinical studies on PD focusing on novel therapeutic development. In particular, the focus was on methods to quantify features of dopamine neurons, characterise them, and on the development and optimisation of reporter assays.

The specific aims of the study were:

1. Optimise and develop imaging-based quantitative methods for counting cells and measuring neuromorphometrics in animal models of PD (I and II)

2. Develop and characterise features of cell-based genetic reporter assays for a therapeutic drug target for PD (III and IV)

3. Provide ultrastructural insight of dopaminergic neurons *in vitro* to be used in neuropathological modelling of PD (V)

4 Materials and methods

The methods used in the publications and manuscript (I-V) and the contribution of the author are listed in Table 2. The main methods used by the author to produce the results reported in this dissertation are briefly described. More detailed descriptions of materials, methods, and procedures can be found in the original publications and manuscript.

Table 2. Methods and author (I.P.) contribution

Method	Original publication	Author contribution
Molecular		
Molecular cloning	I, IV	IV
Viral vectors (production)	I, III, IV	IV
RNA interference	IV	IV
Luciferase assay	III, IV	IV
cDNA production	III	III
Quantitative PCR	III	
Genotyping	V	
Cell culture		
Mammalian cell lines	III, IV	IV
Mouse primary neuronal cultures (cortical III midbrain V)	III, V	V
Transfection of cells	III, IV	IV
Production of stable cell lines	IV	IV
Animal		
Stereotaxic injections	I, II, III	I, II, III
Tissue processing	I, II, III	I, II, III
Pharmacological treatments	I, III, IV	I, III, IV
Behavioural		
Cylinder test	I	I (unpublished)
Rotation assay	I	I (unpublished)
Immunological methods		
Immunohistochemical staining	I, II	I, II
Immunocytochemical staining	IV	IV
ELISA	I	
Imaging		
Confocal microscopy	I	I
High-content image analysis	IV	IV
Fluorescence microscopy	IV, V	IV, V
Transmission electron microscopy	V	
Quantitative image analysis	I, II, IV	I, II, IV
Statistics	I, II, III, IV	I, II, IV

4.1 Experimental animals

Female NMRI mice, male TH-GFP (Tg(Th-EGFP)DJ76Gsat/Mmnc, C57BL/6NHsd background), and male Wistar rats (Harlan/Envigo, Horst, the Netherlands) were housed at a 12 h light-dark cycle, with water and food *ad libitum*. The well-being of the animals was observed on a regular basis. All animal experiments were approved by the Finnish National Board of Animal Experiments (license numbers: ESAVI/13959/2019, ESAVI/7812/04.10.07/2015) and performed according to the European legislation (EU directive 2010/63/EU) and local laws and regulations [Finnish Act on the Protection of Animals Used for Scientific or Educational Purposes (497/2013) and Government Decree on the Protection of Animals Used for Scientific or Educational Purposes (564/2013)].

4.2 Stereotaxic injections and administration of drugs

Stereotaxic surgeries were performed under isoflurane anaesthesia (4% induction and 2.5% maintenance) using a stereotaxic frame (Stoelting Co., USA) and post-operative analgesic carprofen was administered (5 mg/kg, s.c.). Animals were randomly allocated to treatment groups for the viral vector injections. 4.5 µl of scAAV1-pre-α-pro-GDNF, scAAV1-pre-β-pro-GDNF or scAAV1-eGFP was equally distributed to three sites in the right striatum. The injection coordinates according to bregma were (1) A/P +1.6 L/M −2.8 D/V −6.0 from the skull, A/P 0.0 L/M −4.1 D/V −5.5 from the skull, and 3) A/P-1.2 L/M −4.5 D/V −5.5 from the skull. Injections were done at a 10° angle at a rate of 0.5 µl/min. The microinjection needle was kept in place for an additional 5 min to avoid the backflow of the solution. For study III, three weeks later 3 × 2 µg of 6-OHDA (Sigma Aldrich, St. Louis, MO) was injected into the same sites as the viral vectors to induce a partial lesion of the nigrostriatal pathway. A single injection of saline (s.c.), methamphetamine [(+)-Methamphetamine hydrochloride; Sigma-Aldrich, St. Louis, MO, USA] (Meth, 2.5 mg/kg, s.c.), dimethyl sulfoxide (DMSO, i.p.) or a combination of levodopa (L-3,4-Dihydroxyphenylalanine methyl ester hydrochloride, Sigma-Aldrich, St. Louis, MO, USA) (LD, 10 mg/kg, i.p.), carbidopa (Sigma-Aldrich, St. Louis, MO, USA) (CD, 30 mg/kg, i.p.) and entacapone (Sigma-Aldrich, St. Louis, MO, USA) (ENT, 10 mg/kg, i.p.) diluted in DMSO (vehicle) was administered 31 weeks after 6-OHDA (34 weeks after AAV-injections).

4.3 Tissue processing

In brief, for immunohistochemistry and immunofluorescence, the animals were deeply anaesthetised with sodium pentobarbital (100 mg/kg) and perfused transcardially with phosphate buffered saline (PBS) and 4% paraformaldehyde (PFA). The removed brains were postfixed overnight in 4% PFA at 4°C and stored in 20% sucrose in PBS at 4°C. The brains were taken out of the sucrose solution, frozen briefly at -80°C and cut into 40-µm-thick coronal sections with a cryostat at -20°C (Leica CM3050, Leica Biosystems, Germany). The sections were stored in a cryoprotective buffer at −20°C until continuing with staining.

For quantitative real-time polymerase chain reaction analyses of GFP and α-GDNF messenger RNA (mRNA) levels, rat brain samples were collected 2, 4, and 8 h after saline, Meth or LD+CD+ENT injections by euthanising them with CO_2, extracting the brains and snap-freezing them in dry ice-cooled isopentane. After this, the striatum was collected and RNA was extracted using the RNAeasy Mini kit (Qiagen GmbH, Hilden, Germany) according to the manufacturer's instructions. RNA was quantified with a NanoDrop ND-1000 Spectrophotometer (NanoDrop Technologies, Wilmington, DE, USA) followed by cDNA synthesis using reverse transcription and the protocol provided in the Super-Script III first-strand synthesis kit by the manufacturer (Invitrogen, Carlsbad, CA, USA).

4.4 Immunohistochemistry and immunofluorescence

For colourimetric optical density analysis and cell counting, endogenous peroxidase activity was quenched in the free-floating sections with 0.3% hydrogen peroxide (Sigma Aldrich) and incubated with 2% normal goat serum and 0.3% Triton X-100 (mouse) or with 4% bovine serum albumin (BSA) and 0.1% Triton X-100 in PBS (rat) for 1 h at room temperature (RT). Next, the sections were incubated overnight with anti-TH antibody (for mouse sections polyclonal rabbit anti-TH, MAB152 and rat sections monoclonal mouse anti-TH MAB318, Millipore, Billerica, MA, both 1:2000) at 4°C, followed by incubation with the biotinylated secondary antibody (anti-rabbit or anti-mouse, both 1:200, Vector Laboratories, Burlingame, CA) for 1 h at RT. The staining was visualised with 3,3'-diaminobenzidine (DAB) adhering to the manufacturer's instructions (Vectastain ABC peroxidase kit, Vector Laboratories).

For infrared optical density analysis, the sections were incubated with blocking solution (4% BSA and 0.3% Triton X-100 in PBS) for 1 h followed by 1 h incubation with the first primary antibody (mouse anti-TH, MAB318, 1:2000) at RT. After this, the second primary antibody (rabbit anti-GFP, A11122, 1:2000 or goat anti-GDNF, AF-212-NA, 1:1000) was added and the sections were incubated at 4°C overnight. The next day, sections were incubated in anti-mouse IRDye® 800CW secondary antibody for 15 min, and after this, the 2nd secondary antibody (anti-goat or anti-rabbit IRDye® 680RD all secondary antibodies 1:2000, LI-COR Biosciences, Lincoln, NE) was added and both incubated for a total of 1 h at RT. The sections were rinsed with ddH2O for 5 min at RT, before mounting them onto glass slides using Vectashield HardSet Antifade Mounting Medium with DAPI (H-1500; Vector Labs, Burlingame, CA).

4.5 Optical density measurements of striatal tyrosine hydroxylase-positive fibres

For the colourimetric analysis, digitised images of rat brain sections were acquired using a whole slide scanner (Pannoramic P250 Flash II, 3DHistech Ltd., Hungary) with extended focus at a resolution of 0.22 µm/pixel. The images were converted to 8-bit greyscale and colour inverted. The striatum was outlined, and the average optical densities (pixel intensities) of TH+ fibres were measured with ImageProplus (Media Cybernetics, Inc., Rockville, MD) from six adjacent sections per animal. Nonspecific background staining was measured from the corpus callosum and these values were subtracted from striatal measurements. The optical density values measured from the 6-OHDA-lesioned or AAV-injected striatum were divided by the values from the intact striatum. The data are presented as a percentage of the intact side.

For the infrared analysis, the sections were scanned with Odyssey Infrared Imaging System (LI-COR Biosciences, Lincoln, NE) with 42-micron resolution. The average optical density of TH+ fibres from the injected and intact striata of four rat brain sections per animal was measured using the Odyssey Infrared Imaging System software without image manipulations. Nonspecific background staining was measured from the cortex or corpus callosum. Then the values from the AAV-injected striatum were divided by the values from the intact striatum, both subtracted for background staining, as was done in the colourimetric analysis. The data are presented as a percentage of the intact side.

4.6 Cell counting using deep neural network algorithms

Deep convolutional neural network (CNN) -based algorithms were trained using supervised learning in a cloud-based image analysis platform provided by Aiforia Technologies Oy, Finland. The final CNN algorithm was trained to recognise TH+ neuron cell bodies from the digital images. The algorithm was trained with 77 megapixels of imaging data and a total of 1,254 TH+ cell bodies to recognise them. The algorithm consisted of two layers, of which the first layer segmented the TH+ neuron bodies and the second layer counted the individual TH+ cell bodies within the first layer. Images of the mice and rat coronal brain sections were acquired similarly as was done with the colourimetric assessment of optical densities using the same whole slide scanner. The extended focus renders the whole section depth in a single focal plane with a total depth of 10 µm. The acquired digitised images were uploaded into the Aiforia™ image processing and management platform and the regions of interest, in this case, the SN of both hemispheres, were outlined from 6-9 sections from each animal brain. Counts using the algorithm were summed and validated by comparing counting to manual counts and counting obtained by stereological assessment using the optical fractionator method.

4.7 Cloning of reporter plasmids

Three different main plasmid constructs were produced and a transfer plasmid for producing lentiviral vectors. The three main plasmids are psiCHECK-CMV-siRNA1-pA-SV40-mCherry-NLS-pA-HSVTK-EGFP-pA, psiCHECK-CMV-miR19b-pA-SV40-mCherry-NLS-pA-HSVTK-EGFP-pA and additionally miR27a instead of miR19b and psiCHECK2_sec_miR19_1xsp and the transfer plasmid pCDH-SV40-Tomato-miR27a-HSVTK-EGFP-WPRE based on the pCDH backbone. psiCHECK-CMV-siRNA1-pA-SV40-mCherry-NLS-pA-HSVTK-EGFP-pA and psiCHECK-CMV-miR19b-pA-SV40-mCherry-NLS-pA-HSVTK-EGFP-pA were stably transfected into FLP-IN 293 T-Rex cells (Thermo Fisher, #R78007) which enable genomic insertion into a specific locus using the Flippase enzyme. This locus also has a tet-ON element which enables the expression of the transgenes to be activated by tetracycline or derivatives such as doxycycline.

All cloning was done in a similar manner using restriction enzymes to digest plasmids and obtain desired linearised fragments or polymerase chain reaction (PCR) amplification to acquire amplicons performed with Phusion Hot-Start DNA polymerase (ThermoFisher Scientific, Waltham, MA). All linearised fragments or PCR amplicons were always purified by electrophoresis of the restriction reaction mixture in a 1% agarose gel, cutting out the linearised DNA containing band or amplicon, and extracting the DNA from the gel by using a gel-extraction kit (Macherey-Nagel, Düren, Germany) according to the manufacturer's protocol. Then they were either ligated using T4 DNA ligase (ThermoFisher Scientific, Waltham, USA) incubating the mix for 60 min at RT or recombined in a single In-Fusion (In-Fusion® HD Enzyme Premix, Clontech, Mountain View, USA) reaction for 15 min at 50°C (Irwin et al. 2012). The specific plasmids, restriction enzymes and primers used can be found in the original manuscript. All intermediate and final plasmids were assessed by diagnostic restriction enzyme digestion with gel electrophoresis to have correct fragments and confirmed to have correct inserts with sequencing.

4.8 Cell culture, transfections, and drug treatments

Human embryonic kidney (HEK293T) cells and FLP-IN 293 T-Rex (T-Rex) (ThermoFisher Scientific, Waltham, MA) cells were maintained in a humidified incubator (37°C, 5% CO_2, saturated humidity, RH 80-100%) in Dulbecco's modified eagle medium (DMEM, pH 7.4) supplemented with 10% fetal bovine serum (FBS) and 100 µg/ml Normocin™ (InvivoGen, San Diego, USA). Cells were re-plated into Greiner CellStar 96-well clear-bottom cell culture plates for a density of ca. 10000 cells/well in DMEM, pH 7.4 supplemented with 10% FBS and 100 µg/ml Normocin and incubated at 37°C, 5% CO_2 for 24 h before transfection or administration of compounds in all assay validation experiments.

T-Rex cells were transfected simultaneously with 1 µg of pTO-GW-FRT-CMV-siRNA1-mCherry-WPRE-EGFP, pTO-GW-FRT-CMV-miR19b-pA-SV40-mCherry-NLS-pA-HSVTK-EGFP-pA or pTO-GW-FRT-CMV-miR27a-pA-SV40-mCherry-NLS-pA-HSVTK-EGFP-pA, and 5 µg pOG44 (expresses the flippase enzyme to insert the pTO plasmid into a specific genomic region of the T-Rex cells) using 1 µg/µl polyethylenimine (4:1 ratio of PEI/DNA) diluted in OptiMEM (ThermoFisher Scientific, Waltham, MA). After 48 h the media was changed to DMEM supplemented with 10% FBS, 100 µg/ml Normocin, 15 µg/ml Blasticidin S HCl (Sigma-Aldrich, St.

Louis, MO, USA) and 100 µg/ml Hygromycin B (Sigma-Aldrich, St. Louis, MO, USA). Media was changed every 2-4 days for 14 days for selection of cells with the correct insertion, which was confirmed with fluorescence microscopy by detecting expression of mCherry or tdTomato and EGFP. Cells were kept in Blasticidin S and Hygromycin B containing media before validation experiments.

HEK293T cells were transfected with 100 ng of plasmid DNA (psiCHECK2_sec_miR19_1xsp, or psiCHECK2_sec_scramble), using 1 µg/µl polyethylenimine (4:1 PEI/DNA) in OptiMEM and serum-deprived changing the media to DMEM supplemented with 100 µg/ml Normocin.

After 24 h of transfection of the HEK293T cells, or 24 h of plating the stably transfected T-Rex cells, cells were treated with 10 ng/ml doxycycline hyclate (Cat#D9891, Sigma-Aldrich, St. Louis, USA, DOX, in ethanol) and 100 µM enoxacin sesquihydrate (Cat#94426 Sigma-Aldrich, St. Louis, USA, ENX, in DMSO).

4.9 Fluorescence quantification and luciferase assay

Live cells were imaged at RT at 24, 48, 72 and 120 h after administration of compounds. Imaging was done using Thermo Scientific CellInsight™ CX5 High-content screening (HCS) platform at ×10 magnification. Three to nine images per well were acquired, and fluorescence intensities were quantified with CellProfiler and CellProfiler analyst (Carpenter et al. 2006; Jones et al. 2008) using custom-tailored pipelines to detect and segment the cytosol and nuclei. Mean fluorescence intensity ratios per cell per well were calculated and, additionally, in transient transfection experiments, background fluorescence values were subtracted from non-transfected control cells.

After 48 h of treatments, cells were lysed, and the luciferase reaction was induced using the Dual-Glo® Luciferase Assay kit (Promega Corp., Madison, WI). Luminescence was measured with a plate luminometer (Victor3, Perkin-Elmer Corp., Waltham, MA) and luminescence ratios of Renilla and firefly luciferases were determined.

4.10 Postnatal ventral midbrain neuronal cultures

Primary cultures were prepared in part using the David Sulzer laboratory ventral midbrain culture "neuronal preparation" protocol (Lautenschlager et al. 2018). Ventral midbrains were dissected from the brains of 1-4-day-old TH-GFP transgenic mice, cut into pieces, and treated with papain for neurons solution for 10 minutes. The neuron-containing pieces were washed with SF1C or Neurobasal-A medium (NB-A) (Sigma-Aldrich St. Louis, MO, USA), triturated with a siliconised glass Pasteur pipette in NB-A, centrifuged for 5 min with 1000 rpm and cells were plated on various plates and dishes. The cells were maintained in SF1C supplemented with DiPorzio concentrate or NB-A medium (Gibco BRL Waltham, MA) supplemented with 2% B27 (Gibco BRL Waltham, MA), 40 µM L-glutamine (Sigma-Aldrich St. Louis, MO, USA), and 1% penicillin/streptomycin, and maintained in a humidified incubator (37°C, 5% CO_2, saturated humidity, RH 80-100%). On the following day, FDU-solution was added to the cultures for mitotic inhibition of the glia. Half of the culture media supplemented with FDU-solution was changed 3-4 days after seeding.

4.11 Correlative light and electron microscopy

The TH+ primary ventral midbrain neurons were first identified by GFP fluorescence using Zeiss Axio Vert A1 inverted light microscope for correlative light and electron microscopy (CLEM) equipped with a Hamamatsu ORCA-flash 4.0LT CMOS camera. After this, the cells were fixed after 5-7 days *in vitro* with 2% glutaraldehyde (Sigma-Aldrich St. Louis, MO, USA) in 0.1 M sodium cacodylate (NaCac) buffer, pH 7.4, for 20 min at RT, washed twice with NaCac buffer and postfixed with 1% reduced osmium tetroxide in NaCac buffer for 1 h on ice. Samples were further washed with NaCac buffer and dehydrated with varying concentrations of ethanol and acetone. The samples were infiltrated with Epon (TAAB 812) for 2 h prior to 14- h- polymerisation at 60°C. 60-nm or 100-nm thin sections were cut, placed on grids and post-stained with uranyl acetate and lead citrate. The cells were located on the grids based on the fluorescent images and transmission electron microscopy images were acquired using a Jeol JEM-1400 (Jeol, Tokyo, Japan) operating at 80kV equipped with Gatan Orius SC 1000B bottom-mounted CCD-camera (Gatan, Pleasanton, CA) with various magnifications.

4.12 Statistical analysis

Statistical analyses were performed using Prism versions 6-9 (GraphPad Software, Inc., La Jolla, San Diego, CA). Differences between three or more treatment groups were assessed using one-way analysis of variance (ANOVA). Student's two-tailed unpaired t-test was used when comparing two groups. Results are presented as mean ± SEM or mean ± SD. Statistical significance was considered when the p-value was <0.05. Cellular experiments were done in independent duplicates or triplicates.

Correlation between continuous variables was analysed using Pearson correlation. The performance metrics were evaluated by calculating precision (Precision = TP/(TP + FP), recall (Recall = TP/(TP + FN) and F1-score (F1-score = 2*Precision*Recall/(Precision + Recall) in comparing the neuron counts obtained by stereology and the algorithm. The number of true positive, false positive, true negative, and false negative neuron cell body counts were visually counted directly from the digital images.

5 Results

5.1 Optical density measurements of tyrosine hydroxylase-positive fibres in the striatum can be performed with infrared fluorometry (I)

We used a unilateral 6-OHDA rat model of PD to study the effects of GDNF isoforms. We assessed the biochemical effects of the isoforms to the nigrostriatal system in the model by estimating TH+ fibre density in the striatum in both non-lesioned and 6-OHDA-lesioned rats treated with either AAV-vectors expressing GFP or the GDNF isoforms; α-GDNF and β-GDNF. The quantification for estimating TH+ fibre density was done by measuring the optical density of the TH immunolabelled fibres (see section 4.5). Traditionally this has been done by a colourimetric method based on the immunolabelling of the fibres using primary antibodies targeting TH and biotinylated secondary antibodies which enable an avidin-biotin-peroxidase complex reaction with the DAB substrate, resulting in an observable brown colour (Figure 8B and D). This enables visualisation and image-based quantification of TH.

We also measured the optical density of TH+ staining using the infrared dye-conjugated secondary antibody, IRDye® 800CW, and visualised the AAV-injected proteins, GFP and GDNF isoforms with the infrared dye-conjugated secondary antibody IRDye® 680RD (Figure 8F). We noticed that infrared-staining was useful both in the visualisation of TH and injected proteins (GFP and GDNF) and the optical density of TH+ fibres could be quantified with infrared fluorometry using similar principles as used in the colourimetric method. Moreover, the two different staining methods displayed similar variance in the optical density measurements (Figure 8A, C and E).

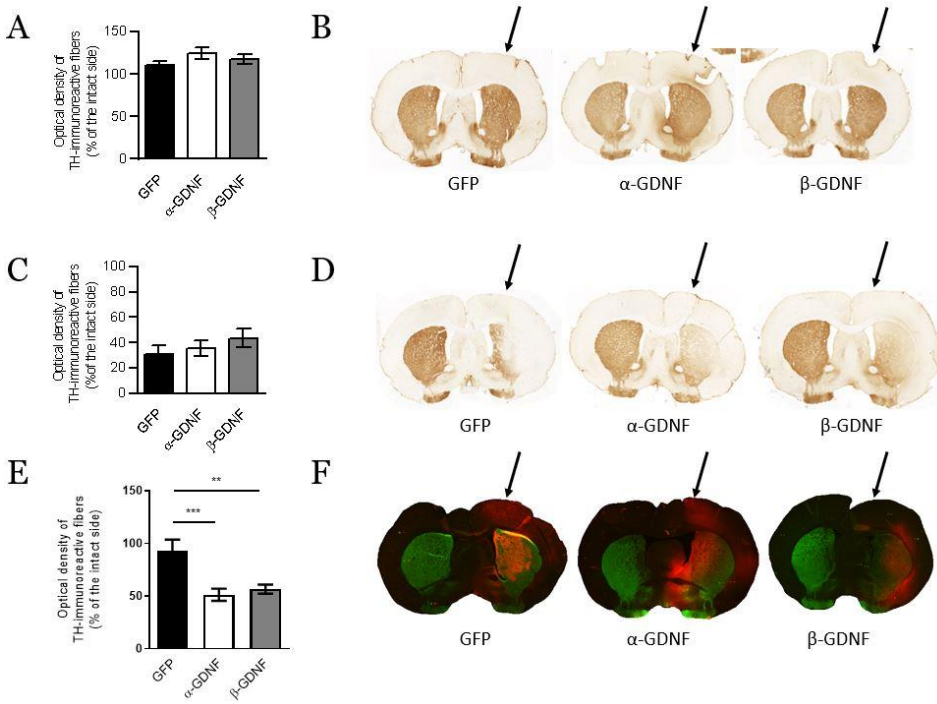

Figure 8. Comparison of staining for optical density measurements. In non-lesioned animals, 3 weeks after the AAV-injections, the optical density of striatal TH-immunoreactive fibres was similar in all treatment groups (GFP 111 ± 4%, α-GDNF 124 ± 7%, and β-GDNF 118 ± 6% of the intact side, n = 8–10 in each group) (**A**). Representative images of TH-stained striatal sections using a primary antibody against TH and a secondary antibody enabling an avidin-biotin-peroxidase complex reaction with DAB, in which the staining is seen as brown (**B**). In lesioned animals, 4 weeks after 6-OHDA administration, the optical density of striatal TH-immunoreactive fibres was decreased in all treatment groups (n = 14–15) (**C**). Representative images of striatal TH-immunoreactivity stained by using the same colourimetric method as in B (**D**). In non-lesioned animals, 7 weeks after the AAV-injections, the optical density of striatal TH-immunoreactive fibres was significantly lower in GDNF-isoform treated groups compared to GFP [one-way ANOVA, $F(2, 28) = 10.56$, $p = 0.0004$, followed by Bonferroni post-hoc test, $^{***}p < 0.001$, $^{**}p < 0.01$ n = 10–11] (**E**). Representative images of TH- and GFP- or GDNF-stained striatal sections using primary antibodies and infrared dye-conjugated secondary antibodies to stain the target proteins (**F**). TH is pseudocoloured as green, and GFP and GDNF are red. Arrows denote the injected side. 6-OHDA: 6-hydroxydopamine, AAV: adeno-associated virus, ANOVA: analysis of variance, DAB: 3,3'-diaminobenzidine, GDNF: glial-derived neurotrophic factor, GFP: green fluorescent protein, TH: tyrosine hydroxylase. All data are expressed as mean ± SEM. Adapted from publication I.

5.2 Deep learning-based counting of tyrosine hydroxylase-positive neurons from the substantia nigra is comparable to stereology (II)

We developed a CNN-based algorithm to detect TH+ neurons from mice and rat brain sections, focusing on the SN. The analysis was validated in two ways; counting by human observers with manual counting and unbiased stereology. The workflow for counting the TH+ neuron platform, using the algorithm, implementing whole-slide scanning, cloud-based image processing, and Aiforia™ is presented in Figure 9A with representative images of the analysed area and CNN performance shown in Figure 9B.

In the manual counting, human observers counted a total of 489 TH+ neurons and algorithm counted a total of 493 TH+ neurons across 26 regions-of-interest with a strong correlation (Pearson correlation 0.98, $p < 0.001$; $R^2 = 0.95$; Figure 9C) and performance metric scores (Precision: 88.5% (85.5–91.4%), Recall: 87.8% (84.9–90.7%), F1-score: 88.2% (85.3–91.0%) with a 95% confidence interval.

Next, with our previous analysis of SNpc TH+ neurons in rat and mice models of 6-OHDA, we compared stereology, using unbiased counting rules with the optical fractionator and disector principle using the StereoInvestigator platform, against the CNN algorithm. We found a strong correlation between the algorithm and stereology across rat samples (Pearson correlation of 0.9, $p < 0.0001$; $R2 = 0.81$; Figure 9D) when comparing the final counts displayed as ratios between the lesioned and unlesioned hemispheres. Additionally, in mouse sections the correlation of the counts obtained with the two methods was significant (Pearson correlation 0.93, $p < 0.0001$ and $R2 = 0.87$; Figure 9E).

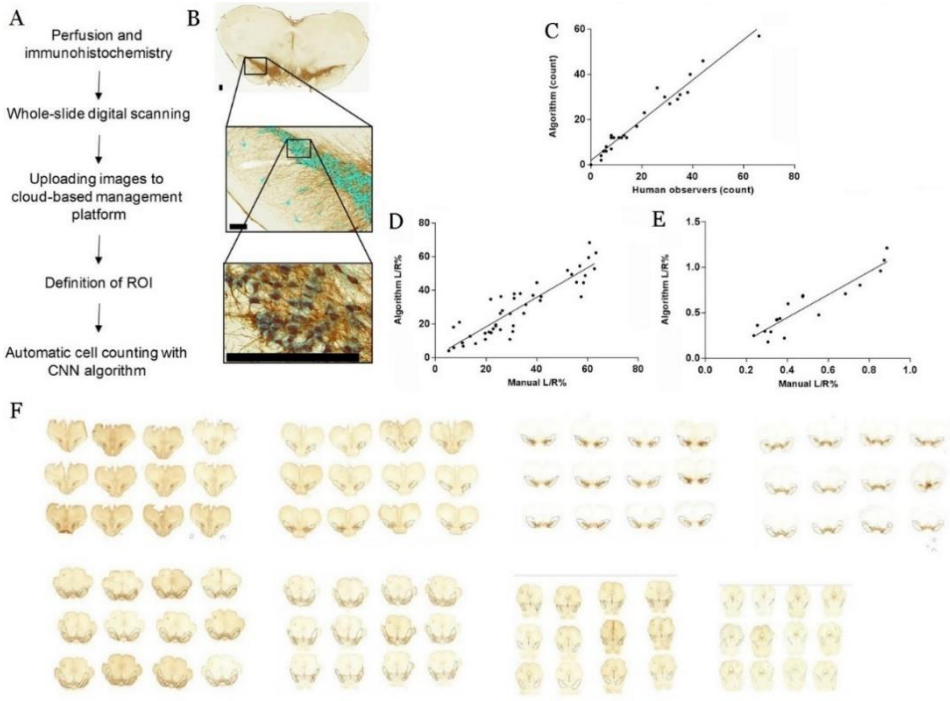

Figure 9. Workflow for counting the neurons using the Aiforia™ platform and validation of counting against manual counting and stereological estimations. Schematic of the workflow to use whole-slide scanning, cloud-based image processing, and the Aiforia™ platform for quantifying TH-positive neurons in the substantia nigra (SN) (**A**). Representative images of the analysed neurons in a region of interest (ROI) and the neurons (circles demarcate neuronal somas) the CNN recognised (**B**), scale bar: 100 µm. Algorithm validation against manual counting done by human observers in rat midbrain sections (R^2 = 0.95; y = 0.95x.) (**C**). Validation of the algorithm against rat samples previously analysed with stereology (**D**). The data is represented as ratios of Left (L; lesion)/Right (R; intact) sides (R 2 = 0.81). Validation of the algorithm against mouse samples previously analysed with stereology (**E**). The data is shown as ratios of Left (L; lesion)/Right (R; intact) sides (R^2 = 0.87). A whole SN volume (96 consecutive 40 µm thick coronal brain sections) was analysed to test the speed of the algorithm in counting the total number of TH+ neurons in the rat SN (**F**). The analysed ROI is shown in each section. Adapted from publication II.

And finally, we tested the speed of the algorithm by using it to count TH+ neurons in a whole rat SN; both hemispheres in 96 consecutive sections including both the pars compacta and pars reticulata (Figure 9F). In total, 29 689 TH+ neurons were detected by the algorithm and the analysis took 3 h which equals a speed of counting 2.7 neurons per second. Taken together, the measurements had a high degree of correlation, and the algorithm was able to perform high-capacity analysis in a relatively short amount of time.

5.3 Cytomegalovirus promoter-driven transgene expression is enhanced by methamphetamine *in vivo* (III)

The drug-induced rotation test has long been used in preclinical PD research to evaluate the function of the dopaminergic nigrostriatal pathway and therapeutic potential of new drugs (Ungerstedt and Arbuthnott 1970; Bjorklund and Dunnett 2019). Hence, we wanted to test whether drugs used in this test, namely Meth, and enhancing more dopamine-specific signalling with drugs that are used by PD patients, could alter CMV-controlled transgene expression. In addition to testing the cytomegalovirus immediate early (CMV-IE) promoter, we wanted to test whether the CMV promoter in our AAV1-CMV-GLuc vector could be enhanced by Meth. The promoter and enhancer region in the used AAV1-CMV-GLuc vector contains a chimeric intron with sequences from the first intron of the human β-globin gene and the intron of an immunoglobulin gene heavy-chain variable region (see study III for promoter sequence). This promoter is hereby referred to as CMV', the vector as AAV1-CMV' and the CMV-IE promoter as CMV. To test whether the intron proportion of the CMV' promoter had a role in Meth-induced increase in transgene expression, we injected rats intrastriatally with AAV1 vectors carrying the GFP transgene under the control of either the CMV' or CMV promoter. Four injections of 2.5 mg/kg Meth administered in 2 h intervals resulted in approximately 5- to 7-fold increases in striatal levels of GFP mRNA at 4 weeks post-transduction (Figure 10A). This supports that the CMV-IE portion of the promoter and enhancer is responsible for the Meth-induced upregulation of transgene expression.

Next, using 6-OHDA-lesioned rats overexpressing GFP or α-GDNF under the CMV' promoter in the striatum, we administered single injections of Meth (2.5 mg/kg) or a combination of LD (10 mg/kg) + CD (30 mg/kg) + ENT (10 mg/kg) to the rats 34 weeks after striatal transduction of AAV-CMV'-GFP (31 weeks after 6-OHDA lesion). We noticed a significant effect of Meth on GFP mRNA levels in the lesioned tissue after a single dose (two-way ANOVA, Meth versus saline [0 h time point in Figure 10B] between effect, $F_{3,16} = 14.8$; $p < 0.001$). Moreover, we detected a time-dependent increase in GFP mRNA levels, with a maximum ~5.6-fold increase 4 h post-injection that returned to baseline levels within 8 h (Figure 10B). Treatment with the combination of LD+CD+ENT (10/30/10 mg/kg) did not have a statistically significant effect on increasing α-GDNF mRNA levels compared to vehicle-treated animals (Figure 10C).

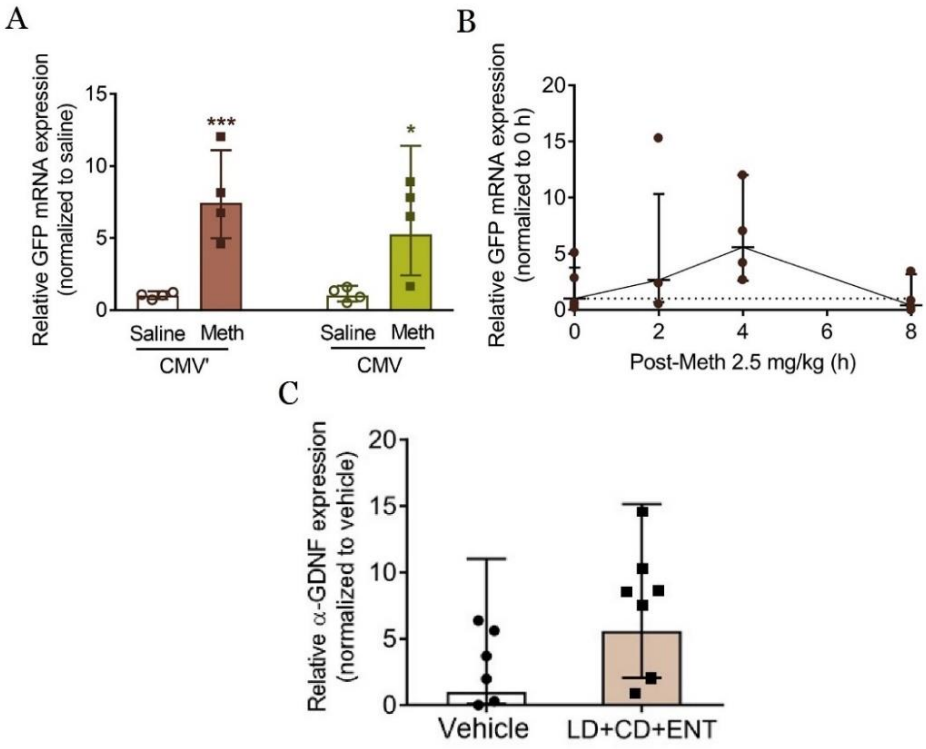

Figure 10. Effects of dopaminergic neuronal activation on CMV promoter-driven transgene expression. Transgene mRNA levels measured from the striatum of rats overexpressing GFP under the CMV' or CMV promoter after administration of four s.c. injections of saline or methamphetamine (Meth 2.5 mg/kg) (n = 4, *p < 0.05, ***p < 0.001, unpaired t test of ΔCt values; CMV': t(6) = 8.744, p = 0.0001; CMV: t(6) = 3.538, p = 0.0122) (**A**). Transgene mRNA levels in the striatum of rats transduced with GFP and lesioned using 6-OHDA 0, 2, 4, and 8 h after a single s.c. injection of 2.5 mg/kg Meth (n = 4–5, one-way ANOVA, $F_{3,13} = 2.608$, p = 0.0960; unpaired t test 0 versus 4 h, t(7) = 2.357, p = 0.0505) (**B**). Transgene mRNA levels in the striatum of 6-OHDA-lesioned rats transduced with α-GDNF after 4 h of a single dose of vehicle or a combination of levodopa (LD) 10 mg/kg, carbidopa (CD) 30 mg/kg and entacapone (ENT) 10 mg/kg (n = 6-7, unpaired t-test vehicle vs. LD+CD+ENT, t(11) = 2.090, p = 0.0607) (**C, unpublished**). Results are presented as $2^{-\Delta\Delta Ct}$ ± upper and lower limits calculated using the ΔCt SD, with individual ΔΔCt values plotted. 6-OHDA: 6-hydoryxydopamine CMV: cytomegalovirus promoter, CD: carbidopa, ENT: entacapone, GDNF: glial-derived neurotrophic factor, LD: levodopa, Meth: methamphetamine. Adapted from publication III. The following sequences were used for target amplification and detection of α-GDNF: agtgactcaaatatgccagaggatt (forward), tcagtcttttaatggtggcttgaa (reverse), tcctgatcagttcgatgat (FAM/BHQ-labelled probe). Further details on methods can be found from publication III.

5.4 Reporter systems using fluorescence or luminescence with exogenous or endogenous control of short-interfering RNAs or microRNAs are a viable approach to measure the activity of Dicer (IV)

Dicer is an RNAse enzyme partaking in the maturation of miRNAs (Bernstein et al. 2001). Dicer has been implicated in a variety of diseases, including PD (Simunovic et al. 2010; Foulkes et al. 2014; Chmielarz et al. 2017). PD patients have reduced levels of Dicer and enhancing Dicer is protective in stressed cultured TH+ neurons. Thus, finding compounds that could enhance the function of Dicer could be studied as potential new drugs for the treatment of PD. We aimed to create sensitive reporter assays that could measure the activity of Dicer and be used for studying Dicer biology and screen for Dicer activating compounds.

The reporter systems express two fluorescent or bioluminescent proteins, one being the indicator and the other an internal control (Figure 11). The transcript of the indicator protein has a binding site for a specific artificially created siRNA implemented into a pre-miRNA backbone, or an added binding site of an endogenous miRNA, and the reporter system either also express these or exploit endogenous microRNA expression. As Dicer is responsible for cleaving pre-miRNAs into mature miRNAs, Dicer activation decreases the expression of the indicator protein and, as such, measuring the ratio of the expressed fluorescent or bioluminescent probes gives an estimate of Dicer activation.

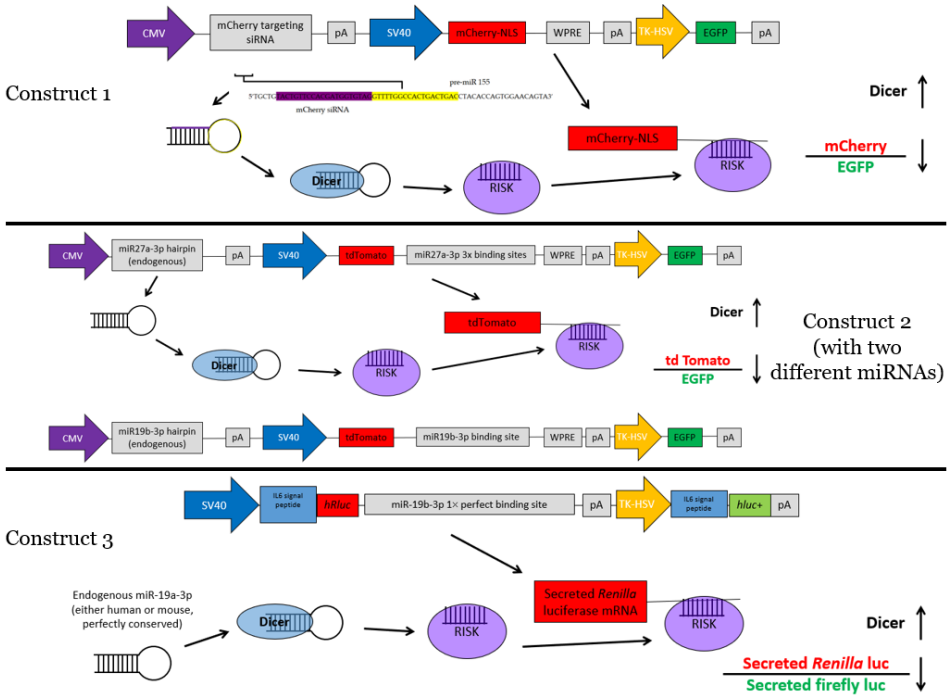

Figure 11. The reporter system constructs to measure the activity of Dicer and how they function. Construct 1 expresses a mCherry transcript targeting siRNA implemented into a pre-miRNA hairpin, under the CMV promoter. This pre-miRNA is processed by Dicer for the siRNA to block translation of the transcript. Construct 2 expresses either miRNA-27a or miRNA-19b and concomitantly with the naturally expressed respective miRNAs silences tdTomato which has the binding sites of these miRNAs incorporated into its transcript. Construct 3 expresses miRNA-19b which, in combination with the naturally occurring miRNA-19b, silences the Renilla luciferase transcript having a mir19b binding site incorporated into the transcript. To summarise, when Dicer is activated, it enhances the maturation of siRNA/miRNAs responsible for repressing the translation of the indicator protein (mCherry, tdTomato, or Rluc) which in turn reduces its ratio to the internal protein (EGFP or FLuc). CMV: cytomegalovirus promoter, EGFP: enhanced green fluorescent protein, IL6: interleukin-6 Fluc: Firefly luciferase, mCherry: modified Cherry (red fluorescent protein), miR: miRNA, microRNA, pA: polyadenylation, pre-miR: precursor microRNA, RISK: RNA-induced silencing complex, Rluc: Renilla luciferase siRNA: small interfering RNA, SV40: simian virus 40 promoter, tdTomato: tandem repeat Tomato (red fluorescent protein), TK-HSV: Herpes simplex virus thymidine kinase promoter, WPRE: Woodchuck Hepatitis virus posttranscriptional regulatory element. Reprinted from manuscript IV.

Plasmids and stable cell lines were developed based on these constructs and their utility as reporter systems was assessed with a small-molecule antibiotic compound, enoxacin, known to activate Dicer. The three reporter systems were validated by quantifying the fluorescence or

bioluminescence ratios of enoxacin treated T-Rex cells stably expressing constructs 1 and 2 or HEK293T cells transiently expressing construct 3 (Figure 12). In the stable cell lines, the induction of the expression of siRNA or miRNAs targeting the transcripts of the indicator proteins, mCherry and tdTomato, was done with doxycycline (DOX) as the reporter systems were stably transfected into the T-Rex cells with DOX-inducible loci. The ratios of mCherry/EGFP, tdTomato/EGFP or RLuc/FLuc were significantly reduced by treatment with 100 µM enoxacin compared to DMSO treatment, indicating Dicer activation (Figure 12A, B and C).

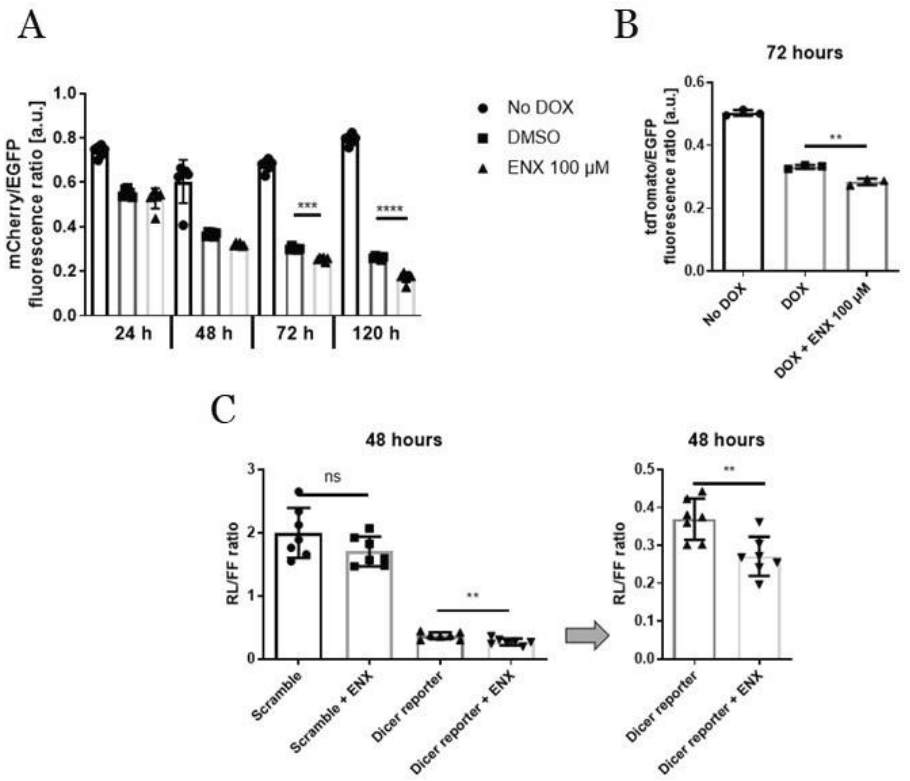

Figure 12. Validation of the constructs and respective reporter assays using a Dicer activating drug, enoxacin. Mean mCherry/EGFP fluorescence ratios measured after 24, 48, 72, and 120 h in FLP-IN 293 T-Rex (T-Rex) cells with DMSO only (No DOX), with DOX and DMSO (DMSO), or DOX and ENX (ENX 100 µM) for validating construct 1 (**A**). No DOX treated cells compared to cells treated with DOX showcase the induction of siRNA expression. Mean mCherry/EGFP ratio was reduced significantly (n = 6 wells per treatment group, one-way ANOVA with Tukey's multiple comparison test, ***p < 0.001,

****p < 0.0001) after 72 and 120 h of treatment in ENX treated cells compared to DMSO. Mean tdTomato/EGFP fluorescence ratio measured after 72 h in T-Rex cells treated with DMSO (No DOX), DOX and DMSO (DOX), or DOX and 100 μM ENX (DOX + ENX 100 μM) for validating construct 2 (**B**). After 72 h of treatment the mean tdTomato/EGFP ratio was significantly reduced in ENX treated cells compared to DMSO (n = 3, average of independent experiments with 4-6 wells per treatment group, unpaired t-test, t(4) = 6,903 **p = 0.0023). Mean RL/LL luminescence ratio measured after 48 h of transiently transfecting the plasmids containing miRNA-19b binding site or scrambled miRNA binding sites in HEK293T cells and treated after 24 h of transfection with DMSO (Scramble or Dicer reporter) or 100 μM ENX (Scramble + ENX or Dicer reporter + ENX) for validating construct 3 (**C**). A significant reduction in the mean RL/LL ratio was detected (n = 7 wells per treatment group, unpaired t-test, t(12) = 3,472 **p=0.0046) in ENX treated cells compared to DMSO. All data are expressed as mean ± SD. [a.u.]: arbitrary unit, DMSO: dimethylsulfoxide, DOX: doxycycline, EGFP: enhanced green fluorescent protein, ENX: enoxacin, FF: firefly (luciferase) mCherry: modified Cherry (red fluorescent protein), RL: Renilla (luciferase), tdTomato: tandem repeat Tomato (red fluorescent protein). Adapted from manuscript IV.

5.5 Cultured postnatal tyrosine hydroxylase-positive neurons from the ventral midbrain seem to have differences in ER sheets and tubules in the somatodendritic areas compared to various areas of the axon (V)

Characterisation of cellular models used for preclinical studies is an important aspect to 1) find out which methods are optimal to use for assessing the desired effects in the model 2) increase reliability and reproducibility by knowing the properties of the model and all variables affecting its integrity 3) elucidate the biology and studied pathophysiology/genesis of the model, which in turn enable 1) and 2). Characterisation of primary cell cultures may include finding out what types of cells are in the culture, how viable they are in certain conditions, how various homeostatic changes, such as stressors, affect them and characterising the morphology and function of the cells (Lautenschlager et al. 2018). Characterisation of the morphology is important for imaging-based methods as changing their native physiological environment may alter their morphology, which may portend changes in function (Westrate et al. 2015). In particular, ultrastructural characterisation gives even more detail as cells function through their organelles and a multitude of changes in the appearance of an organelle has been attributed to specific cellular events (Heald and Cohen-Fix 2014). For example, the formation of autophagosomes indicates increased cellular degradation or autophagy,

and the shedding of ribosomes from the ER points to a change in protein synthesis. As cells have varied morphologies and a myriad of clear differences in their ultrastructure depending on the cell type, it is important to characterise the ultrastructure of a healthy state of a cell so that comparative studies can be performed when looking at how pathologies, insults, or other alterations in homeostasis affect the cell.

The ultrastructure of dopaminergic neurons has been previously studied in animal models but studies thoroughly looking at differences and changes in the ER, especially in cultured dopaminergic neurons is lacking (Nakadate and Tanaka-Nakadate 2015; Öztürk et al. 2020). Therefore, we cultured transgenic TH-GFP mice postnatal (P1-P4) ventral midbrain neuronal cultures specifically looking at the dopaminergic neurons and their ultrastructure. This model is highly suitable for preclinical modelling of PD. We imaged all main compartments of single TH+ neurons using CLEM and made an open-access interactive resource for anyone to utilise the image data for comparative studies (Figure 13).

We qualitatively observed that the TH+ neurons may have distinct ER profiles between the axonal and somatodendritic compartments. The ER in the axons is more tubular and has fewer ribosomes compared to the ER in the dendrites or soma (Figure 13).

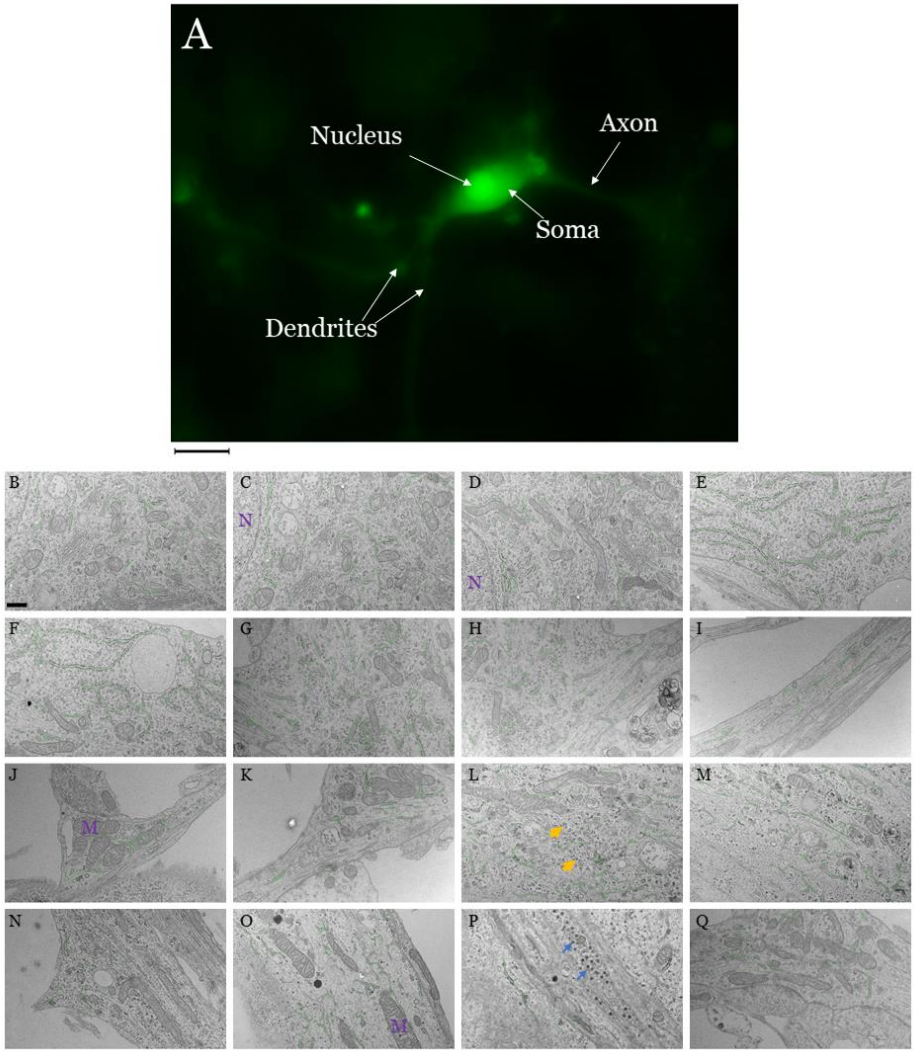

Figure 13. The ER in all main compartments of a cultured TH+ neuron, from postnatal mice expressing GFP under the TH promoter, and imaged using transmission electron microscopy. A fluorescent photomicrograph of the TH+ neuron (**A**). Thin section transmission electron micrographs showcasing the ultrastructure of the soma near the nucleus (**B-D**), somal periphery (**E-F**), base of the axon and a dendrite (**G**), axon hillock (**H**) along the axon (**I**), axonal terminal (**J**), axonal bouton (**K**), dendrite base (**L**), proximal dendrite (**M**), dendritic protrusion (**N**), distal dendrite (**O**), dendritic terminal (**P**) and multiple synapses along a dendrite (**Q**). The ER in the TEM images (**B-Q**) is highlighted in green. The nucleus (N) is displayed in images C and D, and mitochondria (M) in images J and O. Large (yellow) arrows point towards polyribosomes and small (blue) arrows to synaptic vesicles in images L and P respectively. An interactive image of select regions can be found from https://www.helsinki.fi/en/researchgroups/organelle-structure/research#section-106929 (accessed in January 2022). Scale bar: 20 µm (**A**) and 400 nm (**B-Q**). Adapted from publication V with additional unpublished images.

6 Discussion

6.1 Measuring optical density using different labelling methods (I)

Optical density measurements have been used to approximate striatal innervation of TH+ fibres for over 30 years (Burke et al. 1990). Optical density can be reliably used for areas with homogenous staining patterns. Besides computational advancements in image analysis software and utilising different quantification to obtain the measurements, the immunostaining paradigms used in the method has been, mostly, done using colourimetric staining protocols and detection methods as it has been well-established. Some studies have implemented infrared analysis to assess neuronal lesions, however not nearly to the same extent as colourimetric methods in quantifying striatal fibre innervation by measuring average optical densities (Gagnon et al. 2017).

We demonstrated that by merely changing the immunolabelling to use infrared dye-conjugated secondary antibodies, we could achieve results with similar variability to results obtained by the traditional colourimetric method (Figure 8A, C and E). The advantage of using infrared is that in comparison to visible wavelength fluorescent dyes they have reduced background autofluorescence which may cause caveats for some studies, especially with cellular structures having autofluorescence in the lower visible wavelengths (Lopreside et al. 2019). Infrared dye-conjugated secondary antibodies have a wide dynamic linear range and increased detection sensitivity with a better SNR. For example, studies comparing infrared-based detection to chemiluminescent methods have shown that infrared has a broader linear dynamic range avoiding the enzyme kinetics and limitations of substrate availability of chemiluminescence, producing consistent and accurate quantification (Gerk 2011). Compared to colourimetric labelling, infrared dye-conjugated secondary antibodies allow non-overlapping multiplexing (enabling multiple targets to be visualised). Improved visualisation can also be achieved using infrared labelling; however, these are also obtainable by any activatable labelling, essentially immunofluorescence and bio/chemiluminescence, and image manipulation. Nevertheless, using infrared fluorometry may streamline the workflow and decrease the time it takes to analyse a full experimental set of optical density measurements compared to the traditional colourimetric method using DAB.

However, the purpose is not to replace other immunolabeling and detection methods, as they also have considerable advantages, for example in signal amplification, but to provide a useful alternative in addition to them (Lopreside et al. 2019). For instance, colourimetric methods can be used with standard light microscopes if lasers to activate fluorescent dyes are not available. Hence, using infrared expands the toolbox of researchers in conducting optical density measurements to assess fibre density.

6.2 Cell counting using deep learning (II)

Unbiased stereology has been the preferred method to estimate cell counts from brain tissue in preclinical PD studies (Oorschot 1996; Nair-Roberts et al. 2008; Ip et al. 2017). However, as this method is highly laborious and time-consuming, we wanted to develop a method that could overcome these issues with automation and a simplified workflow. Thus, we embarked to develop deep learning-assisted cell counting. With comparative studies, we validated the accuracy of the algorithm against stereology and showed that the method could count TH+ neurons from the SN with similar estimates to those obtained with stereology, with the advantage of increased speed and a less-arduous workflow.

However, unless measuring complete volumes, as we did with the SN (Figure 9F), systematic sampling and some counting rules, i.e. equations to account for neurons in unquantified sections, are still needed for accurate estimation of cell numbers as is the case with any computer-assisted counting methods (Penttinen et al. 2016). Careful consideration is still needed on which sections to choose and knowledge of how many sections cover the total area to be counted and whether there are regional differences in cell numbers that need to be taken into account. Additionally, the issue with using free-floating cryosections is that they must be relatively thick to maintain their integrity. 30-40 µm sections are the preferred choice but depending on the size and positioning of the neuron within the section it is possible that some neurons may not show very well in the sections and can be missed by the imaging as we used extended focus scanning of only 5 layers at 2 µm intervals. Nonetheless, our results are in line with previously published reports on cell numbers and slight differences (within inter-animal variation) do not seem to be an incandescent issue (Oorschot 1996; Nair-Roberts et al. 2008). The differences may also be explained by imprecise demarcation of the counted

areas, with some overlap between the SN and VTA regions accounting for possible extra TH+ neurons counted from the VTA region

The disadvantage of using deep learning algorithms is that the learning parameters and ground truth for the training have to be carefully chosen, as otherwise the algorithm will learn to detect and segment unwanted structures (Laine et al. 2021). Thus, thorough validation is needed across a substantial amount of data for reliability. The advantage of the algorithms is that they can be trained to recognise cells or their features from almost any sort of histological samples, using any kind of labelling method, infrared labelling included, with high accuracy (Turkki et al. 2016; Araujo et al. 2017). Regarding PD, the logical next steps besides just counting TH+ or other neurons of interest would be to quantify pathological markers such as proteinaceous inclusions. Detecting α-synuclein staining in various stages of its pathology up to the formation of LBs is of considerable interest to neuropathologists, as LBs are the foremost searched histopathological findings in *postmortem* PD patient samples (Spillantini et al. 1998; Shahmoradian et al. 2019; Mahul-Mellier et al. 2020). Thus, the next step would be to develop algorithms to recognise LBs and/or stained α-synuclein from brain sections. This has been demonstrated to be successful in assessing tauopathies in which the authors used human expert annotations from 22 patient brains with tauopathies as ground truth and a web-based platform to manage whole-slide images (Signaevsky et al. 2019).

With the wanted remedy of simplified and reduced workflow and work time for cell counting, the Aiforia™ platform with a CNN algorithm provides a user-friendly and convenient method for cell counting (II). Using the algorithm between labs also reduces observer-inflicted bias and therefore could produce more replicable and consistent counts. Digital pathology is also coming of age as studies have shown that ML can assist pathologists in clinical diagnoses (Jahn et al. 2020). If the performance of the algorithm were showcased in human brain samples, it could be valuable in the arsenal of neuropathologists' tools who are interested in rapid quantification of TH+ neurons from brain sections.

6.3 Neuronal activation stimulates cytomegalovirus promoter-driven transgene expression (III)

Indications that CMV-driven expression could be enhanced by neurotransmission were found in studies on neurotoxic effects of Meth, where false-positive results were observed (III). This led us to investigate the effect of various compounds in their ability to activate the CMV promoter. Using *in vitro* and *in vivo* models to study neuronal activation, we observed a strong interaction between neuronal activation and CMV promoter-dependent transgene expression.

Meth increases neuronal activation by releasing dopamine-containing vesicles (Larsen et al. 2002). Amphetamines additionally increase cytosolic dopamine levels by activating TH, impairing VMAT2, and inhibiting MAO (Sulzer et al. 2005; Sulzer 2011). We noticed an increase in the relative GFP levels of rats treated with Meth which presupposes that the expression of GFP was altered due to neuronal activation (Figure 10).

We also noticed a trend toward the increase in transgene expression after LD+CD+ENT treatment. It is tempting to speculate that dopaminergic activation, compared to other neurotransmitter-mediated neuronal activation, would have a prominent role in the activation of CMV-driven transgene expression, however the results we obtained do not support this idea. And considering that methamphetamine potentiates other monoaminergic signalling besides dopaminergic (Sulzer et al. 2005), and our observation that excitatory amino acids, kainic acid and glutamate, enhance CMV-controlled transgene expression (III), it suggests that dopamine-specific signalling would not have a more substantial role compared to other factors inducing neuronal signalling in CMV activation. However, as the number of animals was relatively small and we only assessed specific time points and single dosing of dopamine signalling enhancing agents, the contribution of dopamine-specific activation should be thoroughly assessed with a larger number of animals, different time points and dosing regimens, and in different experimental conditions than 6-OHDA-lesioned rats.

The finding that methamphetamine can activate the CMV promoter has far-reaching implications in the use of viral vectors designated for gene therapy incorporating the CMV promoter, as methamphetamine is used recreationally in humans. The CMV promoter has been used in multiple clinical trials in various diseases and, for example, an open-label phase 1 study aiming to assess the safety, tolerability, and potential clinical effects

of AAV2-GDNF in advanced PD patients leveraging the CMV promoter is currently ongoing, and results should be published in early 2022 (McFarthing et al. 2019; Buck and Wijnholds 2020). Thus, if methamphetamine was used by patients within these studies, it could potentially affect results. As we observed in our studies, two other promoters, the human eukaryotic translation elongation factor 1α and synapsin 1 were not activated, indicating that this seems to be a CMV-specific phenomenon (III). Therefore, extra caution in the use of the CMV promoter in gene therapies should be taken. However, from a more practical point of view, this knowledge can also be exploited in any experiment involving the use of the CMV promoter in neurons. Furthermore, signals from reporter assays, such as the ones developed in study IV to measure the activity of Dicer, could be amplified enhancing the expression of genes under the CMV promoter by concomitant use of methamphetamine in an *in vivo* model. However, this would also add another variable that should be controlled to make sure the effects are not due to the addition of methamphetamine.

6.4 Optimisation of reporter assays for measuring Dicer activity and the role of Dicer in Parkinson's disease (IV)

Dicer activity has previously been studied with enzyme-based and cell-based assays, however, it has not been studied in physiologically relevant conditions using endogenous miRNAs in a cellular context to account for all factors affecting miRNA maturation within a cell (Chiu et al. 2005; Davies and Arenz 2006; Shan et al. 2008; Zhang et al. 2008; Podolska et al. 2014). We developed three different assays taking into account the cellular context for versatile studying of Dicer activation. The results were comparable to previously published assays, supporting the idea that Dicer activity can be measured using siRNA or miRNA implemented cell-based assays. With regards to the sensitivity of the assay, it is important to consider the promoters, which siRNA/miRNA to use, and the use of indicator proteins.

A goal of reporter assays in many cases is to make them robust enough to support HTS (Lorenz et al. 2018). HTS would enable efficient discovery of new ligands that could activate Dicer. For optimal HTS, the assay should have a large enough Z factor, i.e., large effect size (difference in the positive and negative controls) and low variability (coefficient of variation). To

achieve this in the Dicer assays, an increase in expression of the indicators using different promoters or optimising siRNA/miRNA levels could be remedial. Other options would be to optimise the silencing of the transcript, by combining multiple miRNAs or a miRNA sponge as using a singular miRNA was not efficient enough. Additionally, the assays could be made more sensitive and linear by switching EGFP and tdTomato into novel brighter and more stable engineered proteins and similarly switching to NanoLuc instead of RLuc/FLuc, or switching the factors affecting transcription, such as the Woodchuck Hepatitis virus posttranscriptional regulatory element used in our constructs (Zufferey et al. 1999; England et al. 2016; Shen et al. 2017).

As enoxacin activates Dicer through its interaction with TRBP, the mechanism of how Dicer and its partner proteins possibly partake in PD pathogenesis should be further studied (Shan et al. 2008; Felicetti et al. 2020). TRBP and Dicer have been implicated in the ER and the regulation of BDNF, which in turn is a vital neurotrophic factor for neuronal survivability, neuritogenesis, and overall homeostasis of neurons (Antoniou et al. 2018). Dicer dysfunction could therefore be one factor contributing to local miRNA dysregulation and, apropos, dysfunctional neurites. In dopamine neurons, this could further contribute to the degeneration of their axons and ultimately their death.

6.5 Ultrastructure of *in vitro* postnatal dopaminergic neurons (V)

The ER is comprised of a network of sheets, tubules, and vesicles found in virtually all eukaryotic cells, extensively in secretory cells (Shibata et al. 2006; Spang 2018, V). The structure of the ER is conserved and expands throughout the cell. It is the largest organelle and may be up to 10 times in surface area compared to the plasma membrane (Bolender and Weibel 1973; Horton and Ehlers 2003). Considering the vast extensions and arborization of neurons, the organisation of the ER in neurons is remarkable and should be of high consideration when studying neuronal function. The morphofunctional organisation of mature neurons is comprised of the somatodendritic and axonal compartments (Dotti et al. 1988). As neurons undergo stress, they tend to retract neurites and the dying-back phenomenon of axonal degeneration preceding neuronal cell death is seen in many neurodegenerative diseases. Axonal homeostasis is highly dependent on the proper function of the ER and, as such, it is

implicated in axonal degeneration (V). Studying the axonal or dendritic ER is, therefore, a crucial part of figuring out cell death mechanisms in neurodegenerative diseases. To look at the ER in these compartments, traditional light microscopy may not offer high enough resolution to assess alterations in the ER. However, with EM even minor ultrastructural changes can be observed, which is why it is utilised in neuropathology (Walker et al. 2018). However, these changes can be difficult to see, for example, the periodic nature of actin and spectrin in axons was only fully observed after the development and use of super-resolution microscopy, in which stochastic optical reconstruction microscopy demonstrated the organisation of actin rings (Xu et al. 2013). Therefore, the best approach to thorough ultrastructural studies is using CLEM with super-resolution microscopy, which offers a solution to pinpoint minor alterations in neurites (Vassilopoulos et al. 2019). Imminently, these kinds of studies applied to the study of degenerating dopamine neurons could reveal the specific ultrastructural morphological changes seen within PD pathologies and possibly reveal new converging pathogenetic pathways and drug targets within the dopamine neuron ER. This is notable as multiple studies have implicated the ER in PD pathogenesis. For example, α-synuclein may have a role in affecting ER function and vice versa (Belal et al. 2012; Betzer et al. 2018; Colla 2019).

The observations from our data looking at the ultrastructural characteristics of a cultured TH+ neuron gives further confirmation of an important aspect of neuronal homeostasis. As we specifically focused on the ER, we noticed possible differences in the axonal ER compared to the ER seen in the somatodendritic compartments. However, as our observations were preliminary and qualitative, a quantitative assessment of these differences is required for more definitive conclusions. The neuronal ER has been studied previously on many occasions over the past 70 years with similar observations (Palay and Palade 1955; Wu et al. 2017; Terasaki 2018). Dopamine neurons have also been studied to some extent, with comparative ultrastructural studies on VTA and SN dopamine neurons and even 3D reconstruction of a whole neuron (Domesick et al. 1983; Nakadate and Tanaka-Nakadate 2015). However, comparative ultrastructural studies of cultured dopamine neuron ER have been lacking. As these neurons are differentially susceptible to neurodegeneration in culture, and the ER plays a significant role in cellular homeostasis, it would be useful to characterise all features related to dopamine neuron ER when using cultures in modelling PD. As previously discussed, modelling PD pathology in other neurons, such as hippocampal neurons, may not be translatable to dopamine neurons (Er et al. 2020; Mahul-Mellier et al.

2020). Therefore, if there are differences in the neuronal ER of dopamine neurons compared to other neurons, it may give clues to the reasons behind the vulnerability. Although our observations, to some extent, confirm similarities in neuronal ER profiles between types of neurons, there may still be minute differences for example in ribosome amount and distribution. The vast arborization and increased bioenergetic requirements of dopamine neurons may require efficient local translation in axons and the number of ribosomes could thus be crucial to axonal function (Öztürk et al. 2020).

Although quantitative information is what is ultimately aimed at in life sciences, qualitative information still has its role in providing descriptions for which new hypotheses and quantitative methods can be developed upon. However, large-scale imaging studies have predominantly neglected open access to the image sets and thus it would be advised that freely available databases and image repositories were to be made from the acquired images, such as the "Fine Structure of the Aging Brain" by Alan Peters, which provides a collection of electron micrographs acquired throughout studies spanning over 20 years on the ageing rhesus monkey brain (Table 2). Although the database provides mainly data on ultrastructural alterations of the cortex in ageing rhesus monkeys, it can still be invaluable for comparative studies for other areas of the brain, such as the midbrain. A similar database on cellular and animal preclinical models of PD, such as our cultured postnatal dopamine neurons, could be done which could yield a wealth of information on the pathogenesis of PD. As EM data is easier to acquire from 2D cultures, as there is less volume to image, our data on a single TH+ ventral midbrain mouse dopamine neuron is a good start for a comprehensive resource on the ultrastructure of different dopaminergic subtypes for comparative studies. Imaging data, especially information-rich imaging, such as light- and electron microscopy, is still widely used in descriptive studies and are pivotal in highlighting phenotypes of organisms and their structure down to the ultrastructure. Also, for example, extreme phenotypes that are seemingly obvious by visual inspection serve as good pilot studies or preliminary experiments of hypotheses which can then aid in choosing interesting outcomes to further quantify, reducing the time that would go to quantify experiments with lower impact findings (Oates et al. 2009). However, as extreme findings, no matter how seemingly obvious, may still be outliers, generalisations can never be assessed without proper quantification and statistical analyses. Thus, quantitative assessment is crucial for the explanatory power of any experiment.

6.6 Problems in preclinical studies of Parkinson's disease

The most prominent issues that have been raised in preclinical studies on PD have been the lack of translatability of the cellular and animal models of PD towards the human pathology, reproducibility of results, and standardisation of experimentation between research groups.

As an example, studies done on α-synuclein have suffered clearly from all the above-mentioned drawbacks and a review encompassing all of these was recently published where the authors laid out ways how to overcome caveats related to studies on α-synuclein (Oliveira et al. 2021). Currently, no preclinical model of PD can faithfully reproduce the key clinical features of PD. The utility of animal models in PD drug development has been questioned (Merchant et al. 2019). However, animal models are crucial for proof of mechanism studies which in turn serve as the basis for proof of principle and -concept studies in humans. A thorough assessment of outcome measures should be done in each model, such as behavioural effects in the 6-OHDA model (Iancu et al. 2005), which has been lacking with e.g. some of the α-synuclein models (Oliveira et al. 2021). All models are essentially imperfect representations of reality based on current knowledge and the purpose of experiments are to figure out how the models are wrong and correct or refine them based on data acquired from these experiments. However, methods used to analyse and assess outcomes from the models, should also be corrected and refined similarly and purposefully. As demonstrated in the previous example, not all methods apply to all models, and this should be considered thoroughly in preclinical PD research. There is an overt discrepancy between the number of models that have been developed compared to the number of methods used to assess efficacy outcomes within these models.

Another example, brazenly demonstrating multiple issues arising in preclinical studies on PD was shown in a recent systematic review and meta-analysis done on studying baicalein in rodent models of PD (Wang et al. 2020). The authors identified 20 different studies, done between 2008 and 2019, using rodent models mainly based on 6-OHDA, MPTP, and rotenone. The overall quality of the studies was low as only one study reported randomisation and most had unclear reporting in baseline measurements, blinding, and detection bias. The models used were heterogeneous with varied conditions, including different administration routes and doses of neurotoxins. While most looked at neuroprotective

mechanisms and enzymatic activity, only a few studies investigated other measures such as inhibition of oxidative stress, neuroinflammation, neuronal apoptosis, protein aggregation, or restoration of mitochondrial dysfunction. From the 20 studies, 16 reported incomplete outcome data, not to mention possible unreported negative findings which may overestimate the efficacy of baicalein, showcasing that there is still a lot to improve when it comes to conformity and reliability of measuring efficacy outcomes.

Another question is whether the results are biologically significant or meaningful (Lovell 2013). One can find statistically significant effects, but the effect sizes can be so minor that the changes may not be biologically pertinent. This is particularly central to drug development where efficacy should be substantial enough to provide a clear benefit to the patients. The question isn't whether there is a statistically significant effect of a drug in increasing dopamine concentrations in the striatum or protecting dopamine neurons in the SN but whether the effects are significant enough to alleviate motor symptoms and increase the quality of life.

Lastly, perhaps the biggest issue is the heap of unpublished, i.e. unknown, data and results which may lead to unclear, mixed or misrepresented data, the aforementioned overreaching conclusions on the efficacy of drugs and thus, altogether, the unreliability of results (Eisner 2018). In 2012 a pharmaceutical company published results in which they tried to reproduce the results of 53 preclinical cancer studies of which only six were reproducible (Begley and Ellis 2012; Baker 2016). Concerns have been raised towards many other heavily criticised preclinical studies and this has ignited the creation of reproducibility projects. The egregious reproducibility crisis that preclinical research faces is a big burden and needs an overhaul, i.e., a paradigm shift when it comes to how research is conducted and how quality control and assurance is ensured. The development and reviewing of quantitative and unbiased methods used in studies is one part of how scientific quality can be assured and enhanced.

7 Conclusions

Drug development is a laborious and expensive endeavour that requires coordinated work from teams of highly skilled researchers. Drug development for brain diseases suffers from a lack of proper understanding of the pathologies they aim to treat. PD is one of them, a complex neurodegenerative disease with high success in terms of developing therapies for symptomatic relief but multiple failures regarding the development of disease-modifying therapies. For successful outcomes, the evidence supporting the development of a drug acquired from the preclinical phase should be robust and reliable. For this, the models, methods, and assays which intend to showcase the efficacy of a drug must be scientifically sound and thoroughly characterised.

The main objective of this work was to develop and refine tools and methods, and characterise selected features related to them, which are used in preclinical studies on PD. The methods and assays developed and optimised in this dissertation provide new tools for researchers looking to create and combine methods to further study PD pathogenesis and reliably assess the efficacy of new therapeutics in development for PD. Furthermore, the work has provided novel insight that researchers can take advantage of when implementing the use of the CMV promoter in gene expression vectors or aiming to develop new cellular models of PD based on mouse primary postnatal dopaminergic neurons.

The main conclusions from the studies are as follows:

1. Optical density measurements to estimate striatal TH+ fibre density can be reliably assessed using infrared fluorometry (I). Moreover, using a CNN-based algorithm to quantify TH+ neurons from rodent brain sections provides a valid and less laborious and time-consuming alternative to stereology (II).
2. CMV promoter-driven transgene expression after AAV-mediated transduction is enhanced by methamphetamine in the rat. This is noteworthy when considering the use of the CMV promoter in various expression vectors in preclinical PD studies using amphetamines (III). Dicer and miRNA biogenesis pathway activation can be measured by utilising cell-based reporter assays implementing exo- and endogenous Dicer-cleavable small RNAs expressed via the CMV promoter with fluorescent and bioluminescent indicators (IV).

3. Primary postnatal dopaminergic neurons may have structural differences in their ER between the axonal and somatodendritic compartments. This observation suggests that differences in the ER distribution and its relation to functional differences in the neurons' compartments should be further studied, as it could be a reason for the heightened susceptibility of dopamine neurons to degenerate (V).

Taken together, these developments and findings could reduce the time and cost of preclinical research done on PD aimed toward drug development, which in turn could aid in developing a therapy that could arrest or even reverse the progression of the disease ending the growing unmet medical need to treat PD.

Acknowledgements

This work was carried out at the University of Helsinki: in the Institute of Biotechnology, during the years 2017-2019, the Neuroscience Center during the year 2020, and the Division of Pharmacology and Pharmacotherapy, Faculty of Pharmacy during the year 2021 and made possible by a 4-year grant from the University of Helsinki Doctoral Programme in Drug Research. Instrumentarium Science Foundation is acknowledged for additional financial support during this work.

Firstly, I'd like to express my greatest respect and gratitude towards my supervisors Professor Mikko Airavaara and Docent Andrii Domanskyi who gave me the opportunity to start this work and, more importantly, help me finish it. Your constant support and everlasting willingness to discuss matters are highly appreciated. Particularly, your enthusiasm toward science resonated with me from the very first moment we met, and I am infinitely grateful for the inspiration I have gotten to experience just by listening to both of you talk about science. I also enjoyed all the various get-togethers and moments outside of the lab, so thank you for making my doctoral student life memorable in its entirety.

Besides my supervisors, for the important scientific inspiration and highly motivational lectures, I would like to extend my deep gratitude to Professors Raimo Tuominen and Mart Saarma for all the meetings and lectures I have been privileged to attend with you. Your knowledge of pharmacology and neurobiology never ceases to amaze me. The moments of continuously learning something new and exciting from you have been awe-inspiring.

I would like to thank Professor Timo Myöhänen and Docent Šárka Lehtonen for reviewing this dissertation. Their constructive comments and the discussions we had improved the dissertation manuscript considerably. Professor Tomi Rantamäki is acknowledged for agreeing to be on the grading committee. I am also very grateful to Dr. Ari-Pekka Koivisto for accepting the invitation to act as my opponent in the public examination of this dissertation.

The highest appreciation goes to all my co-authors. Without you, none of this work would have been possible: Dr. Anna-Maija Penttinen and Dr. Susanne Bäck are thanked for very fruitful and intriguing experiments. Anna Their for all your help regarding the work in this dissertation but also for keenly taking on one of my projects for your Master's thesis. Dr. Piotr Chmielarz for all the Dicer work. Dr. Sreesha Sree and Professor Eija Jokitalo for all the fascinating EM work. Our collaborators from across the ocean, primarily Professor Brandon Harvey. And of course, all the other authors for their important contributions. Brandon, Eija and docent Ville Paavilainen are also acknowledged for agreeing to be members of my thesis committee and for their extremely helpful guidance throughout this work. The personnel of LMU, BIU and EMU are also thanked for all their assistance.

I also want to thank all the former and current members of the Airavaara, Domanskyi, Voutilainen, and Saarma research groups, and the Division of Pharmacology and Pharmacotherapy who have helped me out directly with my work or indirectly by creating immensely enjoyable working atmospheres both in the labs and offices. Especially from the Domanskyi group, Piotr and Julia for helping me to get started with lab work and introducing a lot of basic concepts to me. Şafak, Irena, Dima, and all the students we've had for helping out with basic day-to-day lab work and everyone for all the talks we've had. From the Airavaara group: Anna-Maija, Maryna, Katrina, Kert, Tseng, Jenni A, Jenni M, Vasse, Helike, Anna S, Anna T, Suvi, Jouni, Abhishek, and all the students we've had both

in Meilahti and Viikki are thanked also for everyday help and nice discussions. From the Voutilainen group, Merja, Jinhan, Jaan, and Anne for help with experiments and everyone for intriguing chitchats. From the Saarma group, Ave, Zheng, and Yu for providing materials and help with cell and tissue culture work, and everyone for enjoyable conversations. Additionally, thanks to all the fascinating discussions I've had with everyone at the Faculty of Pharmacy.

I am extremely grateful for my not only amazing colleagues but close friends within these labs for all the help with research, discussions (both scientific and non-scientific) and, more importantly, for all the fun times we've shared. Abhishek, Şafak, Tuulikki, and Aastha, specifically for all the memes and peer support. Jenni, Janika, Liam, Tuulikki, and Aastha, particularly for all the events, festivities, and banter. I am lucky to have such fond memories. And Aastha I am profoundly grateful to you, whom especially I really do owe, for always reminding me of the important things in life. I am certain those letters will find the correct address.

Warmest gratitude to all my friends outside the lab. The groups that kept together throughout my university years: Pauli, Joonas, Jenni, Roosa, Eeva, and Anna-Mari for the good times and all the repartee about graduation. Arttu, Konsta, Martti, and Sami for everything related to pharmacy studies and beyond. My long-standing closest friends: Johannes, Mika, Alexander, and Matias for all the serious and not-so-serious discussions, laughing, and unforgettable times together. Particularly I am tremendously thankful for äijäviikonloput for my sound mental health, Aksu for all the events we've attended, and Matias for all the late-night (never too late though) game sessions and important discussions on life. The therapeutic value of having such good friends is immeasurable. Anna-Mari, I probably would not have embarked on this journey if it weren't for you, my sincerest gratitude goes to you for all the support and everything else, especially our friendship. Lysti and Metka, I cannot thank you enough for enriching my life. I cherish every single moment with you two, love you both forever.

In closing, above all, I would like to thank my family to whom I am eternally indebted. My father Pekka, not only have I received the best parenting, fatherly advice, and support I could ever ask for, you are also one of the main reasons I got interested in science, so thank you for everything. Especially for bringing Kaisa, Viljami, Tiitu, Romu, and Cahvi into our lives. Tuure, the best big brother I could have. All the things I've learned from you and the moments we've shared are invaluable. Nena and Teo, for being the best sister-in-law and nephew I could have, tackar. Elisa, the best big sister I could have. All the things you've taught me and the moments and laughs we've shared are irreplaceable. And my mother, Merja, your unwavering love, support, empathy, and caregiving are out of this world. Words would never be enough to let you know how grateful I am and how much you mean to me.

Helsinki, February 2022

References

Abercrombie M. 1946. Estimation of nuclear population from microtome sections. *Anat Rec* **94**: 239-247.

Aguila J, Cheng S, Kee N, Cao M, Wang M, Deng Q, Hedlund E. 2021. Spatial RNA Sequencing Identifies Robust Markers of Vulnerable and Resistant Human Midbrain Dopamine Neurons and Their Expression in Parkinson's Disease. *Front Mol Neurosci* **14**: 699562.

Airavaara M, Parkkinen I, Konovalova J, Albert K, Chmielarz P, Domanskyi A. 2020. Back and to the Future: From Neurotoxin-Induced to Human Parkinson's Disease Models. *Curr Protoc Neurosci* **91**: e88.

Alam J, Cook JL. 1990. Reporter genes: application to the study of mammalian gene transcription. *Anal Biochem* **188**: 245-254.

Albert K, Raymundo DP, Panhelainen A, Eesmaa A, Shvachiy L, Araujo GR, Chmielarz P, Yan X, Singh A, Cordeiro Y et al. 2021. Cerebral dopamine neurotrophic factor reduces alpha-synuclein aggregation and propagation and alleviates behavioral alterations in vivo. *Mol Ther* **29**: 2821-2840.

Albert K, Voutilainen MH, Domanskyi A, Airavaara M. 2017. AAV Vector-Mediated Gene Delivery to Substantia Nigra Dopamine Neurons: Implications for Gene Therapy and Disease Models. *Genes (Basel)* **8**.

Anden NE, Carlsson A, Dahlstroem A, Fuxe K, Hillarp NA, Larsson K. 1964. Demonstration and Mapping out of Nigro-Neostriatal Dopamine Neurons. *Life Sci (1962)* **3**: 523-530.

Anden NE, Dahlstrom A, Fuxe K, Larsson K. 1966. Functional role of the nigro-neostriatal dopamine neurons. *Acta Pharmacol Toxicol (Copenh)* **24**: 263-274.

Antoniou A, Khudayberdiev S, Idziak A, Bicker S, Jacob R, Schratt G. 2018. The dynamic recruitment of TRBP to neuronal membranes mediates dendritogenesis during development. *EMBO Rep* **19**.

Araujo T, Aresta G, Castro E, Rouco J, Aguiar P, Eloy C, Polonia A, Campilho A. 2017. Classification of breast cancer histology images using Convolutional Neural Networks. *PLoS One* **12**: e0177544.

Armstrong MJ, Okun MS. 2020. Diagnosis and Treatment of Parkinson Disease: A Review. *JAMA* **323**: 548-560.

Asakawa T, Fang H, Sugiyama K, Nozaki T, Hong Z, Yang Y, Hua F, Ding G, Chao D, Fenoy AJ et al. 2016. Animal behavioral assessments in current research of Parkinson's disease. *Neurosci Biobehav Rev* **65**: 63-94.

Ascherio A, Schwarzschild MA. 2016. The epidemiology of Parkinson's disease: risk factors and prevention. *Lancet Neurol* **15**: 1257-1272.

Athauda D, Foltynie T. 2016. The glucagon-like peptide 1 (GLP) receptor as a therapeutic target in Parkinson's disease: mechanisms of action. *Drug Discov Today* **21**: 802-818.

Athauda D, Maclagan K, Skene SS, Bajwa-Joseph M, Letchford D, Chowdhury K, Hibbert S, Budnik N, Zampedri L, Dickson J et al. 2017. Exenatide once weekly versus placebo in Parkinson's disease: a randomised, double-blind, placebo-controlled trial. *Lancet* **390**: 1664-1675.

Bak IJ, Hassler R, Kim JS. 1969. Differential monoamine depletion by oxypertine in nerve terminals. Granulated synaptic vesicles in relation to depletion of norepinephrine, dopamine and serotonin. *Z Zellforsch Mikrosk Anat* **101**: 448-462.

Baker M. 2016. Biotech giant publishes failures to confirm high-profile science. *Nature* **530**: 141.

Bakkar N, Kovalik T, Lorenzini I, Spangler S, Lacoste A, Sponaugle K, Ferrante P, Argentinis E, Sattler R, Bowser R. 2017. Artificial intelligence in neurodegenerative disease research: use of IBM Watson to identify additional RNA-binding proteins altered in amyotrophic lateral sclerosis. *Acta Neuropathol.*

Barker RA, Parmar M, Studer L, Takahashi J. 2017. Human Trials of Stem Cell-Derived Dopamine Neurons for Parkinson's Disease: Dawn of a New Era. *Cell Stem Cell* **21**: 569-573.

Bassil R, Shields K, Granger K, Zein I, Ng S, Chih B. 2021. Improved modeling of human AD with an automated culturing platform for iPSC neurons, astrocytes and microglia. *Nat Commun* **12**: 5220.

Begley CG, Ellis LM. 2012. Drug development: Raise standards for preclinical cancer research. *Nature* **483**: 531-533.

Belal C, Ameli NJ, El Kommos A, Bezalel S, Al'Khafaji AM, Mughal MR, Mattson MP, Kyriazis GA, Tyrberg B, Chan SL. 2012. The homocysteine-inducible endoplasmic reticulum (ER) stress protein Herp counteracts mutant alpha-synuclein-induced ER stress via the homeostatic regulation of ER-resident calcium release channel proteins. *Hum Mol Genet* **21**: 963-977.

Benedetti MS, Dostert P. 1994. Contribution of amine oxidases to the metabolism of xenobiotics. *Drug Metab Rev* **26**: 507-535.

Bernstein E, Caudy AA, Hammond SM, Hannon GJ. 2001. Role for a bidentate ribonuclease in the initiation step of RNA interference. *Nature* **409**: 363-366.

Berridge MJ. 1998. Neuronal calcium signaling. *Neuron* **21**: 13-26.

Betzer C, Lassen LB, Olsen A, Kofoed RH, Reimer L, Gregersen E, Zheng J, Cali T, Gai WP, Chen T et al. 2018. Alpha-synuclein aggregates activate calcium pump SERCA leading to calcium dysregulation. *EMBO Rep* **19**.

Bjorklund A, Dunnett SB. 2007. Dopamine neuron systems in the brain: an update. *Trends Neurosci* **30**: 194-202.

Bjorklund A, Dunnett SB. 2019. The Amphetamine Induced Rotation Test: A Re-Assessment of Its Use as a Tool to Monitor Motor Impairment and Functional Recovery in Rodent Models of Parkinson's Disease. *J Parkinsons Dis* **9**: 17-29.

Bjorklund A, Kirik D, Rosenblad C, Georgievska B, Lundberg C, Mandel RJ. 2000. Towards a neuroprotective gene therapy for Parkinson's disease: use of adenovirus, AAV and lentivirus vectors for gene transfer of GDNF to the nigrostriatal system in the rat Parkinson model. *Brain Res* **886**: 82-98.

Bolam JP, Pissadaki EK. 2012. Living on the edge with too many mouths to feed: why dopamine neurons die. *Mov Disord* **27**: 1478-1483.

Bolender RP, Weibel ER. 1973. A morphometric study of the removal of phenobarbital-induced membranes from hepatocytes after cessation of treatment. *J Cell Biol* **56**: 746-761.

Bouard D, Alazard-Dany D, Cosset FL. 2009. Viral vectors: from virology to transgene expression. *Br J Pharmacol* **157**: 153-165.

Boucherie DM, Duarte GS, Machado T, Faustino PR, Sampaio C, Rascol O, Ferreira JJ. 2021. Parkinson's Disease Drug Development Since 1999: A Story of Repurposing and Relative Success. *J Parkinsons Dis* **11**: 421-429.

Boussaad I, Cruciani G, Bolognin S, Antony P, Dording CM, Kwon YJ, Heutink P, Fava E, Schwamborn JC, Kruger R. 2021. Integrated, automated maintenance, expansion and differentiation of 2D and 3D patient-derived cellular models for high throughput drug screening. *Sci Rep* **11**: 1439.

Boutros M, Heigwer F, Laufer C. 2015. Microscopy-Based High-Content Screening. *Cell* **163**: 1314-1325.

Boyce RW, Dorph-Petersen KA, Lyck L, Gundersen HJ. 2010. Design-based stereology: introduction to basic concepts and practical approaches for estimation of cell number. *Toxicol Pathol* **38**: 1011-1025.

Brodniewicz T, Grynkiewicz G. 2010. Preclinical drug development. *Acta Pol Pharm* **67**: 578-585.

Buck TM, Wijnholds J. 2020. Recombinant Adeno-Associated Viral Vectors (rAAV)-Vector Elements in Ocular Gene Therapy Clinical Trials and Transgene Expression and Bioactivity Assays. *Int J Mol Sci* **21**.

Burbulla LF, Schelling C, Kato H, Rapaport D, Woitalla D, Schiesling C, Schulte C, Sharma M, Illig T, Bauer P et al. 2010. Dissecting the role of the mitochondrial chaperone mortalin in Parkinson's disease: functional impact of disease-related variants on mitochondrial homeostasis. *Hum Mol Genet* **19**: 4437-4452.

Burke RE. 1998. Programmed cell death and Parkinson's disease. *Mov Disord* **13 Suppl 1**: 17-23.

Burke RE, Cadet JL, Kent JD, Karanas AL, Jackson-Lewis V. 1990. An assessment of the validity of densitometric measures of striatal tyrosine hydroxylase-positive fibers: relationship to apomorphine-induced rotations in 6-hydroxydopamine lesioned rats. *J Neurosci Methods* **35**: 63-73.

Caccia C, Maj R, Calabresi M, Maestroni S, Faravelli L, Curatolo L, Salvati P, Fariello RG. 2006. Safinamide: from molecular targets to a new anti-Parkinson drug. *Neurology* **67**: S18-23.

Caicedo JC, Cooper S, Heigwer F, Warchal S, Qiu P, Molnar C, Vasilevich AS, Barry JD, Bansal HS, Kraus O et al. 2017. Data-analysis strategies for image-based cell profiling. *Nat Methods* **14**: 849-863.

Capdeville R, Buchdunger E, Zimmermann J, Matter A. 2002. Glivec (STI571, imatinib), a rationally developed, targeted anticancer drug. *Nat Rev Drug Discov* **1**: 493-502.

Carlsson A. 1959. The occurrence, distribution and physiological role of catecholamines in the nervous system. *Pharmacol Rev* **11**: 490-493.

Carlsson A, Lindqvist M, Magnusson T. 1957. 3,4-Dihydroxyphenylalanine and 5-hydroxytryptophan as reserpine antagonists. *Nature* **180**: 1200.

Carpenter AE, Jones TR, Lamprecht MR, Clarke C, Kang IH, Friman O, Guertin DA, Chang JH, Lindquist RA, Moffat J et al. 2006. CellProfiler: image analysis software for identifying and quantifying cell phenotypes. *Genome Biol* **7**: R100.

Cassell MD, Mankovich NJ, Gray TS, Williams TH. 1982. Computer-assisted image analysis of the distributions of peptidergic terminals in the central nucleus of the amygdala: a preliminary study. *Peptides* **3**: 283-290.

Charvin D, Medori R, Hauser RA, Rascol O. 2018. Therapeutic strategies for Parkinson disease: beyond dopaminergic drugs. *Nat Rev Drug Discov* **17**: 844.

Chee MS, Bankier AT, Beck S, Bohni R, Brown CM, Cerny R, Horsnell T, Hutchison CA, 3rd, Kouzarides T, Martignetti JA et al. 1990. Analysis of the protein-coding content of the sequence of human cytomegalovirus strain AD169. *Curr Top Microbiol Immunol* **154**: 125-169.

Cheng HC, Ulane CM, Burke RE. 2010. Clinical progression in Parkinson disease and the neurobiology of axons. *Ann Neurol* **67**: 715-725.

Chiu YL, Dinesh CU, Chu CY, Ali A, Brown KM, Cao H, Rana TM. 2005. Dissecting RNA-interference pathway with small molecules. *Chem Biol* **12**: 643-648.

Chmielarz P, Er S, Konovalova J, Bandres L, Hlushchuk I, Albert K, Panhelainen A, Luk K, Airavaara M, Domanskyi A. 2020. GDNF/RET Signaling Pathway Activation Eliminates Lewy Body

Pathology in Midbrain Dopamine Neurons. *Mov Disord* **35**: 2279-2289.
Chmielarz P, Konovalova J, Najam SS, Alter H, Piepponen TP, Erfle H, Sonntag KC, Schutz G, Vinnikov IA, Domanskyi A. 2017. Dicer and microRNAs protect adult dopamine neurons. *Cell Death Dis* **8**: e2813.
Chmielarz P, Saarma M. 2020. Neurotrophic factors for disease-modifying treatments of Parkinson's disease: gaps between basic science and clinical studies. *Pharmacol Rep* **72**: 1195-1217.
Cho NH, Cheveralls KC, Brunner A-D, Kim K, Michaelis AC, Raghavan P, Kobayashi H, Savy L, Li JY, Canaj H et al. 2021. OpenCell: proteome-scale endogenous tagging enables the cartography of human cellular organization. *bioRxiv*.
Colla E. 2019. Linking the Endoplasmic Reticulum to Parkinson's Disease and Alpha-Synucleinopathy. *Front Neurosci* **13**: 560.
Colla E, Jensen PH, Pletnikova O, Troncoso JC, Glabe C, Lee MK. 2012. Accumulation of toxic alpha-synuclein oligomer within endoplasmic reticulum occurs in alpha-synucleinopathy in vivo. *J Neurosci* **32**: 3301-3305.
Croston GE. 2017. The utility of target-based discovery. *Expert Opin Drug Discov* **12**: 427-429.
Dagra A, Miller DR, Lin M, Gopinath A, Shaerzadeh F, Harris S, Sorrentino ZA, Stoier JF, Velasco S, Azar J et al. 2021. alpha-Synuclein-induced dysregulation of neuronal activity contributes to murine dopamine neuron vulnerability. *NPJ Parkinsons Dis* **7**: 76.
Dastjerd NK, Sert OC, Ozyer T, Alhajj R. 2019. Fuzzy Classification Methods Based Diagnosis of Parkinson's disease from Speech Test Cases. *Curr Aging Sci* **12**: 100-120.
Davies BP, Arenz C. 2006. A homogenous assay for micro RNA maturation. *Angew Chem Int Ed Engl* **45**: 5550-5552.
Decressac M, Mattsson B, Bjorklund A. 2012. Comparison of the behavioural and histological characteristics of the 6-OHDA and alpha-synuclein rat models of Parkinson's disease. *Exp Neurol* **235**: 306-315.
Domesick VB, Stinus L, Paskevich PA. 1983. The cytology of dopaminergic and nondopaminergic neurons in the substantia nigra and ventral tegmental area of the rat: a light- and electron-microscopic study. *Neuroscience* **8**: 743-765.
Dotti CG, Sullivan CA, Banker GA. 1988. The establishment of polarity by hippocampal neurons in culture. *J Neurosci* **8**: 1454-1468.
Drews J. 2000. Drug discovery: a historical perspective. *Science* **287**: 1960-1964.
Duty S, Jenner P. 2011. Animal models of Parkinson's disease: a source of novel treatments and clues to the cause of the disease. *Br J Pharmacol* **164**: 1357-1391.

Eglen RM, Gilchrist A, Reisine T. 2008. An overview of drug screening using primary and embryonic stem cells. *Comb Chem High Throughput Screen* **11**: 566-572.

Eisner DA. 2018. Reproducibility of science: Fraud, impact factors and carelessness. *J Mol Cell Cardiol* **114**: 364-368.

Ekstrand MI, Galter D. 2009. The MitoPark Mouse - an animal model of Parkinson's disease with impaired respiratory chain function in dopamine neurons. *Parkinsonism Relat Disord* **15 Suppl 3**: S185-188.

Elkouzi A, Vedam-Mai V, Eisinger RS, Okun MS. 2019. Emerging therapies in Parkinson disease - repurposed drugs and new approaches. *Nat Rev Neurol* **15**: 204-223.

England CG, Ehlerding EB, Cai W. 2016. NanoLuc: A Small Luciferase Is Brightening Up the Field of Bioluminescence. *Bioconjug Chem* **27**: 1175-1187.

Er S, Hlushchuk I, Airavaara M, Chmielarz P, Domanskyi A. 2020. Studying Pre-formed Fibril Induced alpha-Synuclein Accumulation in Primary Embryonic Mouse Midbrain Dopamine Neurons. *J Vis Exp*.

Fahn S. 2003. Description of Parkinson's disease as a clinical syndrome. *Ann N Y Acad Sci* **991**: 1-14.

Fajrial AK, He QQ, Wirusanti NI, Slansky JE, Ding X. 2020. A review of emerging physical transfection methods for CRISPR/Cas9-mediated gene editing. *Theranostics* **10**: 5532-5549.

Fan F, Wood KV. 2007. Bioluminescent assays for high-throughput screening. *Assay Drug Dev Technol* **5**: 127-136.

Fearnley JM, Lees AJ. 1991. Ageing and Parkinson's disease: substantia nigra regional selectivity. *Brain* **114 (Pt 5)**: 2283-2301.

Felicetti T, Cecchetti V, Manfroni G. 2020. Modulating microRNA Processing: Enoxacin, the Progenitor of a New Class of Drugs. *J Med Chem* **63**: 12275-12289.

Foecking MK, Hofstetter H. 1986. Powerful and versatile enhancer-promoter unit for mammalian expression vectors. *Gene* **45**: 101-105.

Foulkes WD, Priest JR, Duchaine TF. 2014. DICER1: mutations, microRNAs and mechanisms. *Nat Rev Cancer* **14**: 662-672.

Fowler PC, Garcia-Pardo ME, Simpson JC, O'Sullivan NC. 2019. NeurodegenERation: The Central Role for ER Contacts in Neuronal Function and Axonopathy, Lessons From Hereditary Spastic Paraplegias and Related Diseases. *Front Neurosci* **13**: 1051.

Fujita KA, Ostaszewski M, Matsuoka Y, Ghosh S, Glaab E, Trefois C, Crespo I, Perumal TM, Jurkowski W, Antony PM et al. 2014. Integrating pathways of Parkinson's disease in a molecular interaction map. *Mol Neurobiol* **49**: 88-102.

Gagnon D, Petryszyn S, Sanchez MG, Bories C, Beaulieu JM, De Koninck Y, Parent A, Parent M. 2017. Striatal Neurons Expressing D1 and D2 Receptors are Morphologically Distinct and Differently Affected by Dopamine Denervation in Mice. *Sci Rep* **7**: 41432.

Ganguly U, Singh S, Pal S, Prasad S, Agrawal BK, Saini RV, Chakrabarti S. 2021. Alpha-Synuclein as a Biomarker of Parkinson's Disease: Good, but Not Good Enough. *Front Aging Neurosci* **13**: 702639.

Gerk PM. 2011. Quantitative immunofluorescent blotting of the multidrug resistance-associated protein 2 (MRP2). *J Pharmacol Toxicol Methods* **63**: 279-282.

German DC, Manaye KF. 1993. Midbrain dopaminergic neurons (nuclei A8, A9, and A10): three-dimensional reconstruction in the rat. *J Comp Neurol* **331**: 297-309.

German DC, Schlusselberg DS, Woodward DJ. 1983. Three-dimensional computer reconstruction of midbrain dopaminergic neuronal populations: from mouse to man. *J Neural Transm* **57**: 243-254.

Giacomotto J, Segalat L. 2010. High-throughput screening and small animal models, where are we? *Br J Pharmacol* **160**: 204-216.

Giguere N, Burke Nanni S, Trudeau LE. 2018. On Cell Loss and Selective Vulnerability of Neuronal Populations in Parkinson's Disease. *Front Neurol* **9**: 455.

Gillespie M, Jassal B, Stephan R, Milacic M, Rothfels K, Senff-Ribeiro A, Griss J, Sevilla C, Matthews L, Gong C et al. 2022. The reactome pathway knowledgebase 2022. *Nucleic Acids Res* **50**: D687-D692.

Gomez-Suaga P, Bravo-San Pedro JM, Gonzalez-Polo RA, Fuentes JM, Niso-Santano M. 2018. ER-mitochondria signaling in Parkinson's disease. *Cell Death Dis* **9**: 337.

Gonzalez-Hernandez T, Cruz-Muros I, Afonso-Oramas D, Salas-Hernandez J, Castro-Hernandez J. 2010. Vulnerability of mesostriatal dopaminergic neurons in Parkinson's disease. *Front Neuroanat* **4**: 140.

Grace AA, Bunney BS. 1983. Intracellular and extracellular electrophysiology of nigral dopaminergic neurons--2. Action potential generating mechanisms and morphological correlates. *Neuroscience* **10**: 317-331.

Graewe S, Retzlaff S, Struck N, Janse CJ, Heussler VT. 2009. Going live: a comparative analysis of the suitability of the RFP derivatives RedStar, mCherry and tdTomato for intravital and in vitro live imaging of Plasmodium parasites. *Biotechnol J* **4**: 895-902.

Greffard S, Verny M, Bonnet AM, Beinis JY, Gallinari C, Meaume S, Piette F, Hauw JJ, Duyckaerts C. 2006. Motor score of the Unified Parkinson Disease Rating Scale as a good predictor of Lewy body-associated neuronal loss in the substantia nigra. *Arch Neurol* **63**: 584-588.

Gregoire L, Jourdain VA, Townsend M, Roach A, Di Paolo T. 2013. Safinamide reduces dyskinesias and prolongs L-DOPA antiparkinsonian effect in parkinsonian monkeys. *Parkinsonism Relat Disord* **19**: 508-514.

Grenn FP, Kim JJ, Makarious MB, Iwaki H, Illarionova A, Brolin K, Kluss JH, Schumacher-Schuh AF, Leonard H, Faghri F et al. 2020. The Parkinson's Disease Genome-Wide Association Study Locus Browser. *Mov Disord* **35**: 2056-2067.

Guardia-Laguarta C, Area-Gomez E, Rub C, Liu Y, Magrane J, Becker D, Voos W, Schon EA, Przedborski S. 2014. alpha-Synuclein is localized to mitochondria-associated ER membranes. *J Neurosci* **34**: 249-259.

Gulley RL, Wood RL. 1971. The fine structure of the neurons in the rat substantia nigra. *Tissue Cell* **3**: 675-690.

Gundersen HJ. 1986. Stereology of arbitrary particles. A review of unbiased number and size estimators and the presentation of some new ones, in memory of William R. Thompson. *J Microsc* **143**: 3-45.

Guzman JN, Sanchez-Padilla J, Chan CS, Surmeier DJ. 2009. Robust pacemaking in substantia nigra dopaminergic neurons. *J Neurosci* **29**: 11011-11019.

Harkavyi A, Abuirmeileh A, Lever R, Kingsbury AE, Biggs CS, Whitton PS. 2008. Glucagon-like peptide 1 receptor stimulation reverses key deficits in distinct rodent models of Parkinson's disease. *J Neuroinflammation* **5**: 19.

Heald R, Cohen-Fix O. 2014. Morphology and function of membrane-bound organelles. *Curr Opin Cell Biol* **26**: 79-86.

Hetz C, Saxena S. 2017. ER stress and the unfolded protein response in neurodegeneration. *Nat Rev Neurol* **13**: 477-491.

Hornykiewicz O. 1998. Biochemical aspects of Parkinson's disease. *Neurology* **51**: S2-9.

Horton AC, Ehlers MD. 2003. Dual modes of endoplasmic reticulum-to-Golgi transport in dendrites revealed by live-cell imaging. *J Neurosci* **23**: 6188-6199.

Hou X, Watzlawik JO, Fiesel FC, Springer W. 2020. Autophagy in Parkinson's Disease. *J Mol Biol* **432**: 2651-2672.

Hughes JP, Rees S, Kalindjian SB, Philpott KL. 2011. Principles of early drug discovery. *Br J Pharmacol* **162**: 1239-1249.

Hutchinson L, Kirk R. 2011. High drug attrition rates--where are we going wrong? *Nat Rev Clin Oncol* **8**: 189-190.

Iancu R, Mohapel P, Brundin P, Paul G. 2005. Behavioral characterization of a unilateral 6-OHDA-lesion model of Parkinson's disease in mice. *Behav Brain Res* **162**: 1-10.

Inglese J, Johnson RL, Simeonov A, Xia M, Zheng W, Austin CP, Auld DS. 2007. High-throughput screening assays for the identification of chemical probes. *Nat Chem Biol* **3**: 466-479.

Ip CW, Cheong D, Volkmann J. 2017. Stereological Estimation of Dopaminergic Neuron Number in the Mouse Substantia Nigra Using the Optical Fractionator and Standard Microscopy Equipment. *J Vis Exp*.

Jahn SW, Plass M, Moinfar F. 2020. Digital Pathology: Advantages, Limitations and Emerging Perspectives. *J Clin Med* **9**.

Jang SE, Qiu L, Chan LL, Tan EK, Zeng L. 2020. Current Status of Stem Cell-Derived Therapies for Parkinson's Disease: From Cell Assessment and Imaging Modalities to Clinical Trials. *Front Neurosci* **14**: 558532.

Jaworski K, Jankowski P, Kosior DA. 2017. PCSK9 inhibitors - from discovery of a single mutation to a groundbreaking therapy of lipid disorders in one decade. *Arch Med Sci* **13**: 914-929.

Jayawickreme CK, Kost TA. 1997. Gene expression systems in the development of high-throughput screens. *Curr Opin Biotechnol* **8**: 629-634.

Jin J, Hulette C, Wang Y, Zhang T, Pan C, Wadhwa R, Zhang J. 2006. Proteomic identification of a stress protein, mortalin/mthsp70/GRP75: relevance to Parkinson disease. *Mol Cell Proteomics* **5**: 1193-1204.

Jones TR, Kang IH, Wheeler DB, Lindquist RA, Papallo A, Sabatini DM, Golland P, Carpenter AE. 2008. CellProfiler Analyst: data exploration and analysis software for complex image-based screens. *BMC Bioinformatics* **9**: 482.

Jumper J, Evans R, Pritzel A, Green T, Figurnov M, Ronneberger O, Tunyasuvunakool K, Bates R, Zidek A, Potapenko A et al. 2021. Highly accurate protein structure prediction with AlphaFold. *Nature* **596**: 583-589.

Jung J, Michalak M, Agellon LB. 2017. Endoplasmic Reticulum Malfunction in the Nervous System. *Front Neurosci* **11**: 220.

Kalia LV, Lang AE. 2015. Parkinson's disease. *Lancet* **386**: 896-912.

Keller KK, Andersen IT, Andersen JB, Hahn U, Stengaard-Pedersen K, Hauge EM, Nyengaard JR. 2013. Improving efficiency in stereology: a study applying the proportionator and the autodisector on virtual slides. *J Microsc* **251**: 68-76.

Kepp O, Galluzzi L, Lipinski M, Yuan J, Kroemer G. 2011. Cell death assays for drug discovery. *Nat Rev Drug Discov* **10**: 221-237.

Khudoerkov RM, Voronkov DN, Dikalova YV. 2014. Quantitative morphochemical characterization of the neurons in substantia nigra of rat brain and its volume reconstruction. *Bull Exp Biol Med* **156**: 861-864.

Kikuchi T, Morizane A, Doi D, Onoe H, Hayashi T, Kawasaki T, Saiki H, Miyamoto S, Takahashi J. 2011. Survival of human induced pluripotent stem cell-derived midbrain dopaminergic neurons in the brain of a primate model of Parkinson's disease. *J Parkinsons Dis* **1**: 395-412.

Kirik D, Rosenblad C, Bjorklund A. 1998. Characterization of behavioral and neurodegenerative changes following partial lesions of the nigrostriatal dopamine system induced by intrastriatal 6-hydroxydopamine in the rat. *Exp Neurol* **152**: 259-277.

Klein AD, Mazzulli JR. 2018. Is Parkinson's disease a lysosomal disorder? *Brain* **141**: 2255-2262.

Ko HS, Lee Y, Shin JH, Karuppagounder SS, Gadad BS, Koleske AJ, Pletnikova O, Troncoso JC, Dawson VL, Dawson TM. 2010. Phosphorylation by the c-Abl protein tyrosine kinase inhibits parkin's ubiquitination and protective function. *Proc Natl Acad Sci U S A* **107**: 16691-16696.

Kobayashi M, Tanaka A, Hayashi Y, Shimamura S. 1997. The CMV enhancer stimulates expression of foreign genes from the human EF-1 alpha promoter. *Anal Biochem* **247**: 179-181.

Kordower JH, Olanow CW, Dodiya HB, Chu Y, Beach TG, Adler CH, Halliday GM, Bartus RT. 2013. Disease duration and the integrity of the nigrostriatal system in Parkinson's disease. *Brain* **136**: 2419-2431.

Kraus OZ, Grys BT, Ba J, Chong Y, Frey BJ, Boone C, Andrews BJ. 2017. Automated analysis of high-content microscopy data with deep learning. *Mol Syst Biol* **13**: 924.

Kumer SC, Vrana KE. 1996. Intricate regulation of tyrosine hydroxylase activity and gene expression. *J Neurochem* **67**: 443-462.

Laine RF, Arganda-Carreras I, Henriques R, Jacquemet G. 2021. Avoiding a replication crisis in deep-learning-based bioimage analysis. *Nat Methods* **18**: 1136-1144.

Lanciego JL, Luquin N, Obeso JA. 2012. Functional neuroanatomy of the basal ganglia. *Cold Spring Harb Perspect Med* **2**: a009621.

Lang C, Campbell KR, Ryan BJ, Carling P, Attar M, Vowles J, Perestenko OV, Bowden R, Baig F, Kasten M et al. 2019. Single-Cell Sequencing of iPSC-Dopamine Neurons Reconstructs Disease Progression and Identifies HDAC4 as a Regulator of Parkinson Cell Phenotypes. *Cell Stem Cell* **24**: 93-106 e106.

Larsen KE, Fon EA, Hastings TG, Edwards RH, Sulzer D. 2002. Methamphetamine-induced degeneration of dopaminergic neurons involves autophagy and upregulation of dopamine synthesis. *J Neurosci* **22**: 8951-8960.

Lautenschlager J, Mosharov EV, Kanter E, Sulzer D, Kaminski Schierle GS. 2018. An Easy-to-Implement Protocol for Preparing Postnatal Ventral Mesencephalic Cultures. *Front Cell Neurosci* **12**: 44.

LeCun Y, Bengio Y, Hinton G. 2015. Deep learning. *Nature* **521**: 436-444.
Leggio L, Vivarelli S, L'Episcopo F, Tirolo C, Caniglia S, Testa N, Marchetti B, Iraci N. 2017. microRNAs in Parkinson's Disease: From Pathogenesis to Novel Diagnostic and Therapeutic Approaches. *Int J Mol Sci* **18**.
Lehtonen S, Sonninen TM, Wojciechowski S, Goldsteins G, Koistinaho J. 2019. Dysfunction of Cellular Proteostasis in Parkinson's Disease. *Front Neurosci* **13**: 457.
Lein ES Hawrylycz MJ Ao N Ayres M Bensinger A Bernard A Boe AF Boguski MS Brockway KS Byrnes EJ et al. 2007. Genome-wide atlas of gene expression in the adult mouse brain. *Nature* **445**: 168-176.
Li B, Zhao G, Zhou Q, Xie Y, Wang Z, Fang Z, Lu B, Qin L, Zhao Y, Zhang R et al. 2021. Gene4PD: A Comprehensive Genetic Database of Parkinson's Disease. *Front Neurosci* **15**: 679568.
Li BD, Cui JJ, Song J, Qi C, Ma PF, Wang YR, Bai J. 2018. Comparison of the Efficacy of Different Drugs on Non-Motor Symptoms of Parkinson's Disease: a Network Meta-Analysis. *Cell Physiol Biochem* **45**: 119-130.
Lindholm P, Voutilainen MH, Lauren J, Peranen J, Leppanen VM, Andressoo JO, Lindahl M, Janhunen S, Kalkkinen N, Timmusk T et al. 2007. Novel neurotrophic factor CDNF protects and rescues midbrain dopamine neurons in vivo. *Nature* **448**: 73-77.
Linsley JW, Reisine T, Finkbeiner S. 2019. Cell death assays for neurodegenerative disease drug discovery. *Expert Opin Drug Discov* **14**: 901-913.
Lipinski CA. 2000. Drug-like properties and the causes of poor solubility and poor permeability. *J Pharmacol Toxicol Methods* **44**: 235-249.
Litwin JA. 1979. Histochemistry and cytochemistry of 3,3'-diaminobenzidine. A review. *Folia Histochem Cytochem (Krakow)* **17**: 3-28.
Liu L, Wang Q, Adeli E, Zhang L, Zhang H, Shen D. 2016. Feature Selection Based on Iterative Canonical Correlation Analysis for Automatic Diagnosis of Parkinson's Disease. *Med Image Comput Comput Assist Interv* **9901**: 1-8.
Lopreside A, Wan X, Michelini E, Roda A, Wang B. 2019. Comprehensive Profiling of Diverse Genetic Reporters with Application to Whole-Cell and Cell-Free Biosensors. *Anal Chem* **91**: 15284-15292.
Lorenz DA, Vander Roest S, Larsen MJ, Garner AL. 2018. Development and Implementation of an HTS-Compatible Assay for the Discovery of Selective Small-Molecule Ligands for Pre-microRNAs. *SLAS Discov* **23**: 47-54.
Lovell DP. 2013. Biological importance and statistical significance. *J Agric Food Chem* **61**: 8340-8348.

Luarte A, Cornejo VH, Bertin F, Gallardo J, Couve A. 2018. The axonal endoplasmic reticulum: One organelle-many functions in development, maintenance, and plasticity. *Dev Neurobiol* **78**: 181-208.

Luk KC, Kehm V, Carroll J, Zhang B, O'Brien P, Trojanowski JQ, Lee VM. 2012. Pathological alpha-synuclein transmission initiates Parkinson-like neurodegeneration in nontransgenic mice. *Science* **338**: 949-953.

Ma SY, Roytta M, Rinne JO, Collan Y, Rinne UK. 1997. Correlation between neuromorphometry in the substantia nigra and clinical features in Parkinson's disease using disector counts. *J Neurol Sci* **151**: 83-87.

Maggi A, Ciana P. 2005. Reporter mice and drug discovery and development. *Nat Rev Drug Discov* **4**: 249-255.

Mahul-Mellier AL, Burtscher J, Maharjan N, Weerens L, Croisier M, Kuttler F, Leleu M, Knott GW, Lashuel HA. 2020. The process of Lewy body formation, rather than simply alpha-synuclein fibrillization, is one of the major drivers of neurodegeneration. *Proc Natl Acad Sci U S A* **117**: 4971-4982.

Malpartida AB, Williamson M, Narendra DP, Wade-Martins R, Ryan BJ. 2021. Mitochondrial Dysfunction and Mitophagy in Parkinson's Disease: From Mechanism to Therapy. *Trends Biochem Sci* **46**: 329-343.

Mamoshina P, Vieira A, Putin E, Zhavoronkov A. 2016. Applications of Deep Learning in Biomedicine. *Mol Pharm* **13**: 1445-1454.

Manne S, Kondru N, Jin H, Serrano GE, Anantharam V, Kanthasamy A, Adler CH, Beach TG, Kanthasamy AG. 2020. Blinded RT-QuIC Analysis of alpha-Synuclein Biomarker in Skin Tissue From Parkinson's Disease Patients. *Mov Disord* **35**: 2230-2239.

Matsuda W, Furuta T, Nakamura KC, Hioki H, Fujiyama F, Arai R, Kaneko T. 2009. Single nigrostriatal dopaminergic neurons form widely spread and highly dense axonal arborizations in the neostriatum. *J Neurosci* **29**: 444-453.

McCulloch WS, Pitts W. 1990. A logical calculus of the ideas immanent in nervous activity. 1943. *Bull Math Biol* **52**: 99-115; discussion 173-197.

McFarthing K, Buff S, Rafaloff G, Dominey T, Wyse RK, Stott SRW. 2020. Parkinson's Disease Drug Therapies in the Clinical Trial Pipeline: 2020. *J Parkinsons Dis* **10**: 757-774.

McFarthing K, Prakash N, Simuni T. 2019. Clinical Trial Highlights: 1. Gene Therapy for Parkinson's, 2. Phase 3 Study in Focus - Intec Pharma's Accordion Pill, 3. Clinical Trials Resources. *J Parkinsons Dis* **9**: 251-264.

Mei J, Desrosiers C, Frasnelli J. 2021. Machine Learning for the Diagnosis of Parkinson's Disease: A Review of Literature. *Front Aging Neurosci* **13**: 633752.

Meiser J, Weindl D, Hiller K. 2013. Complexity of dopamine metabolism. *Cell Commun Signal* **11**: 34.
Mercado G, Valdés P, Hetz C. 2013. An ERcentric view of Parkinson's disease. *Trends Mol Med* **19**: 165-175.
Merchant KM, Cedarbaum JM, Brundin P, Dave KD, Eberling J, Espay AJ, Hutten SJ, Javidnia M, Luthman J, Maetzler W et al. 2019. A Proposed Roadmap for Parkinson's Disease Proof of Concept Clinical Trials Investigating Compounds Targeting Alpha-Synuclein. *J Parkinsons Dis* **9**: 31-61.
Michel PP, Hirsch EC, Hunot S. 2016. Understanding Dopaminergic Cell Death Pathways in Parkinson Disease. *Neuron* **90**: 675-691.
Mitchell T, Lehericy S, Chiu SY, Strafella AP, Stoessl AJ, Vaillancourt DE. 2021. Emerging Neuroimaging Biomarkers Across Disease Stage in Parkinson Disease: A Review. *JAMA Neurol*.
Mohs RC, Greig NH. 2017. Drug discovery and development: Role of basic biological research. *Alzheimers Dement (N Y)* **3**: 651-657.
Monzon-Sandoval J, Poggiolini I, Ilmer T, Wade-Martins R, Webber C, Parkkinen L. 2020. Human-Specific Transcriptome of Ventral and Dorsal Midbrain Dopamine Neurons. *Ann Neurol* **87**: 853-868.
Mouton PR, Phoulady HA, Goldgof D, Hall LO, Gordon M, Morgan D. 2017. Unbiased estimation of cell number using the automatic optical fractionator. *J Chem Neuroanat* **80**: A1-A8.
Nair-Roberts RG, Chatelain-Badie SD, Benson E, White-Cooper H, Bolam JP, Ungless MA. 2008. Stereological estimates of dopaminergic, GABAergic and glutamatergic neurons in the ventral tegmental area, substantia nigra and retrorubral field in the rat. *Neuroscience* **152**: 1024-1031.
Nakadate K, Tanaka-Nakadate S. 2015. Three-Dimensional Electron Microscopy Reconstruction of Degenerative Dopaminergic Neurons Surrounded by Activated Microglia in Substantia Nigra. *Ultrastruct Pathol* **39**: 369-377.
Nakajima Y, Ohmiya Y. 2010. Bioluminescence assays: multicolor luciferase assay, secreted luciferase assay and imaging luciferase assay. *Expert Opin Drug Discov* **5**: 835-849.
Noyce AJ, Bestwick JP, Silveira-Moriyama L, Hawkes CH, Giovannoni G, Lees AJ, Schrag A. 2012. Meta-analysis of early nonmotor features and risk factors for Parkinson disease. *Ann Neurol* **72**: 893-901.
Ntetsika T, Papathoma PE, Markaki I. 2021. Novel targeted therapies for Parkinson's disease. *Mol Med* **27**: 17.
Nunes A, Silva G, Duque C, Januario C, Santana I, Ambrosio AF, Castelo-Branco M, Bernardes R. 2019. Retinal texture biomarkers may help to discriminate between Alzheimer's, Parkinson's, and healthy controls. *PLoS One* **14**: e0218826.

Oates AC, Gorfinkiel N, Gonzalez-Gaitan M, Heisenberg CP. 2009. Quantitative approaches in developmental biology. *Nat Rev Genet* **10**: 517-530.

Oliveira LMA, Gasser T, Edwards R, Zweckstetter M, Melki R, Stefanis L, Lashuel HA, Sulzer D, Vekrellis K, Halliday GM et al. 2021. Alpha-synuclein research: defining strategic moves in the battle against Parkinson's disease. *NPJ Parkinsons Dis* **7**: 65.

Onate M, Catenaccio A, Salvadores N, Saquel C, Martinez A, Moreno-Gonzalez I, Gamez N, Soto P, Soto C, Hetz C et al. 2020. The necroptosis machinery mediates axonal degeneration in a model of Parkinson disease. *Cell Death Differ* **27**: 1169-1185.

Oorschot DE. 1996. Total number of neurons in the neostriatal, pallidal, subthalamic, and substantia nigral nuclei of the rat basal ganglia: a stereological study using the cavalieri and optical disector methods. *J Comp Neurol* **366**: 580-599.

Ovallath S, Deepa P. 2013. The history of parkinsonism: descriptions in ancient Indian medical literature. *Mov Disord* **28**: 566-568.

Overton PG, Clark D. 1997. Burst firing in midbrain dopaminergic neurons. *Brain Res Brain Res Rev* **25**: 312-334.

Öztürk Z, O'Kane CJ, Pérez-Moreno JJ. 2020. Axonal Endoplasmic Reticulum Dynamics and Its Roles in Neurodegeneration. *Front Neurosci* **14**: 48.

Pacelli C, Giguere N, Bourque MJ, Levesque M, Slack RS, Trudeau LE. 2015. Elevated Mitochondrial Bioenergetics and Axonal Arborization Size Are Key Contributors to the Vulnerability of Dopamine Neurons. *Curr Biol* **25**: 2349-2360.

Paillusson S, Gomez-Suaga P, Stoica R, Little D, Gissen P, Devine MJ, Noble W, Hanger DP, Miller CCJ. 2017. alpha-Synuclein binds to the ER-mitochondria tethering protein VAPB to disrupt Ca(2+) homeostasis and mitochondrial ATP production. *Acta Neuropathol* **134**: 129-149.

Pakkenberg B, Moller A, Gundersen HJ, Mouritzen Dam A, Pakkenberg H. 1991. The absolute number of nerve cells in substantia nigra in normal subjects and in patients with Parkinson's disease estimated with an unbiased stereological method. *J Neurol Neurosurg Psychiatry* **54**: 30-33.

Palay SL, Palade GE. 1955. The fine structure of neurons. *J Biophys Biochem Cytol* **1**: 69-88.

Pang X, Hogan EM, Casserly A, Gao G, Gardner PD, Tapper AR. 2014. Dicer expression is essential for adult midbrain dopaminergic neuron maintenance and survival. *Mol Cell Neurosci* **58**: 22-28.

Parent M, Parent A. 2010. Substantia nigra and Parkinson's disease: a brief history of their long and intimate relationship. *Can J Neurol Sci* **37**: 313-319.

Parkinson J. 2002. An essay on the shaking palsy. 1817. *J Neuropsychiatry Clin Neurosci* **14**: 223-236; discussion 222.

Parkkinen L, O'Sullivan SS, Collins C, Petrie A, Holton JL, Revesz T, Lees AJ. 2011. Disentangling the relationship between Lewy bodies and nigral neuronal loss in Parkinson's disease. *J Parkinsons Dis* **1**: 277-286.

Patel JL, Goyal RK. 2007. Applications of artificial neural networks in medical science. *Curr Clin Pharmacol* **2**: 217-226.

Penttinen AM, Suleymanova I, Albert K, Anttila J, Voutilainen MH, Airavaara M. 2016. Characterization of a new low-dose 6-hydroxydopamine model of Parkinson's disease in rat. *J Neurosci Res* **94**: 318-328.

Pereira CR, Pereira DR, Rosa GH, Albuquerque VHC, Weber SAT, Hook C, Papa JP. 2018. Handwritten dynamics assessment through convolutional neural networks: An application to Parkinson's disease identification. *Artif Intell Med* **87**: 67-77.

Peters A, Kemper T. 2012. A review of the structural alterations in the cerebral hemispheres of the aging rhesus monkey. *Neurobiol Aging* **33**: 2357-2372.

Pham TD. 2018. Pattern analysis of computer keystroke time series in healthy control and early-stage Parkinson's disease subjects using fuzzy recurrence and scalable recurrence network features. *J Neurosci Methods* **307**: 194-202.

Plate L, Cooley CB, Chen JJ, Paxman RJ, Gallagher CM, Madoux F, Genereux JC, Dobbs W, Garza D, Spicer TP et al. 2016. Small molecule proteostasis regulators that reprogram the ER to reduce extracellular protein aggregation. *Elife* **5**.

Podolska K, Sedlak D, Bartunek P, Svoboda P. 2014. Fluorescence-based high-throughput screening of dicer cleavage activity. *J Biomol Screen* **19**: 417-426.

Poewe W, Seppi K, Tanner CM, Halliday GM, Brundin P, Volkmann J, Schrag AE, Lang AE. 2017. Parkinson disease. *Nat Rev Dis Primers* **3**: 17013.

Postuma RB, Aarsland D, Barone P, Burn DJ, Hawkes CH, Oertel W, Ziemssen T. 2012. Identifying prodromal Parkinson's disease: pre-motor disorders in Parkinson's disease. *Mov Disord* **27**: 617-626.

Postuma RB, Poewe W, Litvan I, Lewis S, Lang AE, Halliday G, Goetz CG, Chan P, Slow E, Seppi K et al. 2018. Validation of the MDS clinical diagnostic criteria for Parkinson's disease. *Mov Disord* **33**: 1601-1608.

Prasad EM, Hung SY. 2021. Current Therapies in Clinical Trials of Parkinson's Disease: A 2021 Update. *Pharmaceuticals (Basel)* **14**.

Prasher DC, Eckenrode VK, Ward WW, Prendergast FG, Cormier MJ. 1992. Primary structure of the Aequorea victoria green-fluorescent protein. *Gene* **111**: 229-233.

Prior MJW, Bast T, McGarrity S, Goldschmidt J, Vincenz D, Seaton A, Hall G, Pitiot A. 2021. Ratlas-LH: An MRI template of the Lister hooded rat brain with stereotaxic coordinates for neurosurgical implantations. *Brain Neurosci Adv* **5**: 23982128211036332.

Przedborski S. 2017. The two-century journey of Parkinson disease research. *Nat Rev Neurosci* **18**: 251-259.

Qin JY, Zhang L, Clift KL, Hulur I, Xiang AP, Ren BZ, Lahn BT. 2010. Systematic comparison of constitutive promoters and the doxycycline-inducible promoter. *PLoS One* **5**: e10611.

Rayport S, Sulzer D, Shi WX, Sawasdikosol S, Monaco J, Batson D, Rajendran G. 1992. Identified postnatal mesolimbic dopamine neurons in culture: morphology and electrophysiology. *J Neurosci* **12**: 4264-4280.

Renaud JP, Chari A, Ciferri C, Liu WT, Remigy HW, Stark H, Wiesmann C. 2018. Cryo-EM in drug discovery: achievements, limitations and prospects. *Nat Rev Drug Discov* **17**: 471-492.

Reyes S, Fu Y, Double K, Thompson L, Kirik D, Paxinos G, Halliday GM. 2012. GIRK2 expression in dopamine neurons of the substantia nigra and ventral tegmental area. *J Comp Neurol* **520**: 2591-2607.

Robertson MJ, Meyerowitz JG, Skiniotis G. 2021. Drug discovery in the era of cryo-electron microscopy. *Trends Biochem Sci.*

Rodriguez EA, Campbell RE, Lin JY, Lin MZ, Miyawaki A, Palmer AE, Shu X, Zhang J, Tsien RY. 2017. The Growing and Glowing Toolbox of Fluorescent and Photoactive Proteins. *Trends Biochem Sci* **42**: 111-129.

Runeberg-Roos P, Piccinini E, Penttinen AM, Matlik K, Heikkinen H, Kuure S, Bespalov MM, Peranen J, Garea-Rodriguez E, Fuchs E et al. 2016. Developing therapeutically more efficient Neurturin variants for treatment of Parkinson's disease. *Neurobiol Dis* **96**: 335-345.

Sadeghian M, Mullali G, Pocock JM, Piers T, Roach A, Smith KJ. 2016. Neuroprotection by safinamide in the 6-hydroxydopamine model of Parkinson's disease. *Neuropathol Appl Neurobiol* **42**: 423-435.

Schapira AH, Cooper JM, Dexter D, Jenner P, Clark JB, Marsden CD. 1989. Mitochondrial complex I deficiency in Parkinson's disease. *Lancet* **1**: 1269.

Schapira AHV, Chaudhuri KR, Jenner P. 2017. Non-motor features of Parkinson disease. *Nat Rev Neurosci* **18**: 509.

Schenborn E, Groskreutz D. 1999. Reporter gene vectors and assays. *Mol Biotechnol* **13**: 29-44.

Schmid AW, Fauvet B, Moniatte M, Lashuel HA. 2013. Alpha-synuclein post-translational modifications as potential biomarkers for Parkinson disease and other synucleinopathies. *Mol Cell Proteomics* **12**: 3543-3558.

Schmitz C, Hof PR. 2005. Design-based stereology in neuroscience. *Neuroscience* **130**: 813-831.
Schweitzer JS, Song B, Herrington TM, Park TY, Lee N, Ko S, Jeon J, Cha Y, Kim K, Li Q et al. 2020. Personalized iPSC-Derived Dopamine Progenitor Cells for Parkinson's Disease. *N Engl J Med* **382**: 1926-1932.
Shahmoradian SH, Lewis AJ, Genoud C, Hench J, Moors TE, Navarro PP, Castano-Diez D, Schweighauser G, Graff-Meyer A, Goldie KN et al. 2019. Lewy pathology in Parkinson's disease consists of crowded organelles and lipid membranes. *Nat Neurosci* **22**: 1099-1109.
Shamir R, Klein C, Amar D, Vollstedt EJ, Bonin M, Usenovic M, Wong YC, Maver A, Poths S, Safer H et al. 2017. Analysis of blood-based gene expression in idiopathic Parkinson disease. *Neurology* **89**: 1676-1683.
Shan G, Li Y, Zhang J, Li W, Szulwach KE, Duan R, Faghihi MA, Khalil AM, Lu L, Paroo Z et al. 2008. A small molecule enhances RNA interference and promotes microRNA processing. *Nat Biotechnol* **26**: 933-940.
Shen Y, Chen Y, Wu J, Shaner NC, Campbell RE. 2017. Engineering of mCherry variants with long Stokes shift, red-shifted fluorescence, and low cytotoxicity. *PLoS One* **12**: e0171257.
Shibata Y, Voeltz GK, Rapoport TA. 2006. Rough sheets and smooth tubules. *Cell* **126**: 435-439.
Shimomura O, Johnson FH, Saiga Y. 1962. Extraction, purification and properties of aequorin, a bioluminescent protein from the luminous hydromedusan, Aequorea. *J Cell Comp Physiol* **59**: 223-239.
Sidransky E, Lopez G. 2012. The link between the GBA gene and parkinsonism. *Lancet Neurol* **11**: 986-998.
Sidransky E, Samaddar T, Tayebi N. 2009. Mutations in GBA are associated with familial Parkinson disease susceptibility and age at onset. *Neurology* **73**: 1424-1425, author reply 1425-1426.
Signaevsky M, Prastawa M, Farrell K, Tabish N, Baldwin E, Han N, Iida MA, Koll J, Bryce C, Purohit D et al. 2019. Artificial intelligence in neuropathology: deep learning-based assessment of tauopathy. *Lab Invest* **99**: 1019-1029.
Simunovic F, Yi M, Wang Y, Stephens R, Sonntag KC. 2010. Evidence for gender-specific transcriptional profiles of nigral dopamine neurons in Parkinson disease. *PLoS One* **5**: e8856.
Sinclair E, Trivedi DK, Sarkar D, Walton-Doyle C, Milne J, Kunath T, Rijs AM, de Bie RMA, Goodacre R, Silverdale M et al. 2021. Metabolomics of sebum reveals lipid dysregulation in Parkinson's disease. *Nat Commun* **12**: 1592.
Sjostedt E, Zhong W, Fagerberg L, Karlsson M, Mitsios N, Adori C, Oksvold P, Edfors F, Limiszewska A, Hikmet F et al. 2020. An atlas of the

protein-coding genes in the human, pig, and mouse brain. *Science* **367**.
Skibinski G, Finkbeiner S. 2011. Drug discovery in Parkinson's disease-Update and developments in the use of cellular models. *Int J High Throughput Screen* **2011**: 15-25.
Smits LM, Reinhardt L, Reinhardt P, Glatza M, Monzel AS, Stanslowsky N, Rosato-Siri MD, Zanon A, Antony PM, Bellmann J et al. 2019. Modeling Parkinson's disease in midbrain-like organoids. *NPJ Parkinsons Dis* **5**: 5.
Spang A. 2018. The endoplasmic reticulum-the caring mother of the cell. *Curr Opin Cell Biol* **53**: 92-96.
Spillantini MG, Crowther RA, Jakes R, Hasegawa M, Goedert M. 1998. alpha-Synuclein in filamentous inclusions of Lewy bodies from Parkinson's disease and dementia with lewy bodies. *Proc Natl Acad Sci U S A* **95**: 6469-6473.
Spillantini MG, Schmidt ML, Lee VM, Trojanowski JQ, Jakes R, Goedert M. 1997. Alpha-synuclein in Lewy bodies. *Nature* **388**: 839-840.
Steinmetz KL, Spack EG. 2009. The basics of preclinical drug development for neurodegenerative disease indications. *BMC Neurol* **9 Suppl 1**: S2.
Sterio DC. 1984. The unbiased estimation of number and sizes of arbitrary particles using the disector. *J Microsc* **134**: 127-136.
Sulzer D. 2007. Multiple hit hypotheses for dopamine neuron loss in Parkinson's disease. *Trends Neurosci* **30**: 244-250.
Sulzer D. 2011. How addictive drugs disrupt presynaptic dopamine neurotransmission. *Neuron* **69**: 628-649.
Sulzer D, Schmitz Y. 2007. Parkinson's disease: return of an old prime suspect. *Neuron* **55**: 8-10.
Sulzer D, Sonders MS, Poulsen NW, Galli A. 2005. Mechanisms of neurotransmitter release by amphetamines: a review. *Prog Neurobiol* **75**: 406-433.
Surmeier DJ, Graves SM, Shen W. 2014. Dopaminergic modulation of striatal networks in health and Parkinson's disease. *Curr Opin Neurobiol* **29**: 109-117.
Surmeier DJ, Obeso JA, Halliday GM. 2017. Selective neuronal vulnerability in Parkinson disease. *Nat Rev Neurosci* **18**: 101-113.
Swinney DC. 2013. Phenotypic vs. target-based drug discovery for first-in-class medicines. *Clin Pharmacol Ther* **93**: 299-301.
Swinney DC, Anthony J. 2011. How were new medicines discovered? *Nat Rev Drug Discov* **10**: 507-519.
Swinney DC, Lee JA. 2020. Recent advances in phenotypic drug discovery. *F1000Res* **9**.
Tadenev ALD, Burgess RW. 2019. Model validity for preclinical studies in precision medicine: precisely how precise do we need to be? *Mamm Genome* **30**: 111-122.

Takebe T, Imai R, Ono S. 2018. The Current Status of Drug Discovery and Development as Originated in United States Academia: The Influence of Industrial and Academic Collaboration on Drug Discovery and Development. *Clin Transl Sci* **11**: 597-606.

Tanudjojo B, Shaikh SS, Fenyi A, Bousset L, Agarwal D, Marsh J, Zois C, Heman-Ackah S, Fischer R, Sims D et al. 2021. Phenotypic manifestation of alpha-synuclein strains derived from Parkinson's disease and multiple system atrophy in human dopaminergic neurons. *Nat Commun* **12**: 3817.

Tenenbaum L, Humbert-Claude M. 2017. Glial Cell Line-Derived Neurotrophic Factor Gene Delivery in Parkinson's Disease: A Delicate Balance between Neuroprotection, Trophic Effects, and Unwanted Compensatory Mechanisms. *Front Neuroanat* **11**: 29.

Terasaki M. 2018. Axonal endoplasmic reticulum is very narrow. *J Cell Sci* **131**.

Terasaki M, Slater NT, Fein A, Schmidek A, Reese TS. 1994. Continuous network of endoplasmic reticulum in cerebellar Purkinje neurons. *Proc Natl Acad Sci U S A* **91**: 7510-7514.

Thakur P, Breger LS, Lundblad M, Wan OW, Mattsson B, Luk KC, Lee VMY, Trojanowski JQ, Bjorklund A. 2017. Modeling Parkinson's disease pathology by combination of fibril seeds and alpha-synuclein overexpression in the rat brain. *Proc Natl Acad Sci U S A* **114**: E8284-E8293.

Thompson L, Barraud P, Andersson E, Kirik D, Bjorklund A. 2005. Identification of dopaminergic neurons of nigral and ventral tegmental area subtypes in grafts of fetal ventral mesencephalon based on cell morphology, protein expression, and efferent projections. *J Neurosci* **25**: 6467-6477.

Tiklova K, Bjorklund AK, Lahti L, Fiorenzano A, Nolbrant S, Gillberg L, Volakakis N, Yokota C, Hilscher MM, Hauling T et al. 2019. Single-cell RNA sequencing reveals midbrain dopamine neuron diversity emerging during mouse brain development. *Nat Commun* **10**: 581.

Trifonova OP, Maslov DL, Balashova EE, Urazgildeeva GR, Abaimov DA, Fedotova EY, Poleschuk VV, Illarioshkin SN, Lokhov PG. 2020. Parkinson's Disease: Available Clinical and Promising Omics Tests for Diagnostics, Disease Risk Assessment, and Pharmacotherapy Personalization. *Diagnostics (Basel)* **10**.

Tsujii S, Ishisaka M, Hara H. 2015. Modulation of endoplasmic reticulum stress in Parkinson's disease. *Eur J Pharmacol* **765**: 154-156.

Turkki R, Linder N, Kovanen PE, Pellinen T, Lundin J. 2016. Antibody-supervised deep learning for quantification of tumor-infiltrating immune cells in hematoxylin and eosin stained breast cancer samples. *J Pathol Inform* **7**: 38.

Uhl GR, Hedreen JC, Price DL. 1985. Parkinson's disease: loss of neurons from the ventral tegmental area contralateral to therapeutic surgical lesions. *Neurology* **35**: 1215-1218.

Uhlen M, Bjorling E, Agaton C, Szigyarto CA, Amini B, Andersen E, Andersson AC, Angelidou P, Asplund A, Asplund C et al. 2005. A human protein atlas for normal and cancer tissues based on antibody proteomics. *Mol Cell Proteomics* **4**: 1920-1932.

Uhlen M, Fagerberg L, Hallstrom BM, Lindskog C, Oksvold P, Mardinoglu A, Sivertsson A, Kampf C, Sjostedt E, Asplund A et al. 2015. Proteomics. Tissue-based map of the human proteome. *Science* **347**: 1260419.

Ungerstedt U. 1968. 6-Hydroxy-dopamine induced degeneration of central monoamine neurons. *Eur J Pharmacol* **5**: 107-110.

Ungerstedt U, Arbuthnott GW. 1970. Quantitative recording of rotational behavior in rats after 6-hydroxy-dopamine lesions of the nigrostriatal dopamine system. *Brain Res* **24**: 485-493.

Valente EM, Arena G, Torosantucci L, Gelmetti V. 2012. Molecular pathways in sporadic PD. *Parkinsonism Relat Disord* **18 Suppl 1**: S71-73.

Van Rompuy AS, Lobbestael E, Van der Perren A, Van den Haute C, Baekelandt V. 2014. Long-term overexpression of human wild-type and T240R mutant Parkin in rat substantia nigra induces progressive dopaminergic neurodegeneration. *J Neuropathol Exp Neurol* **73**: 159-174.

Vassilopoulos S, Gibaud S, Jimenez A, Caillol G, Leterrier C. 2019. Ultrastructure of the axonal periodic scaffold reveals a braid-like organization of actin rings. *Nat Commun* **10**: 5803.

Venderova K, Park DS. 2012. Programmed cell death in Parkinson's disease. *Cold Spring Harb Perspect Med* **2**.

Vila M, Ramonet D, Perier C. 2008. Mitochondrial alterations in Parkinson's disease: new clues. *J Neurochem* **107**: 317-328.

Walker CK, Roche JK, Sinha V, Roberts RC. 2018. Substantia nigra ultrastructural pathology in schizophrenia. *Schizophr Res* **197**: 209-218.

Wang Y, Wei N, Li X. 2020. Preclinical Evidence and Possible Mechanisms of Baicalein for Rats and Mice With Parkinson's Disease: A Systematic Review and Meta-Analysis. *Front Aging Neurosci* **12**: 277.

West MJ, Slomianka L, Gundersen HJ. 1991. Unbiased stereological estimation of the total number of neurons in the subdivisions of the rat hippocampus using the optical fractionator. *Anat Rec* **231**: 482-497.

Westrate LM, Lee JE, Prinz WA, Voeltz GK. 2015. Form follows function: the importance of endoplasmic reticulum shape. *Annu Rev Biochem* **84**: 791-811.

Wise RA. 2004. Dopamine, learning and motivation. *Nat Rev Neurosci* **5**: 483-494.
Wu Y, Jiang JH, Chen L, Lu JY, Ge JJ, Liu FT, Yu JT, Lin W, Zuo CT, Wang J. 2019. Use of radiomic features and support vector machine to distinguish Parkinson's disease cases from normal controls. *Ann Transl Med* **7**: 773.
Wu Y, Le W, Jankovic J. 2011. Preclinical biomarkers of Parkinson disease. *Arch Neurol* **68**: 22-30.
Wu Y, Whiteus C, Xu CS, Hayworth KJ, Weinberg RJ, Hess HF, De Camilli P. 2017. Contacts between the endoplasmic reticulum and other membranes in neurons. *Proc Natl Acad Sci U S A* **114**: E4859-e4867.
Xu K, Zhong G, Zhuang X. 2013. Actin, spectrin, and associated proteins form a periodic cytoskeletal structure in axons. *Science* **339**: 452-456.
Yamada T, McGeer PL, Baimbridge KG, McGeer EG. 1990. Relative sparing in Parkinson's disease of substantia nigra dopamine neurons containing calbindin-D28K. *Brain Res* **526**: 303-307.
Yamano S, Dai J, Moursi AM. 2010. Comparison of transfection efficiency of nonviral gene transfer reagents. *Mol Biotechnol* **46**: 287-300.
Yang W, Hamilton JL, Kopil C, Beck JC, Tanner CM, Albin RL, Ray Dorsey E, Dahodwala N, Cintina I, Hogan P et al. 2020. Current and projected future economic burden of Parkinson's disease in the U.S. *NPJ Parkinsons Dis* **6**: 15.
Zaccaria A, Antinori P, Licker V, Kovari E, Lobrinus JA, Burkhard PR. 2021. Multiomic Analyses of Dopaminergic Neurons Isolated from Human Substantia Nigra in Parkinson's Disease: A Descriptive and Exploratory Study. *Cell Mol Neurobiol.*
Zhang G, Gurtu V, Kain SR. 1996. An enhanced green fluorescent protein allows sensitive detection of gene transfer in mammalian cells. *Biochem Biophys Res Commun* **227**: 707-711.
Zhang Q, Zhang C, Xi Z. 2008. Enhancement of RNAi by a small molecule antibiotic enoxacin. *Cell Res* **18**: 1077-1079.
Zhuo C, Zhu X, Jiang R, Ji F, Su Z, Xue R, Zhou Y. 2017. Comparison for Efficacy and Tolerability among Ten Drugs for Treatment of Parkinson's Disease: A Network Meta-Analysis. *Sci Rep* **8**: 45865.
Zufferey R, Donello JE, Trono D, Hope TJ. 1999. Woodchuck hepatitis virus posttranscriptional regulatory element enhances expression of transgenes delivered by retroviral vectors. *J Virol* **73**: 2886-2892.